UNIVERSITÀ DEGLI STUDI DI TRIESTE
e
UNIVERSITÀ CA' FOSCARI DI VENEZIA

XXXI CICLO DEL DOTTORATO DI RICERCA IN CHIMICA

Development And Optimization Of High-Performance Liquid Chromatography-Tandem Mass Spectrometry Methods As Powerful Tools For The Therapeutic Drug Monitoring In Patients With Gastrointestinal Stromal Tumor

Settore scientifico-disciplinare: CHIM/06

DOTTORANDO
MAURO BUZZO

COORDINATORE
PROF. BARBARA MILANI

SUPERVISORI DI TESI
PROF. FEDERICO BERTI
GIUSEPPE TOFFOLI, M.D.

CO-SUPERVISORE DI TESI
ELENA MARANGON, Ph.D.

ANNO ACCADEMICO 2017/2018

Questo lavoro di tesi è stato svolto presso la Scuola di Dottorato in Chimica interateneo Università degli Studi di Trieste-Università Ca' Foscari di Venezia, diretta dalla Prof.ssa Barbara Milani in collaborazione con la Struttura Operativa Complessa di Farmacologia Sperimentale e Clinica del Centro di Riferimento Oncologico di Aviano, diretta dal Dott. Giuseppe Toffoli.

Contents

ABSTRACT

Gastrointestinal stromal tumor (GIST) is a malignant neoplasm characterised by a marked unresponsiveness to standard chemotherapy regimens and the introduction of the targeted cancer therapy with the tyrosine kinase inhibitors (TKIs) provided evident benefits for the treatment of this pathology. The introduction of imatinib (IMA), an oral TKI, strongly improved the treatment outcomes representing the first valid pharmacologic alternative to surgical resection for GIST patients. IMA is in fact indicated as first-line standard therapy for inoperable, metastatic, or recurrent GISTs. In case of occurrence of resistance to IMA treatment, sunitinib (SUN), another oral TKI, plays an important role in the patients' survival. For its efficacy, SUN is indicated as second-line treatment of GIST after treatment failure with IMA. Despite the indisputable clinical benefits achieved with these TKIs by GISTs patients, their current administration based on the "one-dose-fits-all" paradigm, along with the large inter-individual variability in systemic exposure observed, results in a non-optimized therapy. Moreover, for both IMA and SUN, a positive exposure-efficacy/toxicity relationship exists. For these reasons, therapeutic drug monitoring (TDM) approach, which aims to optimize the therapy by personalizing it through the determination and interpretation of drug concentration in biological fluids, has been suggested as potentially useful for both the TKIs. As related to IMA, a relationship between the trough level (C_{min}, the steady-state concentration before the subsequent administration of the drug) and therapy outcome has been observed, while no consensus is still reached on the precise C_{min} threshold for GIST patients because, in the literature, two different cut-off values have been suggested. As regards SUN, the main problem is its isomerization from the active Z-isomer to the E-one in presence of light. To overcome this problem, which also affects its main metabolite N-desethyl sunitinib (N-DES SUN), several published methods applied light protection conditions to the entire workflow (from blood sampling to plasma analysis) thus making this approach clearly not suitable to be applied for clinical routine analyses.

In this regard, this PhD project aimed to contribute, from the analytical point of view, to the TDM approach for both IMA and SUN in the context of GIST treatment. First, a robust, fast and clinically applicable LC-MS/MS quantification method for IMA and its main active metabolite N-desmethyl imatinib (NOR IMA) needed to be developed from scratch to obtain an applicable tool for the correct definition of the C_{min} thresholds in GIST patients. Regarding SUN, an already developed assay needed to be upgraded to solve the photoisomerization problem without the need for light protection condition during the sample handling. Moreover, a validation according to FDA and EMA guidelines needed to be performed for both the developed methods in order to evaluate their robustness. The two assays were developed and optimized using a Shimadzu Prominence XR chromatographic system coupled with an ESI triple quadrupole API4000 QTrap mass spectrometer from SCIEX.

First, an LC-MS/MS method for the simultaneous quantification of IMA and NOR IMA in human plasma was developed and validated. It requires only 20 µL of plasma to quantify both IMA and its main metabolite in a concentration range of 30-7'500 ng/mL and 6-1'500 ng/mL, respectively. Then, it was successfully applied to real GIST patients' samples thus allowing to highlight possible cases of under-exposure, over-exposure and non-adherence to therapy.

On the other side, the study of SUN and N-DES SUN isomerization in plasma samples led to the introduction, in the already developed LC-MS/MS quantification method, of a simple and fast pre-analytical step to overcome the issue of working in light-protected conditions: only 5 minutes of heated water bath at 70°C were enough to trigger the reconversion from E- to Z- isomer just before the analysis. Lastly, the upgraded method, characterised by optimal accuracy and precision throughout the linear range of 0.1-400 ng/mL and 0.1-200 ng/mL for SUN and N-DES SUN, respectively, was validated thus demonstrating the possibility to perform a quantitative analysis of both SUN and N-DES SUN without the need for light protection conditions.

1 INTRODUCTION

1.1 Gastrointestinal Stromal Tumor

Gastrointestinal stromal tumor (GIST) belongs to the soft-tissue sarcomas family. Although it is responsible for less than 1% of the primary gastrointestinal neoplasms[1], GIST represents the most common non-epithelial tumor of the gastrointestinal tract: the stomach is the most frequent onset site (60%), followed by the small intestine (30%), the colon and the rectum (5%) and the esophagus (5%). It rarely develops outside the gastrointestinal tract and in that cases, the mesentery, the omentum or the retroperitoneum could be involved[2].

Estimates of 2015 show an incidence of 15 new patients out of a million of people per year with a prevalence of 1.3 cases every 10'000 people considering both the cases previously diagnosticated and the new ones. This means that, in Italy, between 6'000 and 7'000 people are affected by GIST[3].

Most of patients are from 40 to 80 years old, with a median age of 60 years, when GIST is diagnosticated[4,5]. Cases of GIST in new-borns and in people under 30 are infrequent[6]. A correlation between gender or ethnicity and the incidence of this tumor is considered to be non-existent[7].

Literature data regarding both the clinical behavior and the epidemiology of GIST before the 21st century are not accurate. This is due to the fact that before the 80's, GIST was classified both as leiomyoma (smooth muscle benign tumor) and leiomyosarcoma (smooth muscle malignant tumor) and only with the introduction of the immunohistochemistry, at the beginning of the 21st century, these two pathologies are recognised as clinically and pathologically distinct.

GISTs are malignant neoplasms, although the small ones with a low mitotic index present a less aggressive behavior and a lower risk of evolution over time[8]. About 40% of GISTs localized at the beginning, subsequently lead to metastases which, in 10–20% of patients affected by this tumor, are already present at the moment of the diagnosis[9]. Metastases sporadically appear outside the abdomen, while they mostly involve the peritoneal cavity, the liver and the omentum[4].

It is known that GIST originates from the interstitial cells of Cajal[10], named also pacemaker cells for their role of intestinal peristalsis coordinators by constituting a

complex cellular web located between the Auerbach plex and the smooth muscle cells of the gastrointestinal tract.

The histological diagnosis is primarily based on the morphology, the immunohistochemistry and, sometimes, on the mutational analysis. Endoscopic examination, echography, computed axial tomography, nuclear magnetic resonance, positron emission tomography exams with Fluorine-deoxy glucose and CD117 expression evaluation represent the diagnostic tools to date[11].

The early stage GISTs, because of small size and their symptomless nature, are often accidentally discovered thanks to examinations (endoscopic or radiographic) for other pathologies.

The antigen CD117 is an epitope of KIT receptor and 95% of tumor cells originated from GISTs are positive for this antigen, regardless of the origin site, the histological appearance or the biological behavior of the tumor. Therefore, this factor is considered one of the most reliable diagnostic markers[12]. As can be seen in figure 1, the KIT receptor is composed by three portions:

1. An extra-cellular portion that incorporates the binding sites for the ligand;
2. A trans-membrane portion;
3. An intra-cellular portion responsible for the tyrosine kinase activity.

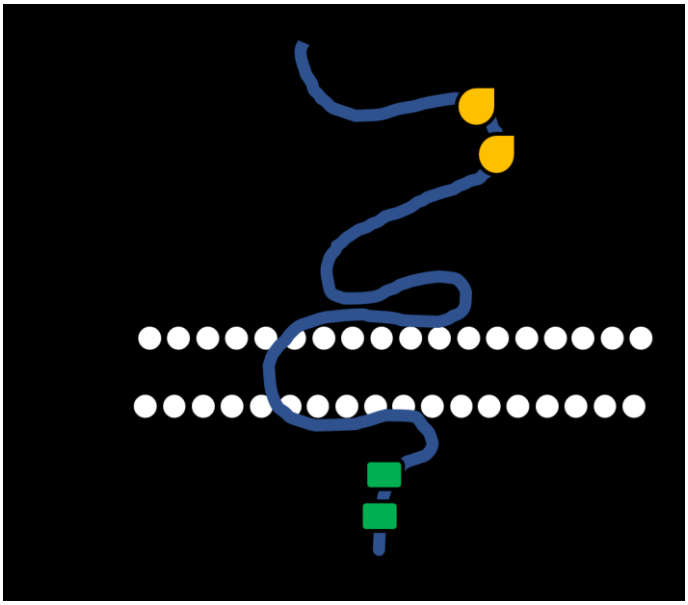

Figure 1. Schematic representation of the KIT receptor structure.

The KIT inactive form is a monomer with intrinsic factors that make its activity self-inhibited. The ligand is a dimeric protein called Stem Cell Factor (SCF), a tissutal and hematopoietic growth factor. When its two domains interact with the two receptors located in the extracellular portion of KIT, the activation begins. This kind of interaction is called homodimerization and leads to a phosphorylation reaction first. Then, the consequences of this interaction are a series of cascade signals with the result of the activation of cellular functions which are fundamentals for carcinogenesis like proliferation, adhesion, differentiation and apoptosis. However, SCF only represents the extrinsic mechanism of KIT activation, which can also be regulated by structural modifications of the protein itself which allow it to be activated in the absence of the ligand (intrinsic mechanism). The latter happens mostly in GISTs, where the structural modifications are the results of oncogene mutations of sequences that code for KIT gene. Most of GISTs (70–80%), in fact, presents KIT mutations[13], which often interest the juxta-membrane domains. These alterations, that are mostly deletions, in frame insertions, missense mutations or combinations of them, could also occur in the extracellular domain or in the intracellular one with a probability of 6 and 2%, respectively.

One third of the 20-25% of GISTs that do not present KIT mutations, have these kinds of alteration in the alpha platelet-derived growth factor receptor (PDGFRα) which determine the constitutive activation of the tyrosine kinase domain with a consequent promotion of cellular differentiation and proliferation and neo angiogenic activity. The discovery of some gain-of-function mutations involving KIT or PDGFRα has significantly changed the biological comprehension and the treatment of the pathology.

Other markers that might be positive in case of GIST are BCL-2 (80%), CD34 (70%), muscle specific actin (50%), smooth muscle actin (35%), s-100 (10%) and desmin (5%)[10]. These data are important to create targeted therapies against the genetic defect present in the tumor. One important example of the application of this strategy is the use of tyrosine kinase inhibitors (TKIs).

1.1.1 Pharmacological treatment

GIST has a very refractory behavior towards standard chemotherapy regimens and for this reason, for patients affected with this pathology, the only therapeutic chances before the introduction of the TKIs was surgery. Actually, only in the case of primary and resectable neoplasm, surgery remains the first therapeutic option[14]. In addition, after the resection of the primary tumor, this neoplasm displays high variability in a way that, even many years after the surgery, recurrences and local metastasis may occur making a long-term follow-up essential for patients. 50% of patients undergoing a potential curative surgery, develops recurrences and local metastasis[15].

Before the introduction of TKIs, the survival rate after 5 years from the complete resection ranged from 35 to 80% and the median survival was 10–20 months for patient with non resectable disease[16]. Imatinib significantly improved the treatment outcome as shown in a randomized phase II trial called B2222: after 5 years of therapy, survival was observed in 54% of patients with metastatic or inoperable GIST[17].

That being said, imatinib does not represent the only weapon against this pathology. Other drugs, such as sunitinib and regorafenib, belonging to the same drug class, play an important role for the patients' survival against GIST. In the following chapters, first-, second-, and third-line treatments are illustrated, particularly going into the details for imatinib and sunitinib, which are the drugs object of this thesis.

1.1.1.1 First-line treatment: imatinib

Imatinib mesylate (IMA) (figure 2) is the active ingredient of the oral anticancer drug Glivec® and Gleevec® (the trade names given in Europe and USA, respectively) and belongs to the TKIs family. This class of drugs acts specifically against a target which is only present in cancer cells, or however, which is more expressed in cancer cells than in normal ones. For this reason, it belongs to the so-called targeted therapies. In general, with this kind of approach, the target is a receptor present on the surface or inside the tumor cell. The drug, therefore, acts selectively on molecular mechanisms that are the basis of the development, growth and spread of the tumor.

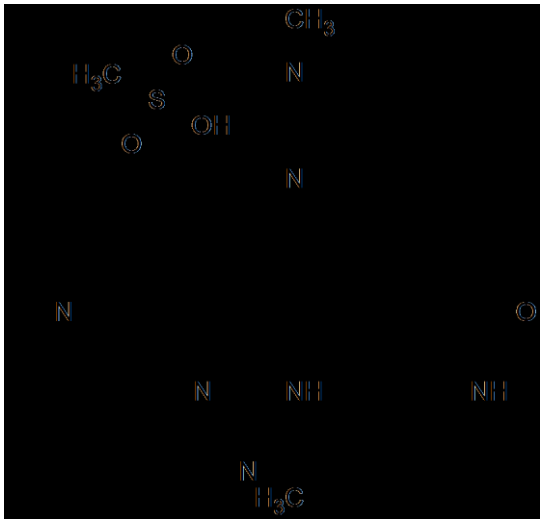

Figure 2. Structural formula of 4-[(4-Methyl-1-piperazinyl) methyl]-N-[4-methyl-3-[[4-(3-pyridinyl)-2-pyrimidinyl] amino]-phenyl] benzamide methane sulfonate, also known as imatinib mesylate.

More in detail, IMA inhibits in a selective and potent way the activity of different tyrosine kinases including Abl, KIT, PDGFRα, the beta platelet-derived growth factor receptor (PDGFRβ) and the receptor for the discoidin domain (DDR1)[10].

The promising results from the American-Finnish clinical trials CSTIB2222[18] and the European organization for research and treatment of cancer[19] convinced the Food and Drug Administration (FDA) in February 2002 and the European Medicines Agency (EMA) in May 2002 to approve IMA as the first treatment line for inoperable, metastatic or recurrent, KIT-positive GIST.

Furthermore, IMA was approved by the FDA in December 2008, and by the EMA in March 2009 for adjuvant treatment following surgical resection of GIST with a high risk of recurrence, due to the increase of the overall survival (OS) observed in patients during the trials[20]. The oral intake of 400 mg/day of IMA represents the actual standard therapy. For patients affected by GIST with exon 9-mutated KIT, the National Comprehensive Cancer Network (NCCN)[6] and the European Society of Medical Oncology (ESMO)[21] guidelines suggest a higher dose (800 mg/day) because it positively correlates with a longer progression-free survival (PFS)[22].

IMA produces a partial response in 45% of patients and a stabilization of the disease in 30%[2], while the complete response is rare. This is why it is described as an oncostatic agent rather than a cytotoxic[23].

Considering that stopping the treatment with IMA is accompanied by a progression of the disease[17], after a complete response or a macroscopic resection of the residual tumor, the therapy should be continued indefinitely and stopped only in the case of tumor progression or occurrence of intolerable side effects.

As most of TKIs do, IMA targets the binding site of adenosine triphosphate (ATP) on the tyrosine kinase proteins KIT, BCR-Abl (especially important in the treatment of both chronic and acute lymphoblastic leukemia), PDGFRα, PDGFRβ and DDR1[10].

The binding between the drug and this site prevents the hydrolysis of ATP (figure 3), thus inhibiting the tyrosine kinase phosphorylation activity and therefore, blocking the downstream signal of the proliferation and survival pathways inside the cell[24].

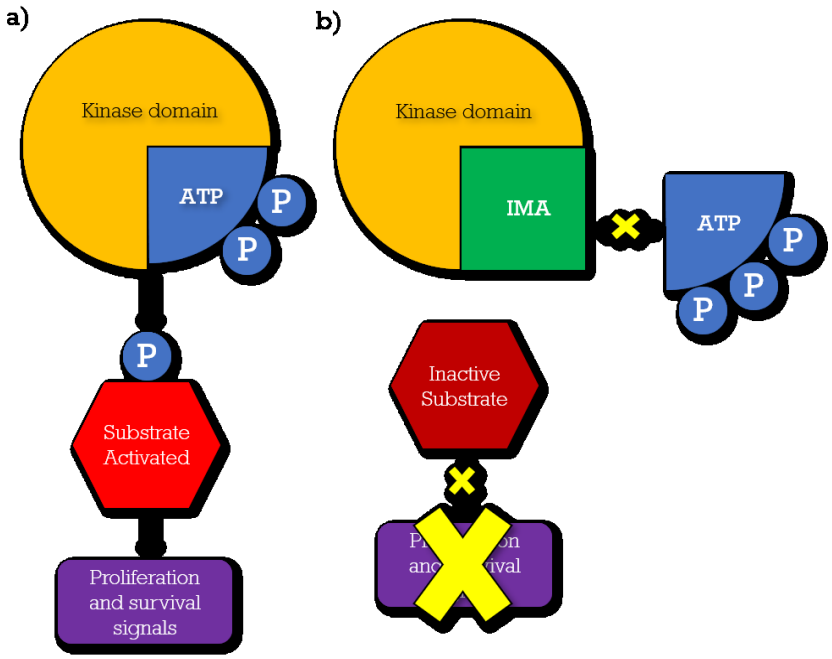

Figure 3. Comparison between the absence a) and the presence b) of IMA at the level of the kinase domain of a generic tyrosine kinase protein. In a), the phosphorilation ATP-mediated activates the substrate that leads to the diffusion of proliferation and survival signals. In b), by occupying the ATP binding pocket of the kinase domain, IMA leads to the block of the substrate activation with a consequent block of proliferation and survival stimuli.

The pharmacokinetic profile of IMA has been evaluated in healthy volunteers, in patients affected by chronic myeloid lukemia (CML), GIST and other neoplasms[25].

The absorption is rapid with a 98% bioavailability regardless of the food intake[26] and for this reason, to reduce the risk of gastrointestinal irritation, patients take IMA

orally during a meal with a large glass of water and the bioavailability is not compromised[27].

After the absorption, IMA undergoes extensive and rapid tissue distribution. A minimum percentage of the drug can penetrate through the blood-brain barrier, without however reaching sufficient concentrations to determine some pharmacological activity in the central nervous system[25]. Approximately 95% of the administered drug is bound to plasma proteins, mainly to albumin and alpha 1 acid glycoprotein[26].

Like most drugs, IMA is metabolized in the liver; mainly by the cytochrome P450 enzymatic system (CYP); in particular from isoforms 3A4 and 3A5 and to a lesser extent from 1A2, 2D6, 2C9, 2C19[25]. The main metabolite of imatinib is N-desmethyl imatinib (NOR IMA), also known as nor-imatinib or CGP74588. NOR IMA is an N-demethylated derivative of piperazine (figure 4), it has a biological activity similar to IMA and represents approximately 20-25% of the steady-state level of the original drug in patients with GIST[28].

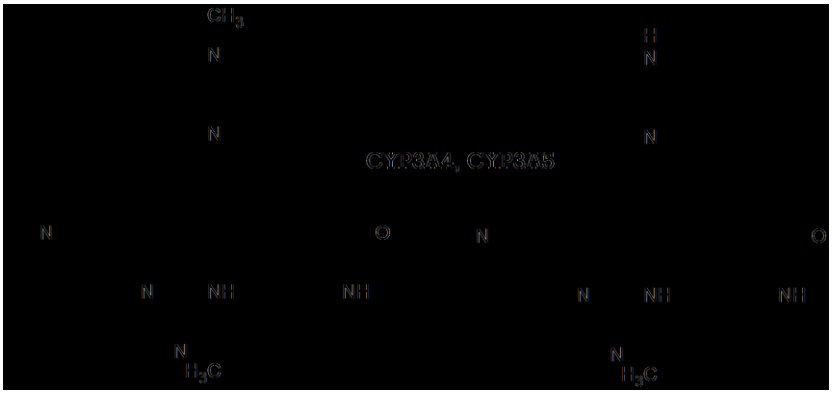

Figure 4. NOR IMA formation through N-demethylation reaction of IMA mediated by isoform 3A4 and 3A5 of cytochrome p450.

Being a substrate of CYP3A4, IMA may interfere with the metabolism of other drugs and natural substances co-administered as follows:

- strong inducers of CYP3A4 such as rifampicin, fluconazole and St John's Wort (ipericum perforatum) increase the metabolism of IMA, thus decreasing its plasma concentration[25].

- strong inhibitors of CYP3A4 such as erythromycin, ketoconazole and grapefruit juice, decrease the metabolism of IMA, thereby increasing its plasma concentration[25,29].

Co-administration of IMA with simvastatin significantly increases the exposure to the statin by 2-3 times[30]. Warfarin is a substrate of both CYP3A4 and CYP2C9 and due to the possible interaction between warfarin and IMA metabolism, patients requiring anticoagulants during treatment with IMA should opt for standard or low molecular weight heparin[27].

It is also necessary to pay attention to the co-administration of IMA with other CYP3A4 substrates with a narrow therapeutic window, such as fentanyl and cyclosporine[27].

Other factors that could reduce IMA metabolism are hepatic and renal impairment and hepatic metastases, while age, race, gender and body weight do not significantly affect its pharmacokinetics in the treatment of GIST[31].

IMA elimination occurs primarily via the fecal route and the half-life ($T_{1/2}$) of this drug and its active metabolite NOR IMA is approximately 18 and 40 h respectively[32].

This drug regimen is generally well tolerated and allows the patient to lead a normal life. Adverse reactions with a high incidence rate (above 10%) are gastrointestinal disorders (nausea, vomiting, diarrhea), abdominal pain, fatigue, myalgia, muscle cramps, rash and superficial edema, in particular periorbital and lower limb edemas[27]. The edemas are rarely severe and can usually be managed with diuretics, with other supportive measures or with a dose reduction. More important disorders, such as hepatic, renal or cardiac failure, hemorrhages and significant changes in hematological values, are rarely observed[27]. Hematological toxicities, such as anemia, neutropenia and leukopenia, have an incidence rate of less than 10%[27]. Furthermore, the continuing use of the drug allows many patients to develop tolerance of these side effects[33].

Although IMA treatment leads many GIST patients to have clinical benefits, four drug resistance mechanisms have been identified[34]:

1. a superimposition of a new KIT or PDGFRα mutation with increased phosphorylation of KIT or PDGFRα over the original one;

2. KIT genomic amplification with overexpression of KIT oncoprotein, without a new point mutation;

3. activation of an alternate receptor tyrosine-kinase protein coupled by loss of expression of KIT oncoprotein;

4. activation of KIT or PDGFRα outside the juxta-membrane region without a secondary genomic mutation.

All these mechanisms occur as secondary resistance to the drug, while the last listed can also occur as primary resistance.

Approximately 10% of patients treated with IMA experience tumor progression within 3-6 months of treatment due to the onset of primary resistance. In addition, a further 40-50% of them develop drug resistance within 2 years of treatment after partial response or disease stabilization. These patients are classified as having delayed or secondary resistance[31].

In the case of drug resistance occurrence or tumor progression, the oncologist can increase the dose of IMA from 400 to 800 mg/day based on two clinical trials (EORTC 62005[35] and SWOGS 0033[36]), which have shown how the dose escalation at the time of disease progression provides clinical benefit in one third of patients. If dose escalation leads to disease progression or drug intolerance, it will be necessary to proceed to the second-line treatment for this pathology which consists of the administration of another TKI: sunitinib.

1.1.1.2 Second-line treatment: sunitinib

Sunitinib malate (figure 5) (SUN), the active ingredient of the oral anticancer drug Sutent®, is able to inhibit multiple tyrosine kinase receptors, involved in tumor growth, tumor neo-angiogenesis and metastatic cancer progression.

This TKI was approved by the FDA for the treatment of both renal-cell carcinoma (RCC) and progressive pancreatic neuroendocrine tumor (PNET). Moreover, thanks to its ability to inhibit KIT protein, it showed enough efficacy to become the second-line therapy for GIST patients[37]. In fact, SUN was approved by the FDA in January 2006 and by EMA in June of the same year for the treatment of unresectable

and/or metastatic malignant GIST in adult patients after treatment failure (resistance or intolerance) with IMA[38].

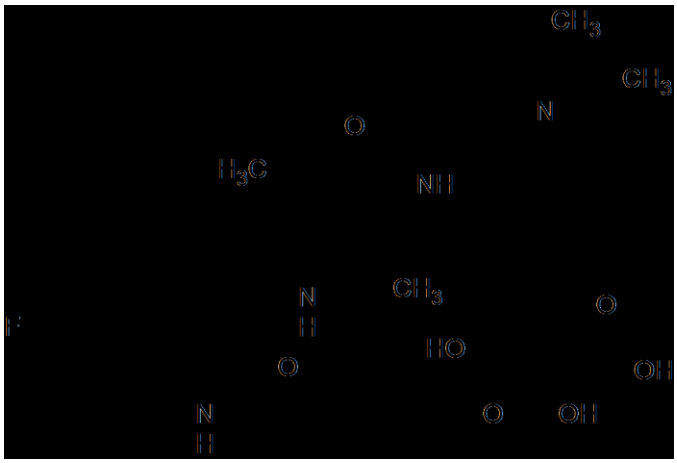

Figure 5. Structural formula of N-[2-(diethylamino) ethyl]-5-[(Z)-(5-fluoro-2-oxo-1,2-dihydro-3H-indol-3-ylidene)-methyl]-2,4-dimethyl-1H-pyrrole-3-carboxamide L-malate, also known as sunitinib malate.

The approved dose is 50 mg/day for 4 weeks, followed by 2 weeks off per 6 weeks (4+2 scheme), until disease progression or the onset of intolerable side effects. In 2006, George et al. demonstrated that also a continuous administration schedule could be used[39]: the administration of 37.5 mg/day of SUN without any treatment discontinuation, in fact, makes only few patients requiring treatment interruption or dose reduction[40].

The results from an international multicenter randomized double-blind placebo-controlled phase III trial, showed that median time to tumor progression (TTP) and PFS in patients with GIST, treated with 50 mg/day of SUN following the abovementioned 4+2 scheme, were 27.3 and 24.1 weeks, respectively, versus 6.4 and 6.0 weeks with placebo (hazard ratio (HR)=0.33, $p<0.0001$ and HR=0.33, $p<0.0001$, respectively)[41]. Moreover, phase I and II clinical trials have shown a response rate of 8-15%, with a further 39-58% of disease stabilization in patients treated with SUN with metastatic, IMA intolerant or resistant GIST[23].

From the pharmacodynamic point of view, there are numerous proteins that SUN is able to inhibit, including PDGFRα, PDGFRβ, VEGFR1, VEGFR2, VEGFR3 and KIT.

Regarding the KIT protein inhibition, both IMA and SUN belong to the class of type II protein kinase inhibitors, where:

- type I inhibitors occupy the ATP pocket of the active conformation of a kinase;
- type II inhibitors occupy the ATP pocket of an inactive conformation of a kinase;
- type III inhibitors are allosteric inhibitors so they do not occupy the ATP pocket[42].

The only difference between IMA and SUN, in this regard, falls into the interaction type: IMA occupies the gate area, the front and the back cleft of the protein while SUN is limited to the gate area and the front cleft. Compounds with the same type of interaction of IMA are named type IIA inhibitors and are characterized by longer residence times than type IIB inhibitors of which SUN is an example[37].

The pharmacokinetic profile of SUN has been evaluated both in healthy volunteers and in patients with solid tumors[43].
After an oral administration, SUN reaches a maximum concentration (C_{max}) after 6-12 h, which indicates a slow absorption from the gastrointestinal tract. The food intake does not show a significant effect on the exposure of the TKI[44], which might be influenced instead by variation in body mass index: patients with severe obesity have shown lower plasma levels than average[45].
With a large apparent volume of distribution (V_d/F) of 2'230 L, SUN undergoes tissue distribution and so does its active metabolite. In vitro experiments have shown that approximately 95 and 90% of the parent drug and its active metabolite respectively are bound to plasma proteins without any concentration dependence (in the range of 100-4'000 ng/mL)[41].
Its main active metabolite is called N-desethyl sunitinib (N-DES SUN) or SU12662 and it is generated through a metabolic N-de-ethylation reaction (figure 6) primarily mediated by the isoform CYP3A4, which is also responsible for the further inactivation reaction[41]. This metabolite significantly contributes to the pharmacological activity of SUN thanks to a combination of similar potency

exhibition and presence at high concentrations level (N-DES SUN comprises 23-47% of the total exposure at steady state, which is reached in 2 weeks)[46].

Being a substrate of CYP3A4 in the same way as IMA, it is important to avoid the contemporary administration of both SUN and other substances with the ability to induce or inhibit the CYP3A4 isoform. If this caution is not taken into account, SUN plasma levels will probably undergo alterations[41].

While in vitro studies have demonstrated that SUN is a substrate for the efflux transporter BCRP, the co-administration with gefitinib (a BCRP inhibitor) has not led to clinically relevant modifications on C_{max} and AUC of SUN or total drug (SUN+N-DES SUN)[47].

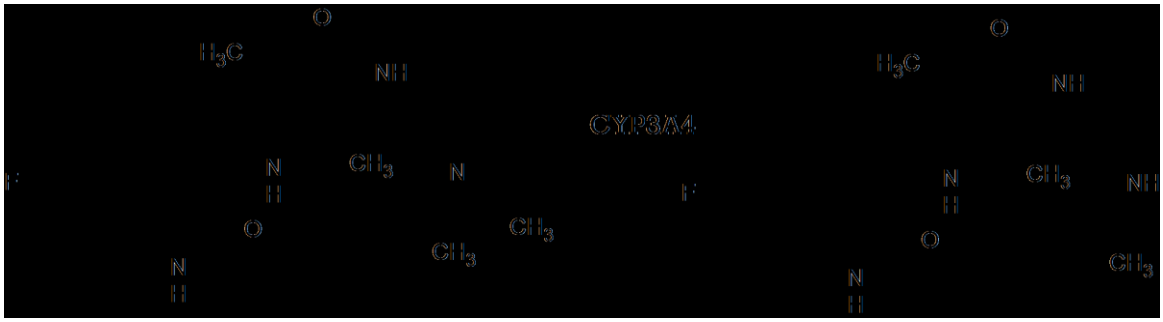

Figure 6. N-DES SUN formation through N-de-ethylation reaction of SUN mediated by the isoform 3A4 of cytochrome p450.

Age, race and gender do not significantly affect SUN pharmacokinetics, and, after a single dose of drug, no systemic exposure variations have been seen in patients with mild and moderate hepatic impairment compared with patients with normal hepatic function (studies of SUN in patients with severe hepatic impairment has not been conducted yet). Regarding patients with severe renal disfunctions, SUN apparent clearance (CL/F) was not affected by creatinine clearance (CrCl) within a range of 42-347 mL/min and the systemic exposure after a single dose of SUN was not different from patients with normal renal function. Only in end stage renal disease (ESRD), the total systemic exposures were lower for SUN and its main metabolite (47 and 31% respectively) in comparison with normal conditions[48].

The main route of excretion for the two compounds is via the feces (61% of the administered dose), while only the 16% undergoes renal elimination. SUN and N-

DES SUN, which present a long $T_{1/2}$ of 40-60 h and 80-110 h respectively, represent the major drug-related compounds identified in plasma, feces and urine[41].

This drug regimen is generally well tolerated and allows the patient to lead a normal life. During treatment of GIST with SUN, adverse reactions with a higher incidence rate (above 25%) are changes in hematological values (neutropenia is experienced by 1 patient in 2, followed in frequency by lymphopenia, thrombocytopenia and anemia), gastrointestinal disorders (diarrhea occurs in 40% of patients, followed by abdominal pain and nausea), fatigue, skin discoloration and anorexia. On a GIST randomized trial[41], 10% of SUN-treated patient experienced a decrease in left ventricular ejection fraction, and nearly a quarter of them needed a dose reduction or cardiac medications. Moreover, in the same trial, severe hypertension occurred in more than 10% of patients leading to the temporary suspension of the drug. Moving on grade 3 or 4 treatment-related adverse reaction, the most common are fatigue and hypertension (as previously mentioned)[43].

In case of disease progression with SUN, the next move involves the third-line drug called regorafenib.

1.1.1.3 Third-line treatment and other therapies

Regorafenib, the active ingredient of the drug Stivarga®, is an inhibitor of several tyrosine-kinase receptors, including kinases involved in tumor angiogenesis (VEGFR1, VEGFR2, VEGFR3), in oncogenesis (KIT, RET, RAF1, BRAF), in metastasis (VEGFR3, PDG FR, FGFR) and in tumor immunity (CSF1R)[49].

Following the results of the clinical study entitled *GIST-Regorafenib In Progressive Disease* (GRID), an international, multicenter, randomized, placebo-controlled phase III trial[50], FDA in February 2013 and EMA in August 2013 have approved regorafenib for the treatment of patients with locally advanced, unresectable or metastatic GIST previously treated with IMA and SUN.

It is an oral therapy, administered at a dose of 160 mg/day following cycles of 4 weeks with a 3+1 scheme (a week off after three weeks of treatment) until disease progression or occurrence of unacceptable toxicity. From the GRID clinical trial, it was possible to determine:

- a median PFS of 4.8 months in the arm treated with regorafenib compared to 0.9 months of the placebo arm (HR=0.27, p<0.0001);
- no statistically significant difference in the OS between the two treatment groups (HR=0.77, p=0.199), due to the possibility of crossing over between the two treatment arms;
- a disease control rate (defined as full or partial response rate plus disease stability for at least 12 weeks) of 52.6% for regorafenib and 9.1% for placebo (p<0.00001)[50].

The most common side effects are: palmar-plantar erythrodysesthesia, fatigue, hypertension, weight loss, alopecia, dysphonia, mucositis and diarrhea[51],[52].
Serious adverse events occur in less than 1% of patients and include severe bleeding, intestinal perforation, liver injury, high blood pressure and heart attack[51].
Very often, due to high toxicity, the oncologist see himself as constrained to reduce the dose of medication.
Alternative treatment options in case of failure of IMA, SUN and regorafenib are still in experimental phase. Any patient who has already been treated with all the three drugs and who needs further treatment should be taken into consideration for enrollment in a clinical study[53].
About 250 clinical trials involving the use of nearly sixty drugs, including other TKIs like sorafenib, nilotinib, dasatinib and pazopanib have been approved worldwide[54].
However, at the moment, the fourth approved treatment line is still missing.

An important parameter to consider for anticancer therapy is the compliance, as it has been shown that, for example, the discontinuity in treatment with IMA is associated with a loss of disease remission and a shorter TTP[26]. Oral anticancer therapies are becoming increasingly common in cancer clinical practice[26]. Although oral administration offers patients the convenience of taking the medicine independently at home, the evidence shows that adherence to oral therapy is far from optimal[55,56]. Factors such as the advanced age, the increasing time from diagnosis or duration of treatment, the lack of understanding of the relevance of the compliance to achieve and maintaining the response, the side effects drug related, a high number of co-medications and the poor physician/patient communication are

strongly associated with non-adherence to therapy[26]. For this reason, and for others which will be mentioned below, a frequent monitoring of drug exposure in patients might be a very useful practice to make anticancer therapy more effective thus gaining more possibility of success.

1.2 Therapeutic Drug Monitoring

Therapeutic Drug Monitoring (TDM) is a branch of clinical chemistry and clinical pharmacology, which aims to optimize the therapy by personalizing it through the determination and interpretation of drug concentration in biological fluids, such as plasma, serum, whole blood or urine[57]. In a more practical way, the data obtained are exploited to verify if the drug concentration is within a therapeutic window (figure 7).

Figure 7. Schematic representation of a therapeutic window. If the drug concentration falls below the lower limit, the efficacy of the treatment might be compromised, while severe toxicity might occur if the drug concentration exceeds the upper limit.

Since the beginning of the 60s, TDM has been used during the clinical treatment of patients with the aim of simultaneously maximizing the therapeutic effect and minimizing the occurrence of toxicity. Nowadays, this approach is widely applied in pharmacological treatments with antiepileptics, cardiovascular drugs, antibiotics, anti-inflammatory agents, antidepressants, airway smooth muscle relaxants, immunosuppressants and some chemotherapeutic drugs as 5-fluorouracil in the treatment of metastatic colorectal carcinoma (mCRC), carboplatin, 6-mercaptopurine in pediatric acute lymphoblastic leukemia (ALL) and Hodgkin's diseases.

1.2.1 The multidisciplinary approach of TDM

An appropriate administration of the drug, an adequate collection and processing of the biological sample, a precise and accurate measurement of the drug and/or of the metabolites and an appropriate interpretation of the results are the distinguishing factors of the correct execution of the TDM practice[58]. TDM is indeed a multidisciplinary approach comprising different professional figures such as the physician, the pharmacist, the nurse, the pharmaceutical chemist/technician and the pharmacokinetic scientist. The entire personnel must be conscious of the limitations and difficulties of the TDM: a criticality that occurs only in one among the steps, is enough to compromise the whole process.

The physician is the first professional figure involved, because, after having visited the patient, he decides the pharmacological therapy according to the diagnosis of the disease.

The pharmacist has the role to dispense the medicine to the patient and, in the case of intravenous administration, to realize the pharmaceutical preparation with the adequate dosage prescribed by the physician.

The nurse is responsible for the correct timing of drug administration, in the case of either an intravenous administration or an oral therapy carried out by an hospital patient. An adequate sampling of the biological fluid both in terms of quality (e.g. some plasma with traces of hemoglobin caused by hemolysis during sample handling is more challenging to be analyzed than clean plasma) and timing also represents a responsibility of the nurse. Correct timing is in fact one of the keys for a good TDM practice: to administrate the drug and to perform the sampling with the correct timing allows an optimal evaluation of the pharmacokinetic parameters. If the actual sampling time is very different from that established, and this is not reported, the pharmacokinetic parameters obtained are not reliable and this could compromise the clinical decisions of the physician regarding the optimal dosage that fits for the patient[59].

The protagonists of the following phase are the professional figures of the clinical chemist or the pharmaceutical technologist, who process the sample and analyse it to determine the concentration of the drug and/or any metabolites in the biological

fluid. Starting from the concentration value, the pharmacokinetic scientist or the pharmacist can extrapolate a pharmacokinetic parameter or contextualize the data thanks to guidelines present in literature. In both cases, the result of the interpretation of the concentration value could be extremely helpful for the physician to make changes in the dosage of the drug according to the clinical outcome, and other biochemical or clinical parameters[60].

The methods that can be used to quantify the analytes of interest must be accurate, precise, simple, rapid, sensitive, specific, not affected by matrix effects, and economically sustainable[61].

1.2.2 LC-MS/MS as a tool for TDM

The reference analytical method for the determination of drug concentration in human plasma samples is the high-performance liquid chromatography (HPLC) coupled with tandem mass spectrometry (MS/MS). In fact, an HPLC is an analytical technique which allows separating the components of a complex matrix (like whole blood, serum or plasma) with high precision and reproducibility, while a mass spectrometer, especially in tandem configuration, provides information regarding both the identity and the exact amount of the analytes[62] present in the biological sample. The HPLC-MS/MS methods can quantify different molecules simultaneously, starting from a small sample volume and ensuring the reliability of the results.

1.2.2.1 Principles of liquid chromatography

Chromatography is a process that allows to separate the compounds contained in a mixture based on their different physico-chemical characteristics such as mass, charge or polarity. The separation of the compounds, under the same conditions, is based on their different distribution between the two phases that compose the system: a fixed, called stationary phase (SP), and the eluent that flows through it, called mobile phase (MP). The analyte, depending on its affinity for each of the two abovementioned phases, tends to partition between them. This phenomenon is identified by the partition coefficient (K) which is compound-dependent and

represents the ratio between the concentration of the analyte in the SP (C_s) and in the MP (C_m).

$$K=C_s/C_m$$

The greater the K value for a certain compound, the higher its affinity for the SP will be. SP being equal, K values vary according to the compound to be eluted and the composition of the MP.

Working on the experimental conditions, a different migration of the compounds present in the mixture and so their separation will be obtained.

The different types of chromatography differ according to the support adopted as SP, to the nature of the MP, and above all, to the separation principle; chromatography can therefore be:

- adsorption chromatography: the separation of the compounds is based on the adsorption coefficient relative to the SP;
- partition chromatography: the separation of the compounds is based on the partition coefficient relative to a biphasic (aqueous/organic) system. If the SP is more polar than the MP it will be called normal phase (NP), while in the opposite situation it is called reverse phase (RP);
- ion exchange chromatography: the separation of the compounds is based on their charge and the ionic bond with the SP, which is an ion exchange resin;
- size exclusion chromatography: the separation of the compounds is based on molecular size. It is also called gel permeation chromatography;
- affinity chromatography: separation of the compounds is based on biochemical, reversible and very specific reactions.

For a RP separation, the technique adopted in the present thesis, derivatized matrices with apolar functional groups (bonded phases) are used. The SP is usually constituted by a matrix (composed, depending on the uses, by silica, polymer or a silica-polymer hybrid) which is derivatized with apolar chains of various length (e.g. octilsilyl, octadecilsilyl, phenyl, etc.). RP chromatography is indicated for the separation of lipophilic molecules, like most of drugs, because the prevailing retention mechanism is due to hydrophobic interactions. The selectivity is therefore

based on the differences in hydrophobicity between the different molecules to be separated.

During the chromatographic process, the lipophilic molecules carried by the MP, are retained on the SP that fills the chromatographic column and which presents similar characteristics. As the MP, constituted by an aqueous-organic mixture, continues to flow through the column, there will be the detachment of the various analytes retained by the SP according to their affinity for the MP.

There are many solvents that can be used as MP, and they differ on their eluting power which is strictly related on their own polarity. Two or more solvents can also be mixed to modulate the elution power of the resulting MP.

In LC, there might be two different types of elution regimes (figure 8):

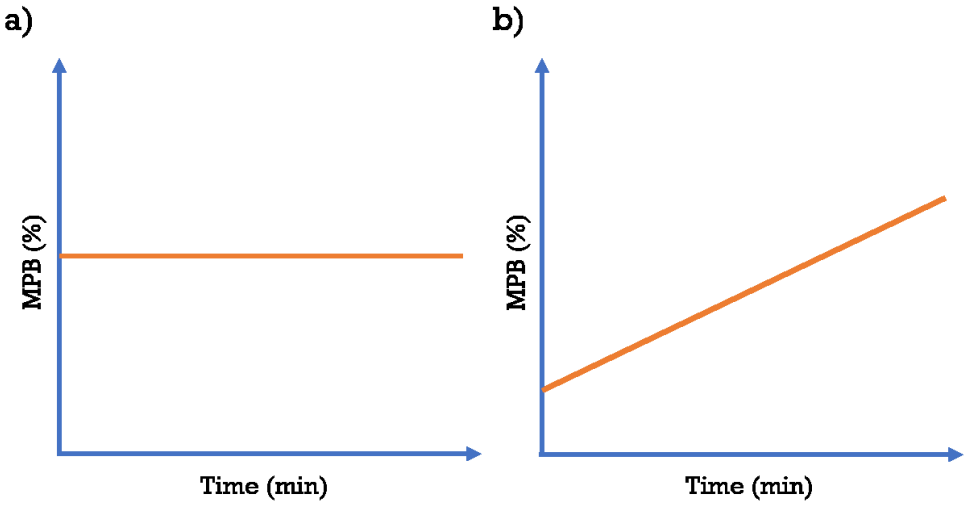

Figure 8. graphic representation of the two elution types: isocratic (a) and gradient (b).

- Gradient elution (figure 8b) consists in the use of a mix of two or more MPs, generally called A (e.g. aqueous phase, called "weak solvent" in RP chromatography) and B (e.g. organic phase, called "strong solvent" in RP chromatography), whose proportions in the mixture vary during the chromatographic run.
- The isocratic elution (figure 8a), on the other hand, consists in the separation by eluent with a fixed composition during the whole chromatographic run.

Generally, gradient elution allows faster separations than isocratic one, because the in-column environment changes very rapidly, allowing the analytes to quickly get into the condition for their detachment from the SP.

At the end of the chromatographic run, a graphic representation called chromatogram is obtained, which shows the detector response (Y-axis) during the chromatographic runtime (X-axis) (figure 9). The elution of a compound is represented by a peak originated by the increment of the detector response.

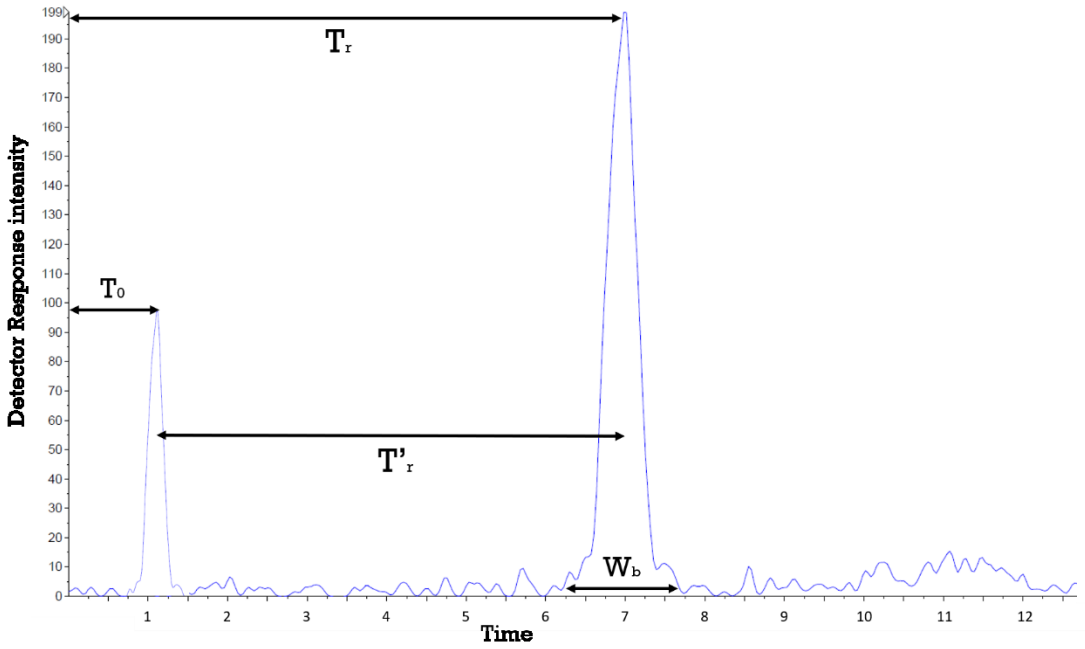

Figure 9. Example of a generic chromatogram. The first lower peak shows the elution of the mobile phase while the second peak describes the elution of the compound of interest. The retention time (T_r), the dead time (T_0) and the adjusted retention time (T'_r) are represented.

For quantitative analysis, the peak area is used as parameter instead of peak height because it is better directly proportioned to the amount of the detected analytes. The retention time (T_r), is the time that the compound of interest takes to be eluted by the MP, while the dead time (T_0) is the elution time of non-retained compound. T_0 also represents the migration rate of the MP molecules, so the adjusted retention time T'_r of an analyte, which represents a qualitative parameter, is the difference between its T_r and T_0. A good chromatographic separation is characterized by narrow, symmetrical and well separated peaks for each substance. In fact, the lower and broader the peak is, the lower the sensitivity of the measurement will be.

The fundamental variables of chromatography are:

- capacity factor (K'): it represents a means of measuring the retention of an analyte on the chromatographic column and it is equal to the ratio between T'_r and T_0.

$$K' = \frac{T'_r}{T_0}$$

The higher the K' value, the longer the time spent in the SP and the later the compound elutes from the column;

- selectivity (α): indicates the ability of the chromatographic system to distinguish between two species A and B. It is expressed by the ratio between the capacity factor of A (K'_A), and the capacity factor of B (K'_B).

$$\alpha = \frac{K'_A}{K'_B}$$

A and B result distinguished only with α value higher than 1. A high selectivity can only be achieved by using the optimal SP-MP combination for the analyte of interest;

- efficiency (N): it is a measure of the dispersion of the analyte band as it travels through the column and it depends on the number of theoretical plates (N) that are the segments in which the volume of the column can be ideally divided. Each plate represents a single equilibrium stage of distribution of the sample between the MP and the SP. The higher the N, the greater the number of exchanges between the two phases, the better the quality of the separation. N value (and therefore efficiency) can be increased by using longer columns, with the collateral effect, however, of increasing the whole run time. Another approach consists in selecting columns filled with smaller sized particle, in order to decrease the plate height (H) and therefore, column length (L) being equal, to increase N.

  The relationship between N, H and L is the following:

$$H = \frac{L}{N}$$

N is instead expressed by the following equation where W_b is the width at the peak base:

$$N=16\left(\frac{T'_r}{W_b}\right)^2$$

- resolution (R): it is the capacity of the system to separate two chromatographic peaks and it relates the abovementioned three variables as shown in the following formula:

$$R=\frac{\sqrt{N}}{4}\left(\frac{\alpha-1}{\alpha}\right)\left(\frac{K'}{1+K'}\right)$$

in fact, R indicates the goodness of the separation between two peaks. It is defined by evaluating the retention times of two different substances eluted in two consecutive peaks. Resolution is good enough when two consecutive peaks are represented as distinct without overlapping themselves. Given two compounds A and B, R is also calculated from the ratio between the distance between the two peaks and the mean value of the peak widths at base:

$$R=2\frac{T_{rB}-T_{rA}}{W_{bA}+W_{bB}}$$

While most of the time HPLC is coupled with UV detectors, the coupling with mass spectrometry (typically a triple quadrupole), for quantitative analysis of compounds in complex matrices (e.g. plasma, whole blood), allows reaching the best selectivity and sensitivity.

1.2.2.2 Principles of tandem mass spectrometry

Mass spectrometry (MS) is a technique that allows the detection of substances based on the ratio between the molecular mass and the charge (*m/z*), with an accuracy that might reach 0.01%. Each spectrometer consists of some essential components which are summarized in figure 10. However, some of the conditions and characteristics described in this thesis are specific of SCIEX spectrometers,

because are the instruments adopted for the method development object of this PhD project.

After the sample introduction, the first step in MS is the ionization of the neutral compound of interest mainly through electron ejection, electron capture, protonation, deprotonation, adduct formation. This process takes place into the source and it is fundamental because the spectrometer can detect only the charged molecules. A variety of ionization techniques are used for MS and are characterized by the internal energy transferred during the ionization process along with the physico-chemical properties of the analyte that can be ionized. In fact, some ionization techniques are very energetic and cause extensive fragmentation. An example of these so called "hard" sources is the electron ionization (EI) source. Other techniques are softer and only produce ions of the molecular species (soft sources), such as chemical ionization (CI), and atmospheric pressure (AP) ionization sources like APCI and electrospray. Matrix-assisted laser desorption ionization (MALDI) source also belongs to the "soft" sources category and it is applied for the production of intact gas-phase ions from a broad range of large, non-volatile and thermally labile compounds such as proteins, oligonucleotides, and synthetic polymers.

One of the most commonly used ionization techniques for a sample coming from a RP separation on a HPLC apparatus is the electrospray ionization (ESI). Since ESI is actually the source used in the HPLC-MS/MS methods reported in this thesis, a detailed description of its operating principles is reported below.

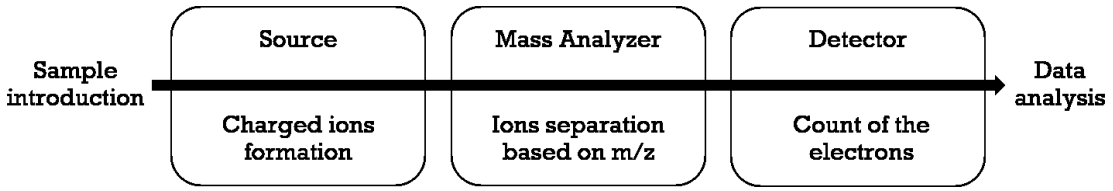

Figure 10. Schematic representation of a mass spectrometer components.

To be analyzed in an ESI source (figure 11), the compound is previously dissolved in a volatile MP added with a small amount (0.1–0.5% V/V) of acid or a weak base, which will help to add a charge to the compound during the ionization process. The MP is let to flow into a stainless-steel capillary called probe. A voltage (2-5 kV)

between the probe and its counter-electrode is applied and, in these conditions, just outside the capillary, a nebulized solution cone (also called Taylor's cone) appears. Its formation is due to the presence of charged species within the solution subjected to the electrostatic field existing between the capillary and the counter-electrode. At the end of the cone, the formation of the charged droplets is observed, in the same way as their migration towards the counter-electrode[63]. The formation of the droplets is strongly influenced by the physical/chemical characteristics of the solvent, by the amount of the ions of the analytes, by the concentrations of inorganic salts and by the applied voltage. The charged droplets, after their formation, have their size lowered due to the solvent evaporation, but they still retain their total charge value.

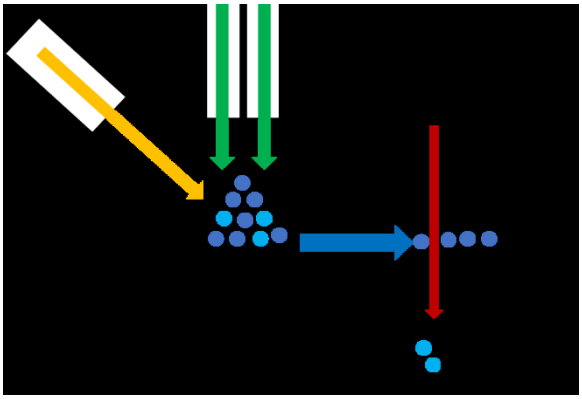

Figure 11. Schematic representation of the an ESI source working in positive mode. Green and yellow arrows represent the nebulizer and the heather gas respectively. The nebulizer gas flow through the probe which is the cathode, while the anode is placed at the entrance of the analyser. The blue arrow indicates the entry of ionized particles (blue rounds) while the neutral ones (light blue rounds) are physically removed by the curtain gas (red arrow) which flows between the curtain plate (the outer one) and the orifice one (the inner one). All the solvent and analyte particles that do not enter the instrument are conveyed towards the waste collection (exhaust).

The energy required for the evaporation of the solvent is provided both by the environmental thermal energy, obtained using a heated capillary and by the collisions with a flow of gas (the nebulizer gas, that flows longitudinally along the capillary perimeter, and the heather gas coming from the sides). As the droplet size decreases, the surface charge density rises higher and higher until the droplet radius reaches the stability limits of Rayleigh, meaning that the electrostatic repulsion equals the surface tension. Overcome that limit, the charged droplets are unstable and decompose through the process called "Coulombic explosion"[64] thus

producing microscopic droplets which, at the end of the process, release desolvated ions.

From the source, the produced ions are transferred to the analyser, where they are discriminated according to their *m/z* values, under high vacuum conditions (10-5 Torr), to prevent impact with atmospheric gas molecules that would lead to a loss of ionization yield. At the entrance of the mass analyser, two conical, center-pierced, steel plates are positioned (orifice plate and curtain plate). In the crawl space, a sheet of gas (curtain gas), usually nitrogen, is let to flow under pressure to prevent the entrance of neutral contaminants.

Several types of mass analysers have been developed since the separation of ions, according to their mass-to-charge ratio, can be based on different principles. For instance, the Time-of-flight (TOF) analyser separates ions, after their initial acceleration by an electric field, according to their velocities when they drift in a free-field region that is called a flight tube. Instead, the quadrupole analyser is a device which uses the stability of the trajectories in oscillating electric fields to separate ions according to their *m/z* ratios. The ion trap analyser works by using a radiofrequency (RF) quadrupolar field that traps ions in two or three dimensions: ions of different masses are present together inside the trap and are expelled according to their masses to obtain the spectrum. Whereas, the analyser based on magnetic sectors selects the ions according to their momentum, given a specific value of magnetic field and a circular trajectory. Also, some mass spectrometers combine several types of analysers.

Among these types of analysers, coupled to an ESI-type source to perform tandem-in space MS analysis for quantitative purposes, a triple quadruple can generally be found.

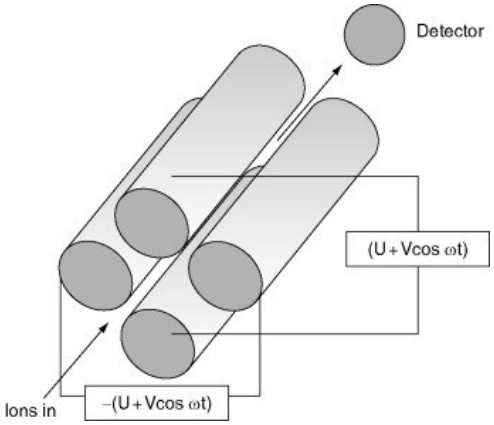

Figure 12. Schematic diagram of a quadrupole. For each couple of rods are showed the connections with both the direct current (U) and the radio-frequency ($V_0 \cos \omega t$) power supplies[65].

This type of analyser consists in a system of three quadrupoles in series: the first and the third ones are filters able to discriminate ions with a specific *m/z* value, while the second one is a collision cell where a controlled fragmentation takes place.

A quadrupole is composed by four parallel metal rods and each opposite rod pair is connected electrically (figure 12[65]). A two components (RF and direct-current (DC)) voltage is applied between adjacent rods: a wide range of *m/z* ions will pass through the quadrupole if only the RF component is applied, allowing to focus the ions.

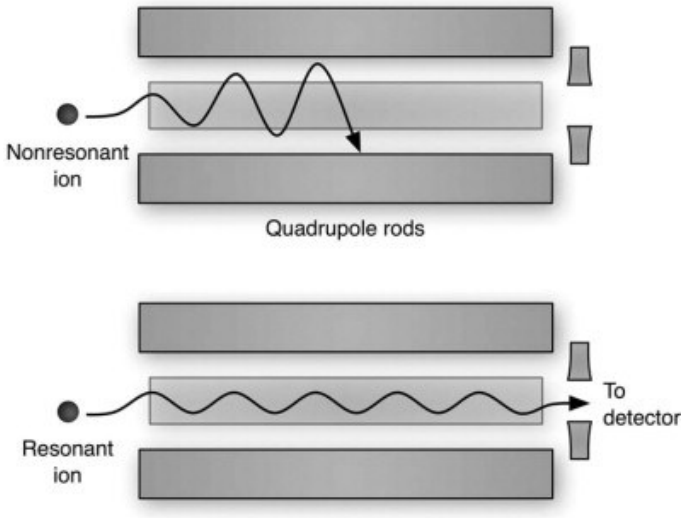

Figure 13. Representation of the functioning principle of a quadrupole mass analyser. The ion whose *m/z* does not lead to a resonance undergoes a collision against one of the four rods thus not being revealed. The resonant ion, instead, will be able to pass through the quadrupole and be recorded by the detector[65].

To select a group of ions with a specific *m/z* value, a DC voltage is added to the RF voltage. In this way, the "wrong" ions (with a higher or lower *m/z* values) will be lost by colliding against the rods due to unstable trajectories, while the "correct" ones are allowed to pass the quadrupole (figure 13[65]). To acquire a mass spectrum, it is necessary to increase both the DC and RF voltages, while keeping their ratio constant, in a way that a certain mass range could be scanned to transmit ions of increasing *m/z.*

Depending on the analysis purpose, the first (Q1) and the third (Q3) quadrupole can be used in different modes to acquire the data. In tandem mass spectrometry (MS/MS or MS^2), the configuration of the instrument allows the controlled fragmentation (also called collision-induced dissociation or CID) of the analyte in the collision cell, represented by the second quadrupole (Q2). Before Q1 there is the Q0, which is a smaller quadrupole equipped only with RF and not with DC, characterized by an ion focusing function.

Through the MS/MS it is therefore possible to obtain information both on the mass of the analyte of interest (parent or precursor ion) and on that of the fragments (product ions) generated by its fragmentation by applying an appropriate collision energy to the cell. Generally, the *m/z* value of an analyte could be considered an information about its identity, but, especially in the case of low-resolution MS, the highest specificity is obtained by considering also the analysis of its fragmentation pattern. Indeed, for each substance, its fragmentation pattern is a sort of proper fingerprint.

The most common scanning mode for quantitative analysis is called selected reaction monitoring (SRM). The application of this scanning mode to more than one fragment ion is called Multiple Reaction Monitoring (MRM) and the mechanism is the following: Q1 act as the first filter that selects the precursor ion of the analyte, which enters the Q2 where the presence of inert gas (Argon or Nitrogen) triggers the CID causing the precursor ion fragmentation and the creation of product ions. The product ions exit from the Q2 and pass through the Q3 which act as the second filter that selects the product ions and sent them to the detector (figure 14). In this way, a spectrum representing the fragmentation products of the selected ion is

obtained. Thanks to the high specificity of this scanning mode, a high signal-to-noise ratio (S/N) can be obtained during the analysis, allowing also a great sensitivity.

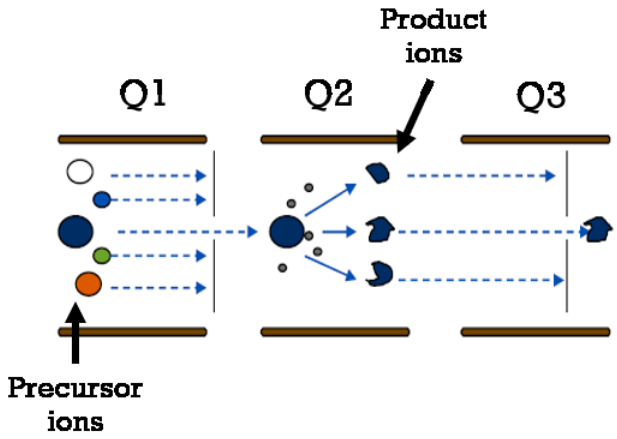

Figure 14. Schematic representation of the ion pathway during the select reaction monitoring mode.

Coupling MS/MS with LC has indeed led to significant improvements making possible to analyse samples with very different concentration ranges. In particular, the increase in sensitivity and specificity given by SRM mode has led to two important advantages:

- the possibility of detecting drugs and metabolites at very low concentration values and, consequently, the possibility of using very small sample volumes;
- the possibility of detecting the analytes of interest in the presence of a complex biological matrix such as tissues or whole blood.

To be used for the quantification of one or more substances in biological samples an LC-MS/MS method needs to be validated according to the FDA[66] or EMA[67] guidelines for the validation of a bioanalytical method.

1.2.2.3 Validation of an LC-MS/MS method

The validation of a bioanalytical method includes all the procedures to demonstrate in a documented way that the method under examination, used for the quantitative determination of the analyte in a given biological matrix (e.g. plasma, urine, blood) is reliable, reproducible and fits for its purpose[66]. In fact, analytical determinations, regardless of the instrument used, must be based on established principles and the operators must use a common and controlled scheme of practices to demonstrate

that the assays provide reliable data. The need to establish the main guidelines for the validation of an analytical method, and to spread them among the pharmaceutical community, emerged in 1990 from the first American Association of Pharmaceutical Scientists (AAPS)/FDA bioanalytical workshop[68].

These validation principles, derived from a team-work between researcher in the bioanalytical field and regulatory bodies, were introduced into the health regulations in Canada in 1992[68] and, subsequently, the FDA published the first edition of its Guidance on Bioanalytical Method Validation in May 2001[68]. This guidance explains the required workflow for the validation of analytical procedures such as gas chromatography (GC), LC, GC-MS, LC-MS, ligand binding assays (LBA), immunological assays and microbiological procedures. Since the publication of the first FDA guidance, the dialog significantly grew throughout scientific conferences not only in the US, but worldwide too. In 2011, EMEA introduced the Guidance on Bioanalytical Method Validation in Europe[67]. Subsequently, in September 2013, the FDA issued a revised draft of the Guidance for Industry Bioanalytical Method Validation that includes a series of changes, the most important of which is the introduction of a further measure of assay reproducibility through the reanalysis of the assayed samples (Incurred Sample Reanalysis or ISR)[69]. Finally, a definitive version of the FDA guidelines was released in May 2018[66].

The validation of selective and sensitive analytical methods for the quantitative assessment of drugs and their metabolites is essential to successfully conduct clinical and non-clinical pharmacological studies. In fact, the quantitative determination of drugs, metabolites and biomarkers provides essential information for assessing the safety and efficacy of drugs. Many clinical studies related to the study phases of the drug frequently have as primary or secondary purpose the determination of plasma concentrations of drugs and/or biomarkers. Consequently, the reliability and quality of such data are the basis of the result of the study[66,70]. For this reason, for the method to be validated, a detailed procedure must be available in which the instrumental conditions, the materials and the reagents to be used, the preparation of standards and samples are clearly defined; moreover, several preliminary tests must be carried out to set up the bioanalytical method sufficient to solve all the critical factors.

Validation can be:

- complete: all the validation parameters are determined because the method is new or literature but not yet validated, or the analysis of other metabolites is added to an already validated method;
- partial: if minor modifications are made to an already validated method (for example: transfer to another laboratory, change of instruments, change of range, limited sample volume, different matrix, change of anticoagulant, modification of sample processing, modification of storage conditions);
- cross-validation: comparison of validation parameters of 2 or more bioanalytical methods used in the same study or comparison of data obtained from different laboratories using the same method.

For the development of the method for the quantitative determination of drugs and metabolites in biological matrices (such as blood, serum, plasma, urine and different tissues) the specific characteristics of the sample (such as expected concentrations) are considered. To guarantee the robustness of the analytical data it is necessary to use a robust method and for this reason the analytical method is validated. In fact, fundamental parameters for the validation of an LC-MS / MS analytical method are: recovery of the analyte from the matrix, linearity of the calibration curve, precision and accuracy intra- and inter-day, reproducibility, sensitivity, lower limit of quantification (LLoQ), selectivity, matrix effect and stability of the analyte in samples and solutions.

The analytical method object of this thesis was developed from scratch, therefore, in accordance with the guidelines of the EMA[67] and FDA[66], a complete validation was performed.

Considering the whole workflow behind the setup of an analytical method and assuming that drug dosage is just a cog in the machine of TDM, it is clear how many are the difficulties and the costs for this kind of practice.

For this reason, it is easy to understand that TDM cannot be performed for every class of drugs: only if some criteria are satisfied, the coordination of the entire personnel for the monitoring of a drug will be taken into consideration.

1.2.3 TDM in the context of anticancer therapy

Actually, dose administration of anticancer drugs is generally based on patient's parameters like body surface area (mg/m^2) or body weight (mg/kg). This dose calculation method is rather unprecise because patients with the same dimensional parameters and taking the same dosage of the same drug might experience different grades of efficacy or toxicity. This marked inter-individual variation on therapeutic response is a distinctive feature of anticancer drug and constitutes one of the criteria that makes TDM recommended for this type of drug. Anticancer drugs are considered good candidates for the TDM practice also for their low therapeutic index, that means that the minimum dose which cause therapeutic response is very close to the toxic one[71]. However, while for drugs like the aminoglycosides, phenytoin and digoxin TDM is largely applied, in the case of the anticancer drugs, despite the high risk of toxicity and therapeutic failure, the dosage of the drug in plasma (or whole blood) to tailor the therapeutic intervention is not common practice. One of the most famous exception is methotrexate, a chemotherapy and immunosuppressant agent whose concentration is commonly measured in human serum by laboratories of pharmacology and clinical toxicology. This because the data obtained is useful to decide if the administration of folic acid as counter poison is a good choice in the case of too prolonged permanence of the drug in blood during a high-dose regimen[72].

Clinical usefulness of TDM in the context of anticancer drugs is actually limited by several factors[73]. First, for most of anticancer drugs the knowledge of pharmacokinetic and pharmacodynamic aspects is not thorough. For this reason, the most evident limiting factor is the difficulty to establish a clear relationship between the concentration value obtained and the therapeutic effect; without these relationships, the TDM approach becomes a random approach. The abovementioned difficulty is unavoidable, since in oncology practice, therapeutic and toxic effects need a long-term evaluation (the gap between the drug dosage and the evidence of the pharmacologic effect is wide). In addition to that, cancer is often treated with more than one drug thus making even more challenging to target the therapeutic and toxic effect at the pharmacodynamic level[74]. If the dose-

response relationship is missing, a therapeutic window, which is the essential element for TDM, cannot be defined. Not to mention that, due to the ample heterogeneity of cancers (identical tumors do not exist: they show different sensitivity and resistance towards anticancer drugs[75]), every case must be analyzed from scratch.

Despite the abovementioned problems, the high potential of TDM (if correctly applied) in the context of chemotherapy is evident because the anticancer drugs generally meet two important criteria: they show both a very low therapeutic index and a large pharmacokinetic inter-individual variability[76,77]. Secondly, anticancer therapy must be characterised by the maximum effectiveness to be useful: undertreatments, which could further compromise the low probability of recovery, are critical in the same way as the cytotoxic adverse reactions, that are typical of most anticancer drugs and could be very dangerous for patient's life. Many studies showed the benefits of a high intensity treatment[73], suggesting that treating patients with dosages which lead to drug concentrations very close to the upper limit of the therapeutic window may represent a winning strategy. Therefore, if a concentration threshold for unacceptable toxic effect was defined for each anticancer drug, TDM would be exploited to subjecting the patients to a high intensity treatment while minimizing the risks. Other consequent benefits of this strategy would include the increment of the compliance (due to the low occurrence of toxicity), the reduction of the pharmacokinetic inter-individual variability, the possibility of correctly adjusting the dosage in patient with hepatic and/or renal impairment[75] and the accessibility of useful data to better detect the drug-drug interactions[58].

In the last years, cancer treatment care has moved from the use of cytotoxic drugs and unspecific chemotherapy to oral molecular-targeted treatments (e.g. TKIs). These new therapies are very specific and usually they are directed against key cellular components (e.g. several types of kinases) implicated in cancer process. This new paradigm in cancer care involves a revolution in patients management, since therapies are administrated orally and for extended periods of times, transforming, in some cases, previously deadly diseases into chronically manageable conditions. For many targeted therapies exposure-response and

exposure-toxicity relationships have been described[76]. Nonetheless, these new drugs are usually administered at fixed dose, although plasma concentration levels show a wide inter-patients variability[76]. This variability depends on several factors. Oral administration improves patient's quality of life but also introduces an adsorption step in the pharmacokinetics that may affect the final plasma drug concentration achieved. Moreover, the possible simultaneous presence of other drugs or genetic and environmental factors affecting distribution, metabolism and excretion may be responsible of the wide variation in drug plasma concentration observed, leading to an under- or over-dosing of drug in some patients. Finally, also adherence to therapy is becoming a critical issue to ensure a correct drug exposure.

Considering that TDM practice reaches is full potential in the case of drugs having a narrow therapeutic window, a considerable inter-individual pharmacokinetic variability, a daily and continuous employment for a long time and a well-known relationship between a pharmacokinetic parameter and pharmacological effects[77–79], it is clear that anticancer targeted therapy appears as an excellent candidate.

In the era of personalized medicine, the TDM approach might indeed contribute to the increase in the probability of efficacy and duration of the therapeutic response and to the minimization of the risk of serious adverse reactions in patients receiving these new targeted antineoplastic therapies[80].

Only recently TDM has been recognized as having potential clinical relevance in treatment with some TKI. In fact, the ESMO suggests that measurement of IMA plasma concentrations could be important in all patients and is recommended especially in cases of suboptimal response, therapy failure, toxicity due to overdose or adverse events[81]. Furthermore, several clinical trials demonstrate the safety and feasibility of TDM of TKIs, including sunitinib[82].

1.2.3.1 TDM applicability for imatinib

TDM could be an useful tool for the treatment with IMA because among GIST patients there is a large inter-individual variability of drug concentration in plasma (coefficient of variation 40-50%)[83]. In fact, data from a study conducted on patients with metastatic GIST showed that IMA plasma levels ranged from 256 to 4'582

ng/mL[26]. Several factors are responsible for these differences in concentration, such as the intrinsic variability of cytochrome enzyme activity, the presence of drug transporters, such as the P-glycoprotein, protein binding and drug-drug interactions. Therefore, due to this high variability, the dose has not a predictive value for plasma drug levels[84] and this has clear consequences on the response to treatment which, in the case of treatment with IMA, is strongly correlated with the trough level (C_{min}). The C_{min} is defined as the steady-state concentration before the subsequent administration of the drug. It has been reported that, since a month from the beginning of the therapy, patients with a C_{min} less than 1'110 ng/mL (value of the first quartile of concentration values) show a shorter TTP than patients in the other quartiles[83]. However, no consensus was reached for the definition of a precise minimum concentration threshold (defined by the C_{min}) related to the effectiveness of the treatment because for example Eecheoute et al. showed, in a recent study[85], that the C_{min} of IMA decreased by about 30% in the first three months of treatment. Since this finding, it is clear that the one-month value, initially proposed by the Demetri group, should not be used throughout the entire follow up. An increase in drug clearance, which subsequently reaches a plateau, seems to be the responsible factor for this decrease in the C_{min} and this hypothesis is supported by a study[86] conducted by analysing C_{min} more than three months after the beginning of the treatment. In this study, a longer PFS was associated with C_{min} values higher than 760 ng/mL, suggesting the need to repeatedly evaluate IMA plasma concentrations during the treatment period. The decrease in C_{min}, after three months from the beginning of the treatment, also provides an explanation about the increase in drug tolerance over time, and underlines how in some patients this decrease may cause the failure to achieve effective drug concentrations[87].

Furthermore, for GIST patients, surgery further complicates the panorama: it has been described that patients undergoing partial or total gastrectomy show a significant decrease in IMA C_{min}[88].

These studies underline the role of the repeated monitoring of IMA during therapy as a useful tool for managing and optimizing the treatment for each patient. Furthermore, it is also essential to define unequivocally, in GIST patients, the C_{min} threshold that can be used as a reference for TDM in clinical practice.

To improve the knowledge on the potential role of plasma concentration monitoring of IMA during therapy, a study has been launched at the National Cancer Institute of Aviano (PN): "Pilot study to evaluate the feasibility of an innovative approach to monitor patients with gastrointestinal stromal tumor treated with imatinib" (N.EudraCT: 2017-002437-36, Code: CRO-2017-19), of which this thesis reports part of the project. In this protocol, the C_{min} is evaluated at regular time intervals: the patient's plasma concentrations are monitored by collecting a blood sample every 3 months for the first two years of therapy from their enlistment and, thereafter, every time the patient plans a medical examination with the oncologist (approximately every 4-6 months). On the day of the withdrawal blood is collected just before the next dose is administered to determine C_{min}.

The whole process is obviously useless if C_{min} values are unreliable. For this reason, it is necessary to adopt the most accurate and robust analytical technique for the quantitative analysis of small molecules in biological samples. Therefore, one of the aims of this thesis is to actively contribute from the analytical point of view by developing a robust LC-MS/MS analytical method for the quantification of IMA and its main metabolite, NOR IMA, in human plasma.

1.2.3.2 The case of sunitinib and its analytical issue

For SUN, TDM approach has been suggested as potentially useful due to its low therapeutic index, the existence of a positive exposure-efficacy/toxicity relationship and of a large interindividual variability in systemic exposure (± 30%) [76,89,90]. Since its main metabolite N-DES SUN shows similar biochemical activity and potency while reaching similar plasma levels[38], to calculate the target plasma concentration for TDM analysis, the sum of the plasma concentrations of both the analytes has to be considered. More precisely, the total trough plasma concentration (total C_{min}) of SUN plus N-DES SUN has been chosen as TDM target and from pharmacokinetic/pharmacodynamic studies, it was defined in the range of 50–100 ng/mL[46,91]. Further studies have indicated that, in a small cohort of patient with advanced solid malignancies and following a pharmacological regime of 50 mg of SUN once daily with the 4+2 scheme, total trough level higher than 50 ng/mL have been associated with an objective response[46]. Taking into account both the dose

proportionality of plasma exposure at therapeutic doses and the demonstrated efficacy of SUN 37,5 mg continuously daily, a minimal total C_{min} of 37,5 ng/mL has been recommended for GIST patients[57]. Furthermore, dose limiting toxicities have been reported especially when total C_{min} were higher than 90 ng/mL[46,92]. Thus, a robust and adequately ranged assay for the simultaneous quantification of SUN and N-DES SUN is necessary to be applied in clinical routine.

From an analytical point of view, the most challenging peculiarities of SUN which create an obstacle for the development of a clinically suitable quantification method is represented by its photo-isomerization in solution (figure 14). In fact, both SUN and its main active metabolite, N-DES SUN, are 5-fluoro-2-oxindoles linked to a dimethyl pyrrole carboxamide by an exocyclic double bond. Thanks to the presence of an intramolecular hydrogen bond (HB) between the C2 carbonyl group of the oxindole and the N-H group of the pyrrole ring, the Z-isomer is the most thermodynamically stable[93,94]. The E-isomer instead is characterised by a less stable non-planar conformation due to the steric hindrance between the substituted-benzene and pyrrole rings[94].

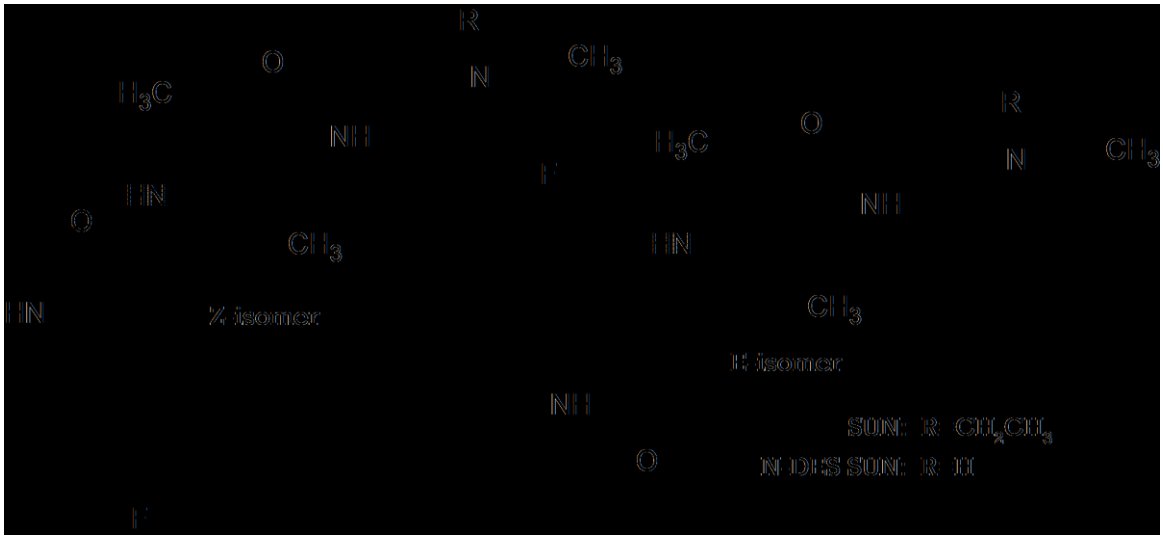

Figure 14. Representation of the two geometric isomers of both SUN and N-DES SUN. For the Z-form is evidenced the portion involved in the intramolecular HB, which does not occur in the E-form due to the steric hindrance between the substituted -benzene and the pyrrole rings.

Under light conditions, this phenomenon only occurs ex vivo in plasma samples and other solutions: for this reason, particular precautions are necessary during

collection, handling, and analysis of biological samples containing SUN and N-DES SUN. Studies of Z- to E-SUN photo transformation in solvent were performed firstly by Maafy and Lee[94] who proposed, as a result, a model named Φ-order kinetics to well described the phenomenon, later verified by the group of Padervand[95]. Other authors in the following years conducted studies regarding Z- to E-SUN conversion though focusing their attention on Z-SUN stability conditions in organic solvents. Different light exposure conditions were tested both in terms of intensity and light sources concluding that Z-SUN is more stable with minimal light intensity (6-7 lx) and using sodium light instead of ambient or UV light[96,97]. Moreover, from these studies, the maximum percentage of Z-isomer converted in E-isomer found by ranged from 30 to 40%, while the time to obtain the total transformation ranged from 6 to 30 minutes[96,97].

On the basis of these results, many published methods overcame the isomerization problem by conducting the blood sampling and the whole handling procedures under light protection in order to avoid the formation of E-isomer[93,97–101]. Surely, in the perspective of an analytical assay applicable to the TDM practice, a manipulation of the sample conducted quickly and with minimal light exposure does not represent a suitable option. In addition to that, there have been some cases where E-SUN has been detected despite light protection was applied during sample handling[97,101,102] and some other situations where the researchers have obtained different proportions of E- and Z-isomers in samples over time[103], since the E-isomer is not stable too and might revert back to the Z-one when the light-exposed solution is placed into the autosampler (in the dark).

The ample heterogeneity in results related to the photodegradation of Z- to E-SUN reported in literature suggests that this phenomenon might be influenced not only by light exposition: other factors such as solvent, pH and concentration might contribute too[95].

Some authors addressed the isomerism issue quantifying the sum of the single reaction monitoring responses of both separated isomers [103–107] thus avoiding the obligation of the light protection conditions during sample handling. However due to the split of the chromatographic peak (see figure 15), they were not able to obtain

an LLoQ value to adequately describe the SUN kinetics, given that it is administered orally at the doses equal or lower than of 50 mg/die[97,99].

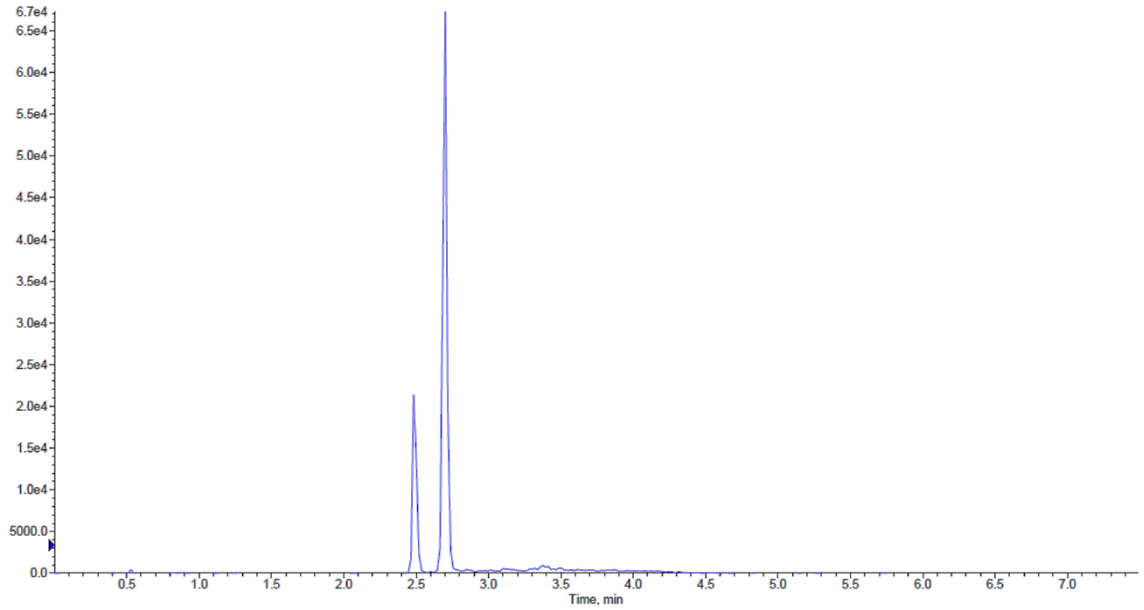

Figure 15. Chromatogram showing the peak split of SUN caused by the photoisomerization.

Thus, to avoid the quantification based on the sum of E- plus Z-isomer, one of the aims of this thesis was to investigate the possibility to revert the E-isomer, formed during the sample processing under light conditions, into the Z-form before LC-MS/MS analysis. The final purpose was, indeed, to setup a simple and rapid procedure to quantitatively reconvert the E-isomer into its Z-form and combined it with an LC-MS/MS assay for the quantification of SUN and its main metabolite, N-DES SUN, in human plasma previously developed by our group. The resulting optimized assay would allow the dosage of both analytes without the need of light-protection conditions during the sample handling thus making the entire analytical workflow more suitable for clinical application, and so, for TDM. Currently, no studies on the E- to Z-SUN reconversion reaction was published so far, and for this reason the starting point of the investigation was a study on the E/Z isomerization of semaxanib, the lead compound of SUN[108] wherein it was observed an increasing in the E- to Z-semaxanib reconversion rate in dark conditions using high temperature (60 °C)[109].

2 AIMS

GIST is a neoplasm extremely resistant to treatments with standard chemotherapy regimens and, prior to the TKIs introduction, surgical resection was the only option available for GIST patients.

IMA, an oral potent TKI indicated as first-line treatment for patients with inoperable, metastatic or recurrent GIST, has dramatically changed the treatment of GISTs, transforming them, in some cases, into chronic diseases that can be treated at home. In the case of IMA resistance occurrence or tumor progression, SUN, another oral effective TKI, represents the second-line treatment for this pathology.

Despite the indisputable advantages brought by the TKIs for the GISTs treatment, some limitations are still related to these drugs. In fact, even if both IMA and SUN show a high interpatient variability in plasma exposure which might affect treatment outcome, nonetheless, they are used with standard fixed doses. Considering that for both this two TKIs a relationship between plasma exposure and treatment outcome has been found, the TDM practice is strongly recommended to identify possible cases of suboptimal response, presence of severe toxicity, drug-drug interactions, cases of non-adherence to therapy, and, thus, to personalize the therapy. As related to IMA, the difficulties to perform this practice are:

- The lack of the definition of a precise C_{min} threshold above which the probability to obtain a better response to treatment would be higher specifically for GIST patients. In literature, in fact, two threshold values were defined in GIST: the first one at 1'110 ng/mL after one month from the treatment beginning and the second one at 760 ng/mL after more than three months of therapy due to an increase in drug clearance;
- The lack of a robust, efficient and simple analytical method for the quantification of IMA C_{min}, more suitable to be applied in clinical practice.

In this context, the first principal aim of this thesis is the development and validation of an LC-MS/MS method for the simultaneous determination of IMA and NOR IMA C_{min} in GIST patients, to evaluate the correlation between plasma drug concentrations and response to therapy in the context of TDM. More in the detail, the following aspects were explored:

- The optimization of both spectrometric and chromatographic conditions for the specific detection of both IMA and NOR IMA in a complex biological matrix (i.e. plasma);
- The optimization of the sample processing for an accurate and precise quantitative analysis: special attention will be paid on simplicity, rapidity and usage of small sample volumes to make the method suitable for the TDM practice;
- The validation, according to the FDA and EMA guidelines, of the developed method;
- The quantification of real samples coming from GIST patients to check the performance and the feasibility of the developed method in a clinical setting.

About SUN, the main difficulty to apply TDM in clinical practice is represented by an analytical issue: in plasma and in presence of light, both SUN and its main active metabolite N-DES SUN undergo a geometric isomerization from the active Z-isomer to the inactive E-one. To avoid this phenomenon, most of the published methods report the preparation and the handling of the sample in dark conditions making their application in a clinical routine difficult.
In this context, the second principal aim of this thesis was to optimize an LC-MS/MS method for the simultaneous quantification of SUN and N-DES SUN by overcoming the analytical issue of the photoisomerization which affects both the compounds, without working in light protection conditions. The avoidance of light protection will lead to an analytical method suitable for TDM practice. More in the detail, the following aspects will be explored:

- The study of the photoisomerization of both SUN and N-DES SUN in human plasma to find the proper experimental conditions to overcome the problem;
- The exploitation of the result of the study to upgrade the LC-MS/MS with a fast and simple preanalytical step to quantify only the Z-isomer of both SUN and N-DES SUN;
- The validation of the upgraded method according to the FDA and EMA guidelines.

3 MATERIALS AND METHODS

3.1 Instrumentation

All the LC-MS/MS analysis in this thesis work were carried out using a Prominence UFLC XR system composed by a SIL-20AC XR auto-sampler, two LC-20AD UFLC XR pumping modules, two FCV-11AL solenoid valve units, a DGU-20A3 degasser, a CBM-20A system controller and a CTO-20AC column oven (Shimadzu, Tokyo, Japan). The LC system was coupled with an API 4000 QTrap (SCIEX, Massachusetts, USA), a mass spectrometer characterized by a Turbo IonSpray (TIS) source and a triple quadrupole analyser. To quantify the analytes, data were processed using Analyst 1.6.3 and the chromatographic peaks were integrated with MultiQuant 2.1 (software package SCIEX). The plasma separation from whole blood samples was performed with a 5810R centrifuge while a 5427R benchtop centrifuge (Eppendorf, Hamburg, Germany) was adopted for the centrifugation which completes the protein precipitation procedure. Analytical standard powders were accurately weighted with a Mettler Toledo DeltaRange XPE205 analytical balance (Columbus, Ohio, USA). For the experiments involving SUN, the ALCO 9157 8W LED lamp (Arnsberg, Germany) was used to standardise the formation of the E-isomer while the water bath Clifton (Nickel-Electro Ltd., Weston-Super-Mare, UK) was utilized to investigate the effect of high temperatures. Working solutions and biological samples were handled with a Pipetman set composed by P1000, P200, P100, P20, P10 and P2 pipettes all purchased from Gilson (Villiers-le-Bel, France). During the analysis, samples were kept in two types of autosampler vials depending on the compound: both borosilicate glass vials with a pre-slit Polytetrafluoroethylene (PTFE) caps purchased from Waters (Milford; Massachusetts, USA) and polypropylene vials with PTFE caps purchased from Agilent Technologies (Santa Clara, California, USA) were used.

3.2 LC-MS/MS method development for the simultaneous quantification of IMA and its main metabolite NOR IMA in human plasma

A bioanalytical method is the set of procedures involved in the conservation, processing and analysis of biological samples containing some analytes of interest. For the method described in this thesis work, the aim was the quantitative analysis of IMA and its main active metabolite NOR IMA in human plasma using an LC-MS/MS apparatus.

The development of this method followed three main steps of instrumental optimization that were necessary to achieve the best sensitivity and selectivity for these two compounds:

1. the optimization of the mass-spectrometric conditions (see section 3.2.2) to achieve the best signal-to-noise ratio (SNR) for the analytes of interest;
2. the optimization of the chromatographic conditions (see section 3.2.3), to obtain the best selectivity and minimize the matrix effect due to other interferents present in plasma (e.g. salts, phospholipids);
3. the optimization of the sample preparation workflow (see section 3.2.4), which includes both the selection of a sample extraction method and the evaluation of the criteria for building a calibration curve. The aim of this optimization is to obtain a sufficient sample cleaning without too difficult and time-consuming techniques and at the same time to obtain a correct instrument calibration in a concentration range that fits for purpose.

3.2.1 Standards and chemicals

The analytical reference standard of imatinib mesylate (batch 017M4710V, purity ≥98%) was purchased from Sigma-Aldrich Co. (Saint Louis, Missouri, USA), while the one of N-desmethyl imatinib free base (batch 2-JST-38-1, purity ≥96%) and the deuterated internal standard (IS) imatinib-D_8 mesylate (batch 2-AJK-132-1, chemical and isotopic purity of 96 and 99,4% respectively) were purchased from Toronto

Research Chemicals Inc. (North York, Ontario, Canada). LC-MS grade acetonitrile (MeCN) and isopropanol (iPrOH) were purchased from Merck Millipore (Burlington, Massachusetts, USA) while analytical grade formic acid (HCOOH) was purchased from Sigma Aldrich; HPLC grade DMSO was purchased from Alfa Aesar (Haverhill, Massachusetts, USA) while LC-MS grade methanol (MeOH) was purchased from Carlo Erba Reagents (Cornaredo, Milano, Italy); type 1 ultrapure water (H_2O) was obtained from a Milli-Q Advantage A10 system from Merck Millipore. The transfusion unit of the National Cancer Institute provided control human plasma/K_2EDTA. Pooled plasma samples belonging to 16 healthy donors (8 males and 8 females), were used to prepare daily standard calibration curves and quality control samples to reduce the bias of the variability between matrices. Only for the matrix effect evaluation (see section 3.3.5), plasma samples from individual donors were adopted.

3.2.2 Mass spectrometric conditions optimization

To achieve the best SNR and the greatest sensitivity for the analyzed compound, two types of parameters had to be tuned: the compound-dependent parameters, which must be optimized individually for each compound based on its ionization efficiency and fragmentation pattern, and the source-dependent parameters, which are dependent on the mobile phase composition and the flow rate. The latter are unique for all the compounds analyzed with the same method. For this reason, their tuning was performed with IMA; which represented the main compound of the assay.

3.2.2.1 Compound-dependent parameters optimization

First, to optimize all the compound-dependent parameters (reported in table 1), three solutions, one for each analyte (IMA, NOR IMA and IS) were prepared in MeOH with 0.1% HCOOH v/v at a concentration of 50 ng/mL. Each solution was directly infused to the TIS source at a flow rate of 15 µL/min and, for each analyte, the following procedure was performed.

With the HPLC disabled, the spectrometer configured in manual tuning mode and all source-dependent parameters set to default values, the first step consisted in the

analyte presence confirmation by the identification of its pseudo-molecular ion $[M+H]^+$.

Declustering Potential (DP)	A parameter that controls the potential difference between Q0 and the orifice plate. It is used to minimize the cluster formation due to the aggregation between ions and solvent droplets.
Entrance Potential (EP)	A parameter that controls the potential which guides and focuses the ions through the high-pressure Q0 region.
Collision Energy (CE)	A parameter that controls the potential difference between Q0 and represents the amount of energy that the precursor ion receives once accelerated into Q2, where it collides with the gas molecules and other fragments.
Collision Cell Exit Potential (CXP)	A parameter that controls the potential which focuses and accelerates ions exiting Q2. It is the potential difference between Q2 and ST3 (a lens that separates Q2 and Q3).

Table 1. Definitions of each compound-dependent parameter.

To do that, a Q1 scan (Q1MS) in positive ion mode was performed: it worked as a single quadrupole scan because no energy was applied to Q2 which, together with Q3, worked in RF only and focused the positive ions from Q1 to the detector without filtering them (figure 16).

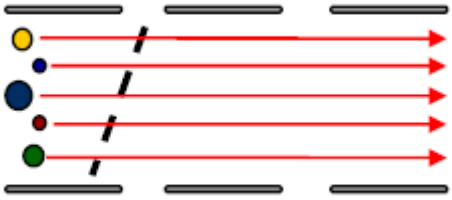

Figure 16. Schematic representation of the triple quadrupole analyser in Q1MS configuration.

The scan was performed in an adequate range of *m/z* values to detect both the pseudo-molecular ion of the analyte and the presence of positive adducts and other ions present in the employed MP (e.g. $[M+Na]^+$, $[M+K]^+$).

In order to obtain an adequate number of duty cycles, the scan time was chosen adopting the following rule:

$$10 \text{ ms} \times \Delta_{amu}$$

Where Δ_{amu} represents the range of *m/z* values analyzed.

After the total ion current (TIC) stabilization, a spectrum was recorded activating the multiple count acquisition (MCA) mode, which summed all the events detected thus increasing the SNR and allowing a more accurate read of the *m/z* value of the pseudo-molecular ion.

For the consequent optimization of the DP and EP parameters, the spectrometer was set in Q1 multiple ions mode (Q1MI), meaning that Q1 did not perform a scan anymore, but worked in selected ion monitoring (SIM) by selecting a specific *m/z* value (i.e. the one of the pseudo-molecular ions found in the previous test) while Q2 and Q3 worked in RF only (figure 17).

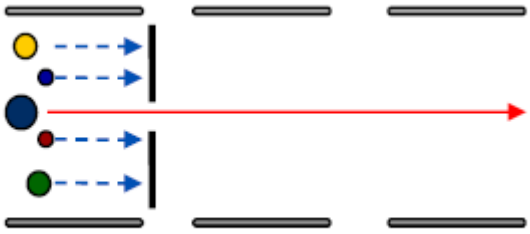

Figure 17. Schematic representation of the triple quadrupole analyser in Q1MI configuration.

By ramping the DP from 20 to 150 V, the intensity trend of the extracted ion current (XIC) was monitored to choose the most correct DP value for the pseudo-molecular ion. Generally, the signal intensity in line with the DP increase has a trend similar to a Gaussian curve and the optimal DP value is the one at the apex of the curve. This because too low DP values will result in lower ion intensity due to interferences from clusters, while too high values might cause an in-source fragmentation.

The optimal EP value (in a range of 1-15 V) was determined in the same way, even if it is often left at 10 V (i.e. the default value) without any impact on analyte detection limit because EP has a minor effect in compound optimization.

While the abovementioned experiments had been done in a single quadrupole configuration (only Q1 was working, while Q2 and Q3 were only focusing ions), to define the remaining compound-dependent parameters (i.e. CE and CXP), all the three quadrupoles were exploited in an MS/MS configuration.

First, an analysis of the fragmentation pattern was carried out for each compound. The spectrometer was set in product ion mode (MS2), that means that Q1 filtered only the pseudo-molecular ions (also called precursor ions, in this kind of experiment), which were fragmented in Q2 and a scan of all fragments (also called product ions) was performed by Q3 (figure 18).

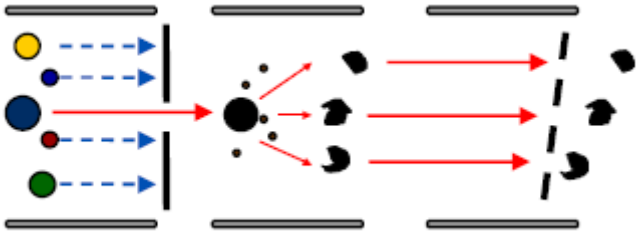

Figure 18. Schematic representation of the triple quadrupole analyser in MS2 configuration.

Several spectra were recorded with different CE values (10, 20, 30, 40, 50, 60, 70 and 80 eV) activating the MCA mode and adopting the correct DP and EP values for the analyzed compound. The *m/z* range explored was 100-500 for all the three analytes because fragments lower than 100 are not informative.

In this way, for each analyte, a first evaluation of the most representative fragments was carried out. Once the main fragments had been selected, the optimal CE value was simultaneously determined for each of them by setting the spectrometer in MRM mode. In this configuration, Q1 behave as a filter by selecting a precise precursor ion, which is fragmented in Q2 and, from the resultant product ions, a further selection is performed in Q3, which behave as a second filter (figure 19).

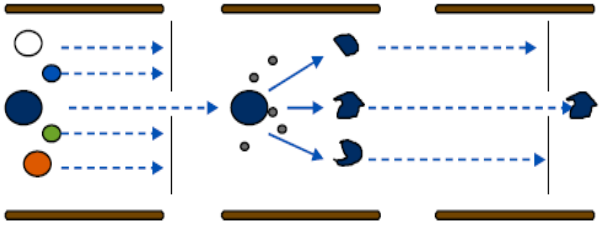

Figure 19. Schematic representation of the triple quadrupole analyser in MRM configuration.

Depending on the number of transitions (fragmentation reactions from precursor to product ion), the dwell time was selected, and a spectrum was recorded by increasing the CE value during the time from 10 to 100 V. The resulting spectrum showed the XIC intensity for each transition in line with the rise of the CE values. The transition with the highest signal intensity was selected as the most suitable for the quantification, while the other two had the function of "qualifiers" to increase the specificity for the analyte of interest. The optimal CE value for each transition is the one at the apex of the XIC signal curve.

A similar experiment was carried out by ramping the CXP value, while the CE was set at its optimum value for each transition. Once the correct values for all the compound-dependent parameter had been obtained, a complete MRM method for the simultaneous quantification IMA and NOR IMA was built up. The precursor ions of IMA, NOR IMA and IS with the optimal value of DP and EP, could be selected and fragmented with the optimal CE and CXP to obtain the desired product ions for the simultaneous quantification and confirmation of the three compounds of interest.

3.2.2.2 Source-dependent parameters optimization

To optimize all the source-dependent parameters (reported in table 2), a solution of IMA was prepared in pure MeOH at a concentration of 200 ng/mL and was directly infused to the TIS source at a flow rate of 15 µL/min into a flowing MP coming from the HPLC pumps. The composition of the MP was 50/50 between A and B, the flow rate was 400 µL/min and the mix with the IMA solution injected was achieved through a tee union. Another union was used as a substitute for the chromatographic column, which was not necessary for this workflow (figure 20) and the whole configuration had the function to mimic the real working conditions of the LC-MS/MS apparatus.

With the HPLC enabled, the spectrometer configured in manual tuning mode and all the source-dependent parameters set to default values (i.e. CUR=10 psi, CAD: medium, IS=5'500 V, TEM=0 °C, GS1=10 psi, GS2=0 psi), the first step consisted in launching a SRM experiment with all the compound-dependent parameters set at the optimal value to analyse the quantifier transition of IMA.

Curtain gas (CUR)	A parameter that controls the pressure of the curtain gas, which flows between the curtain plate and the orifice preventing the contamination of the ion optics by minimizing the entrance of solvent droplets.
CAD gas (CAD)	A parameter that controls the pressure of collision gas in Q2, which in MS/MS experiments has the function of fragment the precursor ions.
IonSpray Voltage (IS)	A parameter that controls the voltage applied to the needle that ionizes the sample, thus influencing the spray stability.
Temperature (TEM)	A parameter that controls the temperature of the turbo gas.
Gas 1 (GS1)	A parameter that controls the pressure of the nebulizer gas, which has the function of helping to generate small droplets of sample flow.
Gas 2 (GS2)	A parameter that controls the pressure of the turbo gas which has the function of helping the evaporation of the spray droplets and avoiding solvent entrance into the analyser.

Table 2. Definitions of each compound-dependent parameter.

With this method the result was a XIC signal (which in SRM are equal to TIC) which, once stabilized, was constant in intensity. By manually varying each source-dependent parameter, a XIC intensity decrease or increase was observed.

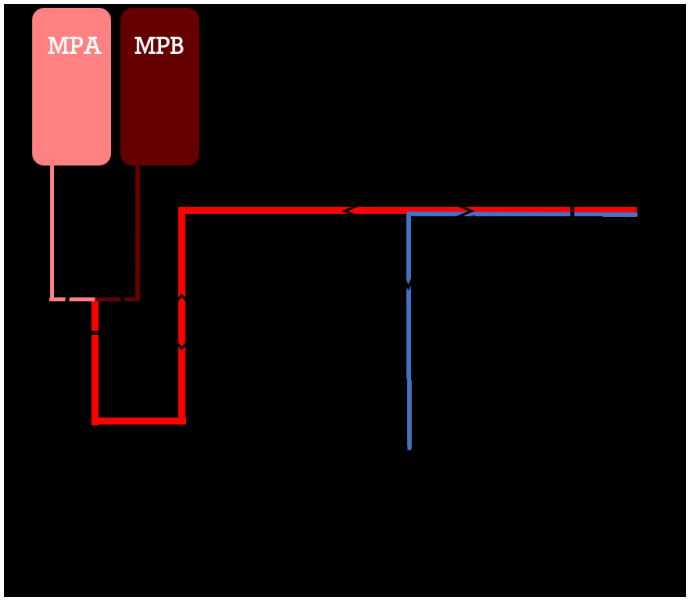

Figure 20. Schematic representation of the instrumental set up for the optimization of the source-dependent parameters. The autosampler was not exploited while the analyte was continuously delivered at low flow rates with an infusion pump.

The goal of this optimization was to reach the maximum signal intensity in order to achieve the greatest sensitivity for the quantification method.

3.2.3 Chromatographic conditions optimization

The development of the chromatographic method implied the determination of the best chromatographic conditions for the separation of IMA from NOR IMA.

The first parameter to consider was the column choice depending on the physicochemical properties of the analytes (type of SP), the number of compounds to be analyzed (length) and required resolution (particle size). The possible addition of a pre-column depending on the sample nature was evaluated too.

Once the SP had been selected, the choice of the column temperature, the flow rate and the MP composition were the next important step. Temperature and flow rate were selected on the basis of the choice of the MP: high viscous solvents might cause too high backpressure into the chromatographic system. This problem could be directly addressed with a lower flow rate while a similar effect could be obtained indirectly with higher column temperature by lowering the mixture viscosity. High temperatures, consistent with the SP chemical nature, generally help to obtain a better chromatographic resolution because of the interchange acceleration of the analytes between the two phases. The evaluation criteria were peak shape, retention time, the degree of carryover and signal stability.

The most time-consuming step was the selection of the chromatographic method: The first step was the choice between a totally isocratic method and a multi-step one.

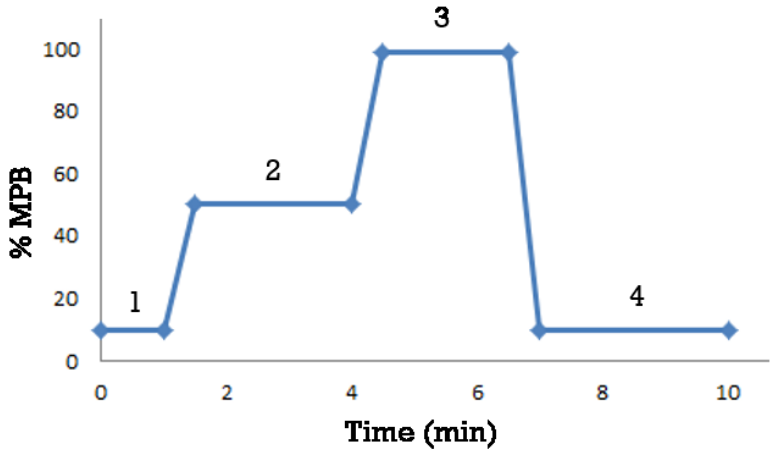

Figure 21. Schematic representation of a multi-step chromatographic method.

While in the former, the MP composition remains unchanged during the whole chromatographic run, in the latter the MPA/MPB ratio changes over time, sometimes following a pattern like the one represented in figure 21 and described below:

1. conditioning phase of the column characterised by a low percentage of MPB which helps the correct packing of the analytes at the head of the column. The initial conditions of the chromatographic run determine the environment encountered by the sample after its injection into the column. In an RP chromatography run, where analytes are eluted in increasing order of affinity for the organic phase, if the initial amount of MPB is too high, it could interfere with the interaction between the analytes and the functional groups on the column particles. This can lead, for example, to an undesired peak-split of the analyte. During the optimization, various percentages of MPB were tested and the possibility to omit this step to save time was considered too. The evaluation criteria were peak shape and the degree of separation between IMA and NOR IMA.
2. Elution phase of the analytes, which might follow an isocratic or a gradient regime. During the optimization, the choice between the two regimes was evaluated, by exploring both different slopes for the gradient approach and different percentages of MPB for the isocratic one; The evaluation criteria were peak shape, retention time and the degree of separation.
3. Washing phase, in which the more lipophilic interferents in the matrix (e.g. phospholipids, peptide residuals, etc.) still bound to the SP, elute from the column thanks to a high percentage of MPB. An adequate washing phase is important to lengthen the life of the column, so during the optimization, different durations of this step were considered by simultaneously monitoring three of the most abundant phospholipids (PLs) in human plasma: phosphatidyl choline, lysophosphatidyl choline and sphingomyelin (figure 22)[110]. The goal was considered achieved when the elution of all the three PLs occurred before the last step and in a reproducible manner during various chromatographic runs.

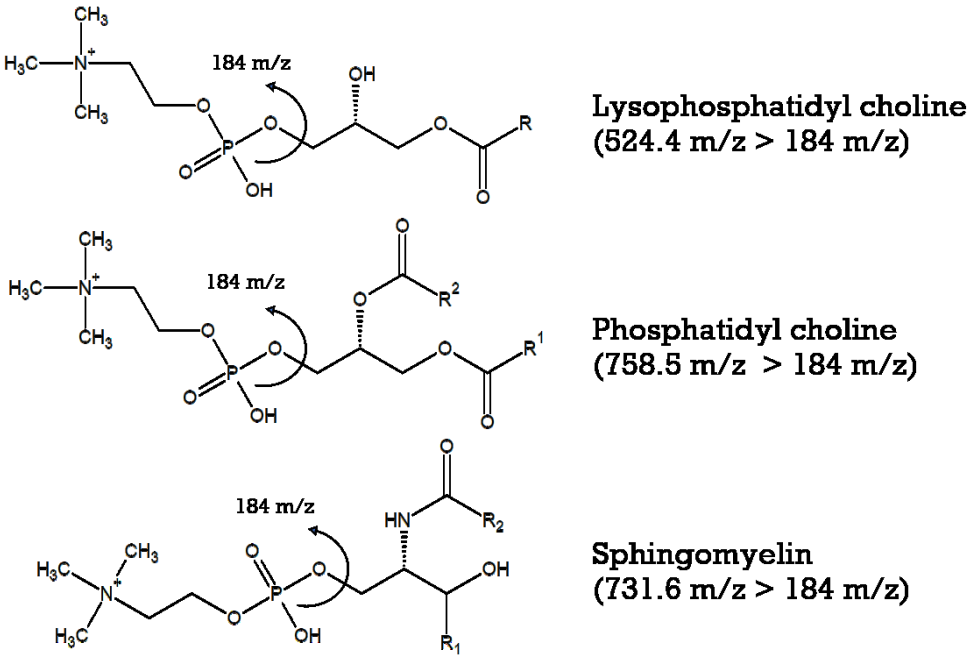

Figure 22. Structure and SRM transitions of three of the most abundant phospholipids in human plasma.

4. Reconditioning phase of the column, in which the MP composition returns to the initial condition. The length of this last step depends on the MP flowrate and the column volume because the column is considered reconditioned only after 10-20 column volumes of MP. Failure to recondition can lead to alterations in retention times and therefore to the lack of reproducibility of repeated runs. In fact, if the analytes at the time of the injection were in a different condition compared to that present at T0, they could behave differently. During the optimization, the reconditioning conditions are kept fixed until the retention times of IMA, NOR IMA and IS remained constant after 3 consecutive runs.

By optimizing all the four steps, the objective was to obtain a chromatographic method with the following characteristics:

- good selectivity, that means adequate separation between IMA and NOR IMA;
- narrow chromatographic peaks with a good symmetry (nor tailing neither fronting were accepted phenomena) for all the three compounds;
- good control over the carryover phenomenon;

- adequate column washing to lengthen column lifetime;
- minimum analysis time.

For the optimization, plasma samples containing both IMA and NOR IMA were prepared at the concentration values corresponding to the LLoQ (30 ng/mL of IMA and 6 ng/mL of NOR IMA) and the Upper Limit of Quantification (ULoQ, 7'500 ng/mL of IMA and 1'500 ng/mL of NOR IMA) of the method. IS was added just before the sample extraction performed in 1.5 mL polypropylene tubes through protein precipitation with 10 volumes of MeOH, followed by a 10 s vortex-mixing. Each sample was then centrifuged at 16'200 g for 15 min at 4 °C and the resulted clean supernatant was stored into an autosampler polypropylene vial just before the analysis. The volume injected was 1 µL. The abovementioned sample preparation workflow was only provisional and allowed us to optimize the chromatographic method in conditions very close to the real ones.

3.2.4 Sample preparation for quantitative analysis

3.2.4.1 Sample extraction optimization

Biological matrices are extremely complex and may contain some endogenous components, such as proteins and lipids, which might interfere with the detection and quantification of the analytes. These interferents might not only dirty and damage both the chromatographic column and the spectrometer source, but they might also cause variations in the analyte ionization efficiency. These ion enhancement or ion suppression phenomena are called "matrix effect" and represent one of the highest concerns during quantitative MS analysis (see section 3.3.5). For this reason, the main purpose in bioanalysis sample preparation is to remove the largest amount of interferents as possible and at the same time to solubilize the analytes in a suitable solvent for their quantification. The most used extraction techniques in the pharmacokinetic field are solid phase extraction (SPE), liquid-liquid extraction (LLE) with immiscible solvents and protein precipitation (PP) with organic solvents miscible in H_2O. Regarding the analysis of drugs in human plasma samples, the simplest and the less time-consuming technique to use is PP: more in detail, organic solvents miscible with H_2O, after their addition to an aqueous

sample like plasma, cause the desolvation of the proteins surface by H_2O molecules displacement, thus leading to the breakage of the weak interactions responsible for their tertiary structure, to the aggregation by attractive electrostatic and dipole forces, and therefore to their precipitation. This extraction method perfectly matches with IMA detection, considering that 95% of the circulating drug is bound to plasma proteins[26]. The most used PP solvents are MeOH and MeCN added in volumes at least three times greater than the sample. The larger the volume of solvent added, the more efficient will be the extraction and the cleaner will be the sample injected on the LC-MS/MS apparatus. At the same time, large volumes lead also to diluted samples which might cause analytical problems if the compound of interest shows low intensity signal. Thus, the volume of solvent added for the PP should be a compromise between the two opposite effects, and it is compound-dependent.

To select the solvent and its amount (expressed as sample:solvent ratio v/v) plasma samples containing both IMA and NOR IMA were prepared at the concentration values corresponding both to the LLoQ (30 ng/mL of IMA and 6 ng/mL of NOR IMA) and the ULoQ (7'500 ng/mL of IMA and 1'500 ng/mL of NOR IMA). These samples, at a known concentration, were extracted with MeOH or MeCN using different volumes and then centrifuged at 16'200 g for 15 min at 4°C. The resulted clean supernatant was stored into an autosampler polypropylene vial just before the analysis.

Several sample:solvent ratio were tested (1:5, 1:6, 1:8, 1:10, 1:15, 1:20, 1:30, 1:40, 1:50, 1:60 and 1:80 v/v) as long as different injection volumes (1, 2 and 3 µL). The aim was to obtain, on equal extraction conditions, a quantifiable peak from the LLoQ sample and a not-over-range signal from the ULoQ sample.

3.2.4.2 Calibration curve preparation

To perform quantitative measurements, it is necessary to calibrate the instrument with a series of known scalar concentration samples, which establishes the relationship between the detected signal and the analyte concentration. These samples are called calibrators and must be realised by using the same matrix type of the real samples for which the quantification method is built for. From the signal

intensities measurement of these calibrators, a curve named calibration curve is identified, characterized by a linear trend in a range of concentration values which show a direct proportionality towards the signal intensity. If this quantitation range of the assay covers the whole drug concentration range expected in a particular study, the developed assay fits for its purpose.

According to the FDA and EMA guidelines, a calibration curve must include at least 6 calibrators, including the LLoQ; For the method subject of this thesis, a seven point-calibration curve was selected, and each calibrator was indicated with a letter of the alphabet, from the less concentrated G, which corresponded to the LLoQ, to the most concentrated A, which corresponded to the ULoQ.

The calibration curve was fitted using the least squares regression method weighted by $1/X^2$. The linear least squares is a technique that allows finding the line that minimizes the sum of the squares of the distances between the experimental points and the extrapolated ones. However, since the absolute variation is larger for higher concentrations, the data at the high end of the calibration curve tend to dominate the calculation of the linear regression. This often results in excessive error at the bottom of the curve, especially for calibration curves that span several orders of magnitude. To compensate for this error and to obtain a better fit of the calibration curve, weighting the curve inversely with the concentration should be appropriate.

It is of fundamental importance that the calibrators undergo the same treatment defined for the real samples.

3.2.4.3 Quality controls preparation

The quality controls (QCs) are samples with a known analyte concentration prepared in the same matrix of the real samples and employed to verify the performance of the bioanalytical method and therefore the integrity and validity of the results, by ensuring the quality of quantification throughout the analysis. A further function of QCs is to evaluate the analyte stability under various stress conditions (e.g. freeze-thaw cycles or storage at RT). In each run, three replicates of low (QCL), medium (QCM) and high (QCH) concentration value QC were

analyzed. The replicates are homogeneously distributed during the analytic run, in order to perform their function towards the entire series of the analyzed samples. The QCs might be purchased or, in the case of the method developed in this thesis work, self-produced. In the latter case, calibrators and QCs must be prepared from separate stock solutions. Moreover, QCs concentration values must differ from the calibrators ones and they must be distributed within the range covered by the calibration curve in the following way:

- QCL: low concentration within to three times the LLoQ;
- QCM: average concentration which falls in the middle of the linear range;
- QCH: high concentration near to 75/85% of the ULoQ.

3.2.4.4 The role of the internal standard

The quantifications carried out in this thesis exploited the internal standard method: during sample preparation a known quantity of a further compound, called an internal standard (IS), was added to each sample (i.e. calibrators, quality controls and real samples) and the analytical parameter used for the quantification was the ratio between the analyte and IS peaks areas. The IS must have very close physical-chemical properties to the analyte of interest, so it might be reasonable to assume that any error introduced during the sample handling has the same impact on both the compounds thus being normalised. The IS addition makes the results of analysis independent from variations in extraction recovery, volume injected and ionization efficiency.

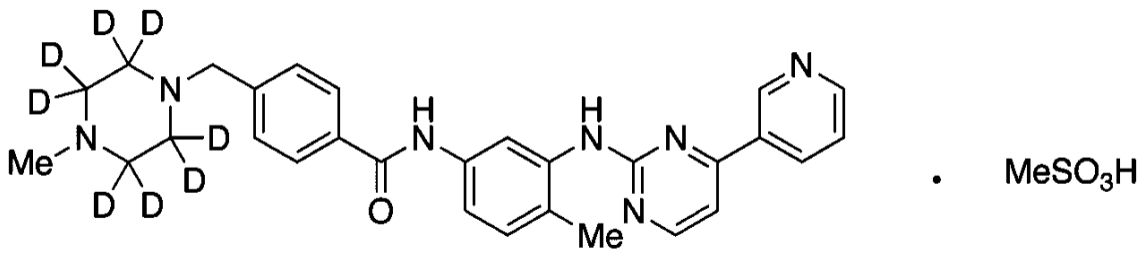

Figure 23. Structure of the imatinib-d8 mesylate, SIL IS used for the quantification method of IMA and NOR IMA. The location of each deuterium (D) minimizes the probability of the H-D exchange in presence of protic solvents.

Excellent candidates for LC-MS/MS analysis are the stable isotopic labelled (SIL) analogs of the analyte (e.g. deuterium-labelled or C^{13}-labelled compounds) because they show a nearly identical chromatographical behavior to the analyte of interest while remaining perfectly distinguishable from it, thanks to the different *m/z* value. During a chromatographic run, the analyte and the SIL IS will co-elute, by suffering in equal measure the matrix effect thus minimizing its impact. For the quantification of IMA and NOR IMA subject of this thesis work, imatinib-D8 mesylate (figure 23) was selected as SIL IS because fitted for purpose and it was not as expensive as the C^{13} labelled analog.

3.3 LC-MS/MS method validation study

The analytical method object of this thesis was developed from scratch and therefore a complete validation was performed in accordance with the EMA[67] and FDA[66] guidelines for the validation of a bioanalytical method. In particular, the validation was carried out by evaluating the following parameters: recovery of the analyte from the matrix, linearity of the calibration curve, intra- and inter-day precision and accuracy, reproducibility, LLoQ and selectivity, matrix effect and stability of the analyte in samples and solutions.

3.3.1 Recovery

The recovery determination of an analyte from a complex matrix allows evaluating the extraction efficiency. Percentage extraction recovery was determined for each analyte (i.e. IMA and NOR IMA) in samples of three concentrations values (QCL, QCM and QCH) prepared in quintuplicate in human pooled plasma without adding the IS. Recovery of the IS was separately evaluated in the same way, but only for a single concentration value of 500 ng/mL.

The recovery was determined by comparing the instrument response from two sample with the same concentration value obtained with different methodologies: for the first one, plasma was spiked with the proper working solution (WS) before the extraction step, while, for the second one, plasma was spiked after that passage. The percentage extraction recovery calculation was given by the following relationship:

$$\text{Recovery } \% = \frac{\text{analyte peak area (in matrix)}}{\text{analyte peak area (in extracted matrix)}} \text{ x } 100$$

The analyte and IS recoveries do not necessarily have to be equal to 100%, however, the most important thing is that, among different analysis, the recovery extent results reproducible and consistent.

3.3.2 Linearity

The linearity of an analytical method is its ability (within a given concentration range) to obtain results directly proportional to the concentration of the analyte present in the sample. The linearity of the calibration curve has been validated in 5 different working days. The calibrators were prepared freshly every day by spiking the pooled human plasma with the proper calibrators WSs, and they were analyzed in order to define the relationship between their concentration values and the instrument response. For each calibrator, the peak area ratio between the analyte (IMA or NOR IMA) and the IS was calculated and plotted against the nominal concentration value.

For the analytical method developed in this thesis work, the weighted least squares method using $1/x^2$ as weighting factor was used in order to evaluate the linearity for each calibration curve of both IMA and its main metabolite.

The fitting quality was calculated using the Pearson correlation coefficient (R^2) and comparing the actual concentrations with the back-calculated ones using the calibration curve.

The accuracy of the back-calculated concentrations must be between ± 15% of their theoretical concentration (± 20% for LLoQ) and at least 66,7% of the calibrators must meet these criteria, LLoQ and ULoQ included.

The reproducibility of each calibration curve was assessed by the arithmetic mean, standard deviation (SD) and the coefficient of variation (CV%) of both m (the slope of the curve equation $y = mx + q$) and R^2.

3.3.3 Intra-day and inter-day precision and accuracy

The intra- and inter-day precision represents the dispersion of a series of measurements around the mean value, while the intra- and inter-day accuracy describes the closeness of the mean value obtained with the assay to the actual concentration value.

The precision of the analytical method was calculated as CV%, which expresses the SD as a percentage of the mean calculated concentration as shown in the following formula:

$$CV\% = \frac{SD}{\bar{X}} x\ 100$$

For each calibrator except the LLoQ, CV% must be ≤15% while for LLoQ, CV% must be ≤20%. The precision was determined both within a single analysis session (intra-run), by determining the analyte in six replicates at three different nominal concentration (i.e. 6 x QCL, 6 x QCM and 6 x QCH) and within different analytical sessions (inter-run) through the analysis in only three replicates (i.e. 3 x QCL, 3 x QCM, 3 x QCH) but in 5 different days. The calibration curve used to determine the real concentrations of the QCs was freshly prepared every day.

The accuracy of the analytical method was reported as a percentage of the nominal concentration and it was determined both intra-run and inter-run in the same way as accuracy.

Accuracy was calculated for calibrator using the following formula:

$$Accuracy\% = \frac{x_{ibc} - x_{in}}{x_{ibc}} x\ 100$$

Where:

x_{ibc} = back-calculated concentration of the i^{th} analyte;

x_{in} = nominal concentration of the i^{th} analyte.

In each run, the concentration measured for at least 6 of the 9 QCs samples must be within ±15% of the nominal value. Only one sample of QCs can be excluded for each concentration level.

3.3.4 Limit of quantification and selectivity

The lower limit of quantification (LLoQ) is defined as the smallest amount of analyte that an assay reaches to quantify (SNR≥5) in the sample with sufficient precision (≤20%) and accuracy (within ±20%). In the analytical method developed in this thesis work, the LLoQ was estimated by adding 1 µL of the least concentrated WS to 6 different samples of control human plasma.

Selectivity identifies the ability of the assay to differentiate and quantify both the analyte of interest and the IS in the presence of other interferents such as matrix

components, metabolites, decomposition products, or other drugs administered concurrently. The selectivity was verified using six independent sources of control human plasma, which were individually analyzed and evaluated for the interference: a single 19 μL aliquot for each one of the six matrices was spiked with the analyte at the LLoQ concentration. Both LLoQ and selectivity had to show an acceptable accuracy (≤20%) and precision (within ±20%).

3.3.5 Matrix effect

Due to the presence of endogenous components in the biological matrix, both the analyte of interest and the IS might experience variations in their ionization efficiency and this phenomenon is called matrix effect. In the ESI source, the analyte in the liquid phase, before entering the analyser, is converted into gas ions through charging and desolvation processes. If one or more endogenous compounds coelute with the analyte of interest, they might interfere with the desolvation and charge steps, altering the ionization of the analyte in a positive (ion enhancement) or negative (ion suppression) way[111]. The endogenous compounds present in the biological matrix (e.g. salts, amines, phospholipids) are the major responsible for the matrix effect but they are not the only ones: even some exogenous components like some plasticizers released from sample containers or some anticoagulants might cause alterations to the ionization process[112]. Other substances capable of generating this phenomenon may be present in the MP too, but in this case, they cannot be considered sources of matrix effect because it is not sample-specific[111].
Both ion enhancement and ion suppression phenomena might compromise precision, accuracy, sensitivity and selectivity of the developed method and, consequently, the reliability of the produced analytical data. For this reason, both FDA and EMA emphasize the importance of the matrix effect assessment. Both guidelines agree that at least six lots of plasma from individual donors must be used to study the variability of the matrix effect, which could be responsible for the lack of reproducibility in the method. For the method developed in this thesis work, the matrix effect variability was evaluated by comparing the response obtained from 6 plasma samples at LLoQ concentration coming from 6 different donors. Matrix effect would be considered irrelevant only if the CV% was within ±20%.

Another method commonly used to qualitatively evaluate the matrix effect is to perform the post-column infusion[113], which allows identifying the chromatographic region where both ion enhancement and ion suppression occur[111]. This method consists of the simultaneous introduction of a constant concentration of the analyte into the ion source through an infusion pump and the launch of a chromatographic run of a blank sample (i.e. extracted matrix). This is made possible thanks to a tee union located after the HPLC column that connects two independent lines into the source: from the one pathway, the extracted matrix injected into the HPLC is transported by the MP, from the second pathway the solution of the analyte was continuously infused (figure 24).

The signal of the infused analyte, monitored by the SRM scan mode, will be steady, unless the endogenous components that elute from the column cause a reduction or an increase in the response. If both ion suppression and enhancement do not occur close to the retention time of the analyte, the influence of the matrix might be considered negligible. For the method developed in this thesis work, the post-column infusion was carried with the solutions of IMA, NOR IMA and IS at a concentration of 200 ng/mL in MeOH with the 0.1% of HCOOH infused at a flow rate of 15 µL/min.

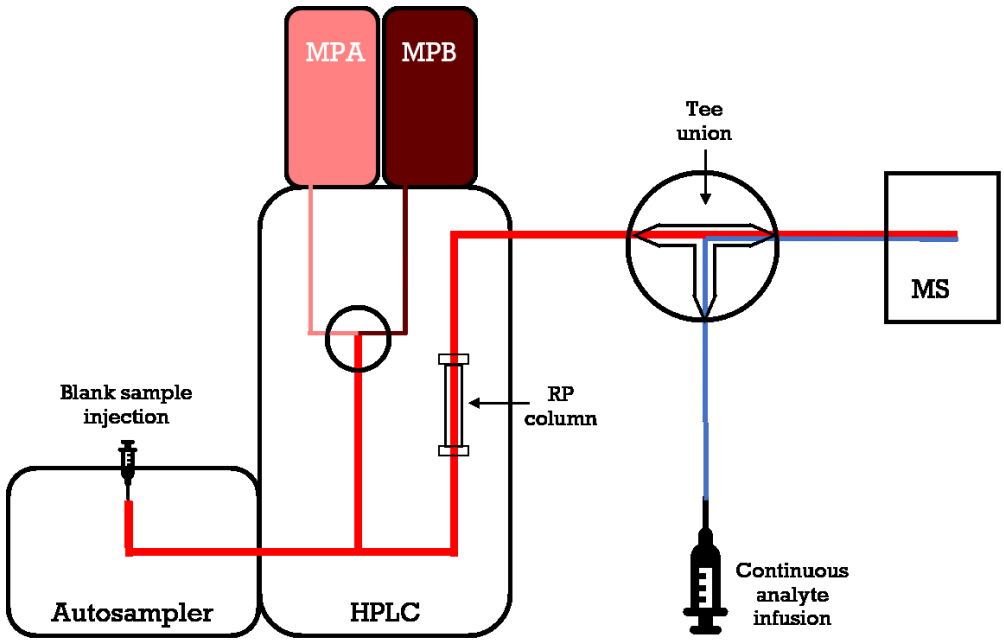

Figure 24. Instrument set up for the post column infusion.

3.3.6 Stability

The stability of an analyte is a function of the matrix in which it is dispersed, of the conditions in which it is stored and of the chemical properties of the analyte itself. Evaluating the stability of the analyte in stock solutions and in the matrix is essential to ensure the reliability of the results obtained from the analytical method. This assessment includes all the situations that can be encountered during the whole analytical procedure such as freeze-thaw stability, short- and long-term stability, stock stability and post-processing stability.

The stability of the analytes of interest was evaluated by analysing in triplicate each of the three QCs levels (i.e. QCL, QCM and QCH).

The bench-top stability in plasma was assessed by leaving the samples 4 h at room temperature (RT) before processing them, while the post-processing stability in the autosampler was evaluated by repeatedly analysing the extracted samples after 24, 48 and 72 h from the first injection. About the freeze-thaw stability, for up to three freeze-thaw cycles the stability of the samples was tested: a fresh aliquot of each QC was prepared, from which a triplicate for each concentration level was obtained, processed and analyzed. The remaining parts of each aliquot were frozen, and in a second time thawed, processed and analyzed thus repeating the whole process for at least three times, always in triplicate. Lastly, for both QC samples in plasma and QC WSs the long-term stability had to be evaluated by storing them at -80 °C. For each one of the abovementioned stability tests, the QCs under stability test should be compared to freshly prepared calibration curves and QCs: each analyte can be considered stable only if the accuracy at each level is within ±15%differences between the freshly prepared samples and the stability of the tested samples was not greater than ±15%.

3.3.7 Incurred Samples Reanalysis

As indicated in the 2013 FDA guidance, which take into account the AAPS/FDA seminar on the reanalysis of the assayed sample[114], an additional measure of the assay reproducibility was introduced: the incurred samples reanalysis (ISR). This evaluation has become an important element into the validation process to verify

the reliability of analyte concentrations in previously quantified samples and, for this reason, it resulted recommended also in the last edition (2018) of the FDA guidance. The ISR was carried out by quantifying a subset of patient samples in two separate runs, performed on different days. This procedure is used to critically support the accuracy and precision measurements established with the QCs. Selection of samples for reanalysis should be performed to ensure adequate coverage of the target concentration profile of the developed method, including at least one high and one low concentration samples. The two runs can be considered equivalent if at least 67% of the retested samples show a percentage difference (%diff) of the results compared to the first analysis within ±20%. To calculate the %diff, the following formula was used:

$$\%\text{diff} = \frac{R-I}{M} x100$$

Where:

R = concentration value found from the repeated analysis;

I = concentration value found from the first analysis;

M = arithmetic mean between R and I.

3.4 Simultaneous quantification of IMA and its main metabolite NOR IMA in GIST patients' plasma for TDM

3.4.1 Patients enrollment

A phase IV clinical trial entitled "*Pilot study to evaluate the feasibility of an innovative approach to monitor patients with gastrointestinal stromal tumor treated with imatinib*" was started at the Aviano (PN) National Cancer Institute. The protocol of this clinical trial (N. EudraCT 2017-002437-36, Code: CRO-2017-19) has been revised and approved by the Comitato Etico Unico Regionale (CEUR) del Friuli Venezia Giulia and by AIFA. The study, which involves the collaboration of the Azienda Ospedaliera Integrata di Verona and the University of Chicago Medical Center, was approved by the ethics committees of each participating center.

3.4.1.1 Patients' characteristics

The expected eligibility criteria were:

- age greater than or equal to 18 years;
- diagnosis of GIST confirmed histologically or cytologically and eligible for treatment with imatinib according to the routine clinical practice criteria both in adjuvant and first-line therapy;
- performance status, determined with the Eastern Cooperative Oncology Group (ECOG) criteria, of 0 or 1 and adequate liver, renal and bone marrow function;
- life expectancy greater than 3 months;
- for patients already treated with imatinib, therapy had to start more than 3 months before the first sample was collected (to reach a stable drug concentration in the blood);
- signature of the informed consent.

Expected exclusion criteria were pregnancy status, non-collaborative and/or unreliable patients, informed consent refusal and the absence of possibility for the patient to undergo periodic clinical check-ups.

3.4.1.2 Treatment and sampling

Standard therapy with Glivec (imatinib) at a dose of 400 mg/day is given to all enrolled patients as starting dosage. For each patient who is eligible for the study, the collection of three tubes of 4.9 mL and one of 2.7 mL (all of them with K_2EDTA as anticoagulant agent) of peripheral blood is proposed for genetic analysis and for TDM respectively. These samplings are scheduled every three months for the first two years of therapy, after which they will be performed at every clinical check-up (i.e. every 4-6 months blood samples were obtained just before the next dose).
After the withdrawal, the patient's whole blood sample for TDM is centrifuged at 2'450 g for 10 min at 4° C and the obtained plasma is transferred into a 1.5 mL polypropylene tube and stored at -80 °C until the analysis.

3.4.2 Real samples processing procedure

Once the validation had been completed, it was possible to proceed with the quantification of the patients' samples. The sample preparation method previously developed for calibrators and QCs was applied also for this real samples:
each plasma sample was thawed at RT, vortex-mixed for 10 s and centrifuged at 2'450 g for 5 min. Thereafter, 20 µL of each sample were transferred into 1.5 mL polypropylene tubes, 1 µL of the IS WS was added and, after 5 s of vortex-mixing, proteins were precipitated with the addition of 1 mL of MeOH.
Each tube was vortex-mixed for 10 s and then centrifuged at 16'200 g for 15 min at 4 °C. Then, 200 µL of obtained clean supernatant were transferred into PP autosampler vials and put into the autosampler (thermostatically controlled at 4 °C) and, for each sample, 1 µL was injected into the HPLC system for the analysis.
These unknown samples were analyzed together with the calibrators and the QCs to calibrate the instrument and to monitor the analysis conditions respectively.

At the beginning of each analysis, a series of few samples called system suitability test (SST) must be checked. These samples serve to ensure that all the necessary conditions for starting a reliable quantification are met and they consist of:

- a first blank, containing only the extracted matrix (blank);
- a zero sample, which is a blank added with IS;
- the LLoQ.

The FDA guidelines describe the criteria for the analysis to be considered accepted:

- the SST must guarantee the quantification of the LLoQ and the absence of a quantifiable signal of the analyte into the blank sample;
- Calibrators must have a precision, expressed as CV%, less than or equal to 15% and an accuracy ranging from 85 to 115%, with the exception of the LLoQ, which for definition must have an accuracy of less than or equal to 20% and an accuracy ranging from 80 and 120%; at most one point can be excluded from the calibration curve, provided it does not constitute one of the two extremes of the curve;
- the QCs must have a precision of less than or equal to 15% and an accuracy ranging from 85 to 115%; at most one QC can be excluded for each triplet corresponding to the same concentration.

3.5 Study of the light-induced geometric isomerization of SUN and N-DES SUN in human plasma by LC-MS/MS

Regarding SUN and its metabolite N-DES SUN, a standard LC-MS/MS quantification method has been already set up, but the validation step was hampered by the issue of the photoisomerization from Z-form to the E-one during the sample preparation (see section 1.2.3.2). To validate the method and to make it suitable for the analysis of real samples in the context of the TDM practice, a solution to the analytical issue had to be found. By excluding the possibility to perform the whole sample handling (from the sampling to the analysis) in dark condition, due to the absence of feasibility in the clinical routine, the E-isomer formation remains unavoidable. The only strategy that could be applied dealt with finding the right conditions to trigger the reverse reaction: the aim was to find a fast and simple way to reconvert both E-SUN and E-N-DES SUN to their Z-forms just before the analysis, in a way to quantify just one peak for analyte thus simplifying the analysis and reaching an adequate LLoQ value. First, in order to identify the abovementioned right conditions, a study of the behavior of both the compounds was carried out. A similar work was conducted by Sistla et al.[109] for the lead compound of SUN called semaxanib wherein it was observed an increase in the E- to Z-isomer reconversion rate in dark conditions using high temperatures (60 °C). After having confirmed the same behavior for SUN, the next step was to create a simple and fast preparative step to supplement the already existing LC-MS/MS method. Once the quantitative assay had been upgraded, a validation following the EMA and FDA guidelines was carried out.

3.5.1 Standards and chemicals

The analytical reference standard of sunitinib malate (batch n° 030M4706V, purity: >99%) was purchased from Sigma-Aldrich Co. (Saint Louis, Missouri, USA), while the one of N-desethyl sunitinib free base (batch n° 1-WHH-100-3, purity: 98%) and the deuterated IS sunitinib-D_{10} (batch n° 3-THT-159-3, chemical and isotopic purity

of 96 and 99,4% respectively), were purchased from Toronto Research Chemicals, Inc. (North York, Ontario, Canada). LC-MS grade MeCN, analytical grade HCOOH and trifluoroacetic acid (TFA) acids were purchased from Sigma-Aldrich Co.; LC-MS grade MeOH and DMSO were purchased from VWR (Radnor, Pennsylvania, USA); type 1 ultrapure H_2O was produced by a Milli-Q Advantage A10 system from Merck Millipore (Burlington, Massachusetts, USA). Pooled plasma samples belonging to 16 healthy donors (8 males and 8 females) were used to prepare daily standard calibration curves and QC samples, to reduce the bias of the variability between matrices. Only for the matrix effect evaluation, plasma samples from individual donors were adopted.

3.5.2 Working solutions preparation

A 1 mg/mL stock solution was prepared in DMSO for both SUN and N-DES SUN. The two solutions were then mixed together and diluted with MeCN obtaining three WSs with the concentration values of 50, 500, and 8'000 ng/mL for SUN and 50, 500, and 4'000 ng/mL for its metabolite. The concentration values of these combined WSs (each solution contained both the two analytes) were selected in order to obtain, after the dilution with the matrix, spiked samples with the final concentration values of 2.5, 25 and 400 ng/mL for SUN and 2.5, 25 and 200 ng/mL for N-DES SUN. Aliquots of these WSs were kept in polypropylene tubes and stored at -80 °C.

3.5.3 Chromatographic conditions

Samples were separated on a Synergy Fusion-RP (4 μm, 80 Å, 50 x 2.0 mm) coupled with a Security Guard Cartridge (Fusion-RP 4 x 2.0 mm), both provided by Phenomenex and thermostatically controlled at 50 °C. The flow rate was kept constant at 300 μL/min following the multi-step elution scheme reported in table 3, where the MPs used for chromatographic separation were 0.1% HCOOH/H2O (MPA) and 0.1% HCOOH/acetonitrile (MPB).

The retention times of SUN and N-DES SUN were 2.45 and 2.41 min respectively while the total run time was 7.5 min.

Time (min)	MPB (%)	MPA (%)
0.50 (initial condition)	10	90
1.50	70	30
2.70	70	30
3.00	40	60
3.50	10	90
7.50 (stop)	10	90

Table 3. Parameters of the multi-step chromatographic method adopted for the elution of SUN and N-DES SUN in human plasma samples.

3.5.4 Mass-spectrometric conditions

The biological samples were analyzed in positive ion mode, and the compound- and source-dependent parameters employed are reported in table 4.

CUR	20 psi		
CAD	5		
IS	5000 V		
TEM	625°C		
GS1	30 psi		
GS2	70 psi		
Analytes	SUN	N-DES SUN	SUN-D10 (IS)
Q1 (DP)	399.2 *m/z* (72 V)	371.2 *m/z* (57 V)	409.2 *m/z* (67 V)
Q3 (CE)	326.2 *m/z* (28 V)	283.2 *m/z* (27 V)	326.2 *m/z* (30 V)
	283.2 *m/z* (36 V)	326.2 *m/z* (22 V)	283.2 *m/z* (39 V)
	238.1 *m/z* (60 V)	238.1 *m/z* (54 V)	238.1 *m/z* (63 V)

Table 4. Values of the tuned compound- and source-dependent parameter for the detection and quantitation of SUN and its main active metabolite N-DES SUN.

Quantification was done in SRM mode using the following transitions: *m/z* 399.2>326.2 for SUN, *m/z* 371.2>283.2 for N-DES SUN, *m/z* 409.2>326.2 for IS. The other product ions were employed for the qualification of the analyte improving the specificity.

3.5.5 Formation of the E-isomer

As already reported, the light exposure of plasma samples during the handling procedures triggers the geometric isomerization of both SUN and N-DES SUN from the Z-form to the E-one. For this reason, to monitor this process was necessary to obtain a standardized starting condition (the maximum percentage of E-isomer) for the subsequent experiments. First, 15 µL of SUN and N-DES SUN WS (L, M, or H) were added to 285 µL of pooled blank human plasma and, after 5 s of vortex-mixing, protein precipitation was performed adding 1.5 mL of pure MeOH to the mixture. The tube was vortex-mixed again for 10 s and centrifuged at 16'200 g for 10 min at RT. It is important to underline that all these steps were performed under light protection to avoid the uncontrolled formation of the E-isomer. Then, from the resulting supernatant, seven aliquots were obtained by splitting the whole volume into seven borosilicate glass vials (150 µL each). Six of them were exposed to the LED lamp for increasing time (5, 10, 20, 30, 60, and 120 min) just before the LC-MS/MS analysis while the first one was immediately put into the autosampler and analyzed. The experiment was carried out for all the three concentration levels (L, M and H) of SUN and N-DES SUN in order to evaluate the existence of a relationship between the isomerization rate and the analytes concentration. Moreover, only for the medium concentration level, the effect of pH was tested: the experiment was performed also on spiked plasma samples extracted with MeOH added with 0.1% v/v of an organic acid. Both HCOOH or TFA, two acids with different strength and commonly used in mass spectrometry, were tested. Each test was conducted at least in triplicate (figure 25). The results were shown as percentage of E-SUN (and N-DES SUN) peak area respect to the sum of E- and Z-SUN (and N-DES SUN) peak areas.

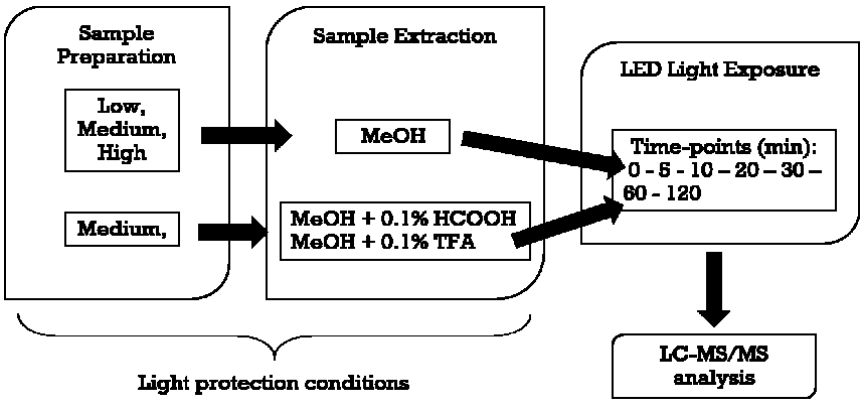

Figure 25. Schematic representation of the experiment steps for the formation of the E-isomer under LED light exposure.

3.5.6 Reconversion from E- to Z-isomer into the autosampler

This experiment, similar to the previous one, was conceived to monitor the reconversion kinetics of E- to Z-isomer when plasma samples were placed in dark condition (e.g. into the autosampler). Plasma samples containing SUN or N-DES SUN at M concentration, prepared as reported in the section 3.5.5 except for the light protection, were initially placed under LED lamp for 30 min. In this way, as resulted from the previous experiment, all the samples reached the maximum percentage of the E-isomer of both the drug and its metabolite, thus standardizing the starting experimental conditions. Then, the samples were directly inserted into the autosampler and repeatedly analyzed at different time points: 0 (immediately analyzed), 0.25, 0.5, 1, 1.5, 2, 2.5, 3, 4, 5, 6, 7, 8, 9, 10, 12 h. This experiment was conducted setting the autosampler at three different temperatures (4, 25, 40 °C) and it was repeated at least three times for each temperature. In the case of the experiment conducted at 4 °C, the samples were analyzed at fewer time points: 0, 0.5, 1, 2, 4, 8, and 12 h.

Moreover, at 40 °C (when the reconversion rate was higher) both the effect of acids and the possible influence of different analyte concentrations on the E- to Z-isomer reconversion rate were investigated. To investigate the effect of SUN and N-DES SUN concentration, samples were prepared using L, M, and H solutions. To

determine the effect of acids the spiked plasma samples (only at the medium concentration level) were processed using MeOH added with 0.1% of HCOOH v/v, as protein precipitating solvent. As in the previous section (3.5.5), all these experiments were conducted in triplicate (figure 26). The results were shown as percentage of Z-SUN (and N-DES SUN) peak area respect to the sum of E- and Z-SUN (and N-DES SUN) peak areas.

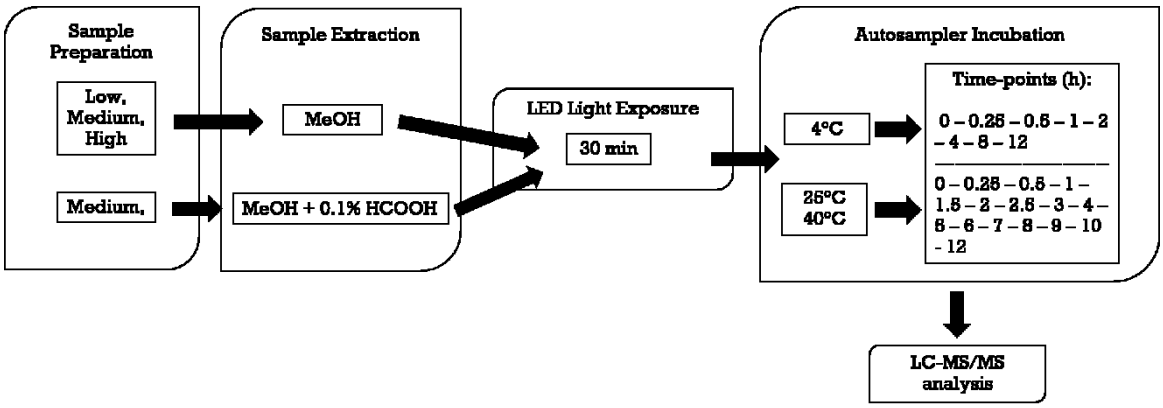

Figure 26. Schematic representation of the experiment steps for the E-to Z-isomer reconversion into the autosampler.

3.5.7 Reconversion from E- to Z-isomer into a heated water bath

The effect of the temperature on the reconversion rate from E- to Z-isomer was further investigated using a heated water bath (HWB), set at different temperatures: 40, 50, 60, 70, 80, 90 °C. Three samples at each concentration (L, M, and H) of SUN and its metabolite were prepared as reported in section 3.5.6, (including the 30 min of LED light exposition). After that, the glass vials were put into the HWB (dark condition) set at the starting temperature (40 °C) for 5 min and, after a transfer conducted in light protection condition, analyzed immediately by LC-MS/MS. Exactly the same procedure was repeated with the HWB set at the higher temperatures reported above.

To investigate the effect of the presence of acids on the reconversion kinetics, the same experiments were conducted using plasma samples obtained as described

above, with the difference that they were treated with MeOH added with 0.1% of TFA or HCOOH v/v for the protein precipitation. In this case, the test was conducted only at the M concentration of SUN and N-DES SUN, although always in triplicate (figure 27). The results were shown as percentage of Z-SUN (and N-DES SUN) peak area respect to the sum of E- and Z-SUN (and N-DES SUN) peak areas.

Figure 27. Schematic representation of the experiment steps for the E- to Z-isomer reconversion into the HWB.

3.5.8 Stability test of SUN and N-DES SUN at high temperatures

To be sure that a temperature-related degradation of the analytes did not occur, a stability test was conducted as follows: three samples at each concentration (L, M, and H) of SUN and its metabolite were prepared as reported in section 3.5.5 (under light protection) and immediately analyzed by LC-MS/MS method to have the initial concentration of Z-isomer.

Figure 28. Schematic representation of the experiment steps to assess the analytes stability under high temperatures. Two HWB cycles were performed.

Then, samples were incubated in the HWB at 70 °C (which is the temperature chosen from the previous experiment as sufficient to quantitatively reconvert the E-isomer into the Z-one) for 5 min and re-analyzed.
The results were shown as percentage variation between Z-SUN (and N-DES SUN) peak area measured before the HWB respect to the same parameter measured after the HWB. The stability was assessed for two incubation (figure 28).

3.6 Validation of the optimized LC-MS/MS method for the simultaneous quantification of SUN and N-DES SUN in human plasma

For the validation procedures according to the FDA and EMA guidelines, the same steps for the developed method for IMA and NOR IMA were followed (see section 3.3). Concerning the ISR, a set of real samples from patients were obtained thanks to the approval of the clinical protocol entitled "*Cross-validation study of new devices for the quantification of sunitinib versus the gold standard technique (LC-MS/MS) on patient samples*" (Code: CRO 2016 18) from the Internal Review Board (IRB) of the National Cancer Institute of Aviano. The study was conducted according to the principles expressed in the Declaration of Helsinki. All blood samples were collected only after the signature of the informed consent from all the patients enrolled in the clinical study.

3.6.1 Working solutions preparation

Two different sets of stock solutions for SUN and N-DES SUN were prepared in DMSO at a concentration of 1 mg/mL. By mixing together the solutions of the first set and diluting the mix with MeCN, seven WSs for the preparation of calibrators were obtained with the following concentrations: 2, 10, 50, 200, 1'000, 5'000, 10'000 ng/mL and 2, 10, 50, 200, 1'000, 2'000, 8'000 ng/mL (from G to A) for SUN and N-DES SUN respectively. Stock solutions belonging to the second set were mixed together and diluted with MeCN obtaining three WSs for the preparation of quality controls (QCs) with the following concentrations: 5, 500, 8'000 ng/mL and 5, 500, 4'000 ng/mL (L, M, H) for SUN and N-DES SUN, respectively. The stock solution for IS was prepared in DMSO at a concentration of 1 mg/mL and was diluted in MeCN to 100 ng/mL obtaining the IS WS. All the solutions were kept in polypropylene tubes and stored at -80 °C.

3.6.2 Calibrators and quality controls preparation

A seven-point calibration curve in plasma was prepared freshly every day during the validation study. For each calibrator, 1.5 µL of the respective WS from G to A were spiked to 28.5 µL of pooled blank human plasma to obtain the final concentrations reported in table 5. Each calibration curve included a blank sample (plasma processed without IS) and a zero-blank sample (plasma processed with the IS). QCs were used at least in triplicate for each concentration level and to prepare them, 1.14 mL aliquots of control human plasma were mixed with 60 µL of each WS (L, M and H) obtaining the final concentrations reported in table 5. Several 30 µL-aliquots of the three QCs were stored at –80 °C to check the stability of the analytes and as controls for future assays.

Sample types	SUN (ng/mL)	N-DES SUN (ng/mL)
G	0.10	0.10
F	0.50	0.50
E	10.00	2.50
D	50.00	10.00
C	100.00	50.00
B	250.00	100.00
A	500.00	250.00
QC L	0.25	0.25
QC M	25.00	25.00
QC H	400.00	200.00

Table 5. Final concentration values of calibrators and QCs for both SUN and N-DES SUN.

3.6.3 Samples processing

After having thawed plasma samples at RT, they were vortex-mixed for 10 s and centrifuged at 2'450 g for 10 min at nominally 4 °C. An aliquot of 30 µL of the actual sample, calibrator or QC was transferred to a 1.5 mL polypropylene tube (figure 29a), spiked with 1.5 µl of the IS WS (100 ng/mL) and the resulting mixture was vortex-mixed for 5 s.

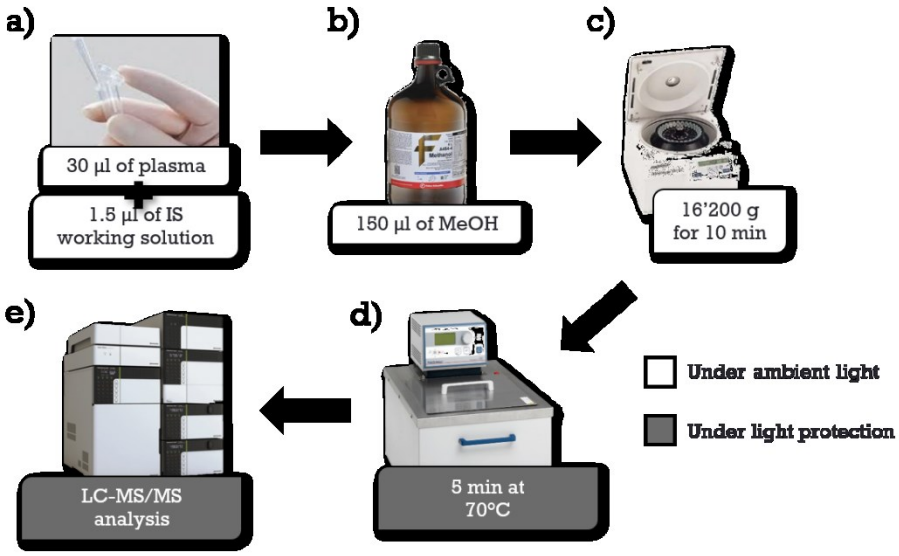

Figure 29. Schematic representation of the sample preparation procedure.

After that, proteins were precipitated with the addition of 150 µL of MeOH (figure 29b) and after vortex mixing for 10 s, each tube was centrifuged at 16'200 g for 10 min (figure 29c). Then, 100 µL of the obtained clear supernatant were transferred to a borosilicate glass vial with a pre-slit PTFE cap. Since all the sample handling steps described above occur without any light-protection, an additional step based on the results of the experiments done in section 3.5 was introduced to revert the isomerization and thus to obtain only the active Z-isomer: the vials containing the supernatant were heated at 70 °C for 5 min in a thermostated water bath (figure 29d). Then, the transfer from the bath to the autosampler represented the only step in the entire sample processing that needed to be done in the dark (figure 29e). To address the carry-over effect, after the injection of the ULOQ, four samples of MP were injected. This procedure guaranteed that no peak higher than 20% of LLOQ was detected.

3.6.4 Sampling protocol for the ISR

Serial blood samples were collected, from one patient treated with 37.5 mg/day SUN, into 4.9 mL polypropylene tubes containing K_2-EDTA and the sampling schedule was the following: before drug administration and at 1, 2, 4, 5, 6, 10, 12 and 24 h following the intake of SUN. In order to avoid confounding factors due to freeze/thaw cycles, plasma will be obtained immediately by centrifugation (2'450 g

for 10 min at 4 °C) of blood samples after the puncture of patients, then split into two aliquots and stored at -80 °C in two different freezers.

4 RESULTS

4.1 LC-MS/MS method development for the simultaneous quantification of IMA and its main metabolite NOR IMA in human plasma

4.1.1 Mass spectrometric conditions optimization

4.1.1.1 Compound-dependent parameters optimization

The monoisotopic mass of IMA is equal to 493.26 Da, so, with the TIS source in positive ion mode, during the first Q1 scan, the presence of the analyte of interest in the infused solution was confirmed by the pseudo-molecular ion $[M+H]^+$ at 494.4 *m/z* (figure 30).

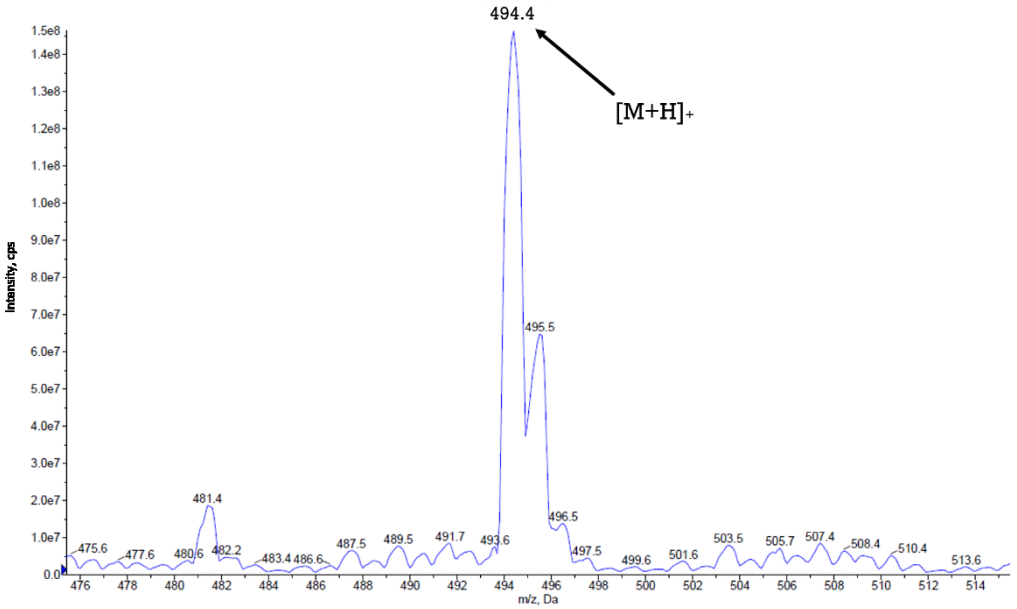

Figure 30. Spectrum obtained in positive mode with a Q1 scan from 450 to 650 Da that confirms the presence of IMA (zoom from 475 to 515 *m/z* to see the isotopic pattern of the pseudo-molecular ion at 494.4 *m/z*).

Through Q1MI scan mode, the XIC signal of the pseudo-molecular ion at 494.4 *m/z* was monitored ramping the DP value from 0 to 400 V. The XIC highest intensity was reached with DP = 130 V (figure 31), which represents the optimal value for a correct removal of clusters. In the same way the value of 10 V was determined as optimal for EP.

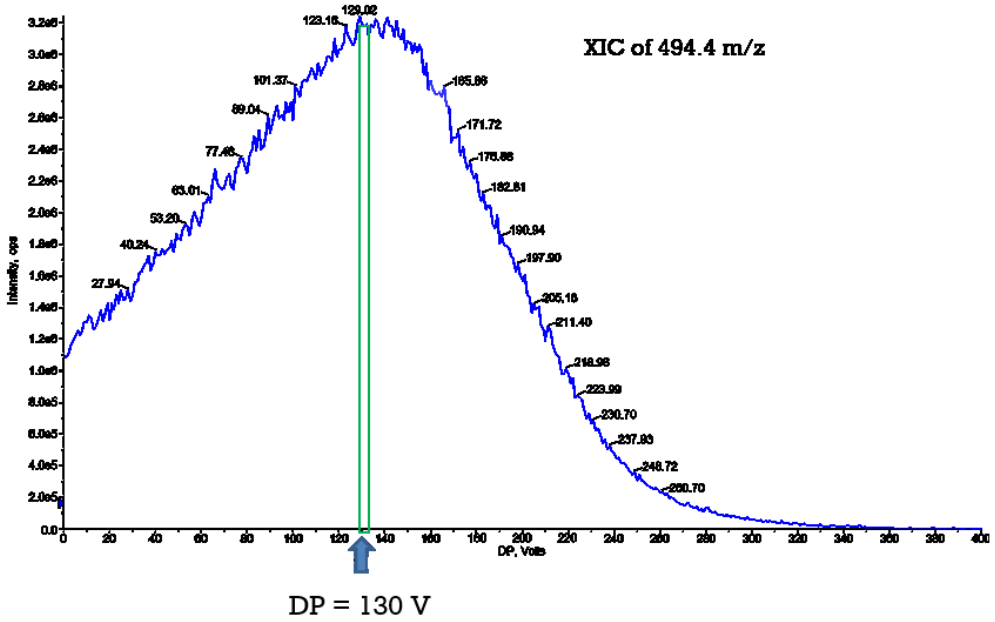

Figure 31. Intensity signal obtained in positive ion mode with Q1 in SIM for 494.4 *m/z*. The apex of the XIC trend was reached at the optimal DP value of 130 V.

In Product ions (MS2) mode, the fragmentation of the IMA precursor ion was evaluated with different CE values (from 10 to 100 V) applied in the collision cell.

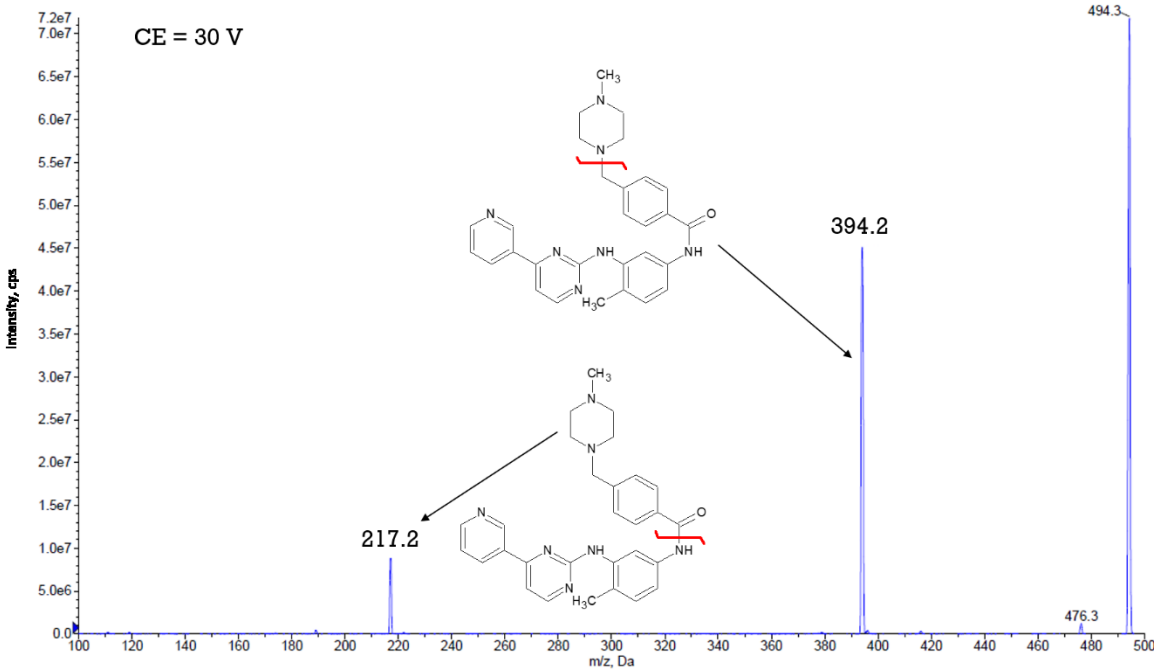

Figure 32. Spectrum recorded in product ion mode showing the fragmentation pattern of IMA precursor ion at 494.4 *m/z* with a CE value of 30 V. The graphic representation of the bond breakage is also shown.

In figure 32, with 30 V of CE applied, the most abundant product ions were found at 394.2 and 217.2 *m/z*, while a third fragment with a similar abundance to the latter was found with 70 V of CE at 378.1 *m/z* (figure 33).

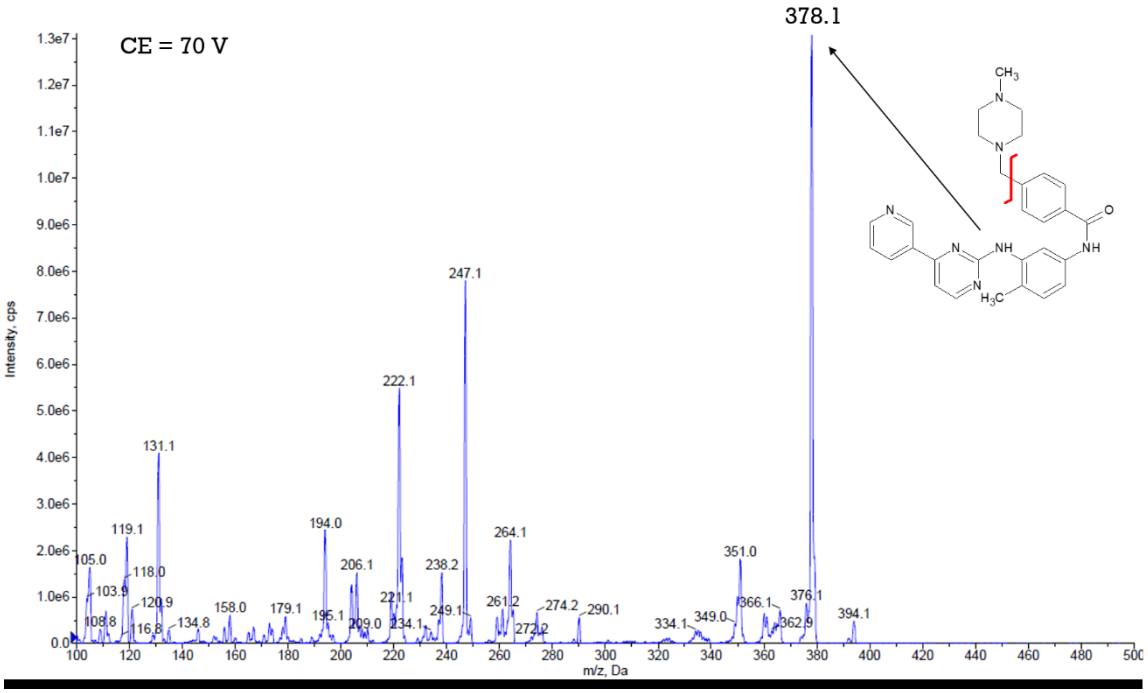

Figure 33. Spectrum recorded in product ion mode showing the fragmentation pattern of IMA precursor ion at 494.4 *m/z* with a CE value of 70 V. Due to the high energy value, the precursor ion is totally fragmented.

To verify the signal intensity of the SRM transition involving the production of these three fragments and to evaluate the optimal CE value for each of them, an MRM scan was performed: the CE value was ramped from 5 to 130 V while the XICs of the following SRM transitions were monitored:

494.4>394.2 *m/z;*

494.4>217.2 *m/z;*

494.4>378.1 *m/z.*

As can be seen in figure 33, the transition 494.4>394.2 *m/z* reached the highest signal intensity and so was selected as the quantifier transition while the other two, showing a lower signal, were selected as qualifiers for the identity confirmation of the analyte.

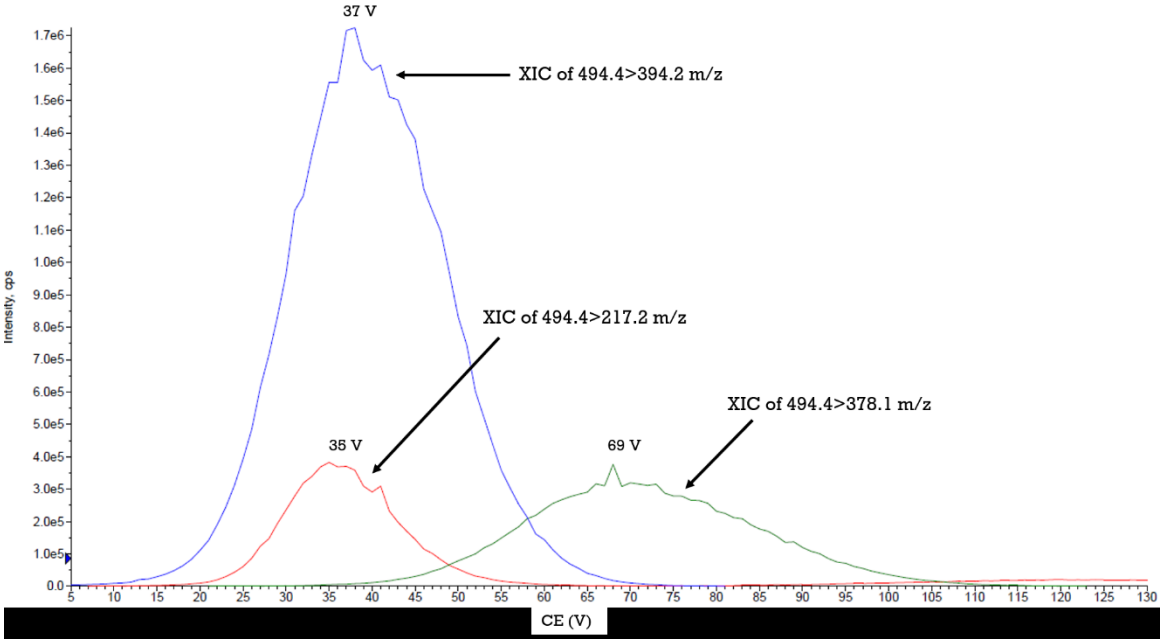

Figure 34. Intensity signal obtained in MRM mode following the transition from the precursor ion at 494.4 *m/z* to the three selected product ions. The XIC intensity of each transition is reported as a function of the CE variation.

The optimal CE values for the formation of each fragment were (figure 34):

37 V for the quantifier product ion at 394.2 *m/z;*

35 V for the first qualifier product ion at 217.2 *m/z;*

69 V for the second qualifier product ion at 378.1 *m/z.*

An optimal CXP value of 10 V for each of the three SRM transitions were obtained thanks to a similar experiment (see section 3.2.2.1).

Moreover, with the precursor ion scan mode it was possible to confirm the direct derivation of the three selected product ions from the precursor ion at 494.4 *m/z*.

The optimized compound-dependent parameters of IMA are reported in table 6.

Precursor ion			Product ions		
Q1 (*m/z*)	DP (V)	EP (V)	Q3 (*m/z*)	CE (V)	CXP (V)
494.4	130	10	394.2	37	10
			217.2	35	10
			378.1	69	10

Table 6. Optimized compound-dependent parameters of IMA.

The monoisotopic mass of NOR IMA is equal to 479.24 Da, so, with the TIS source in positive ion mode, during the first Q1 scan, the presence of the analyte of interest in the infused solution was confirmed by the pseudo-molecular ion $[M+H]^+$ at 480.4 *m/z* (figure 35).

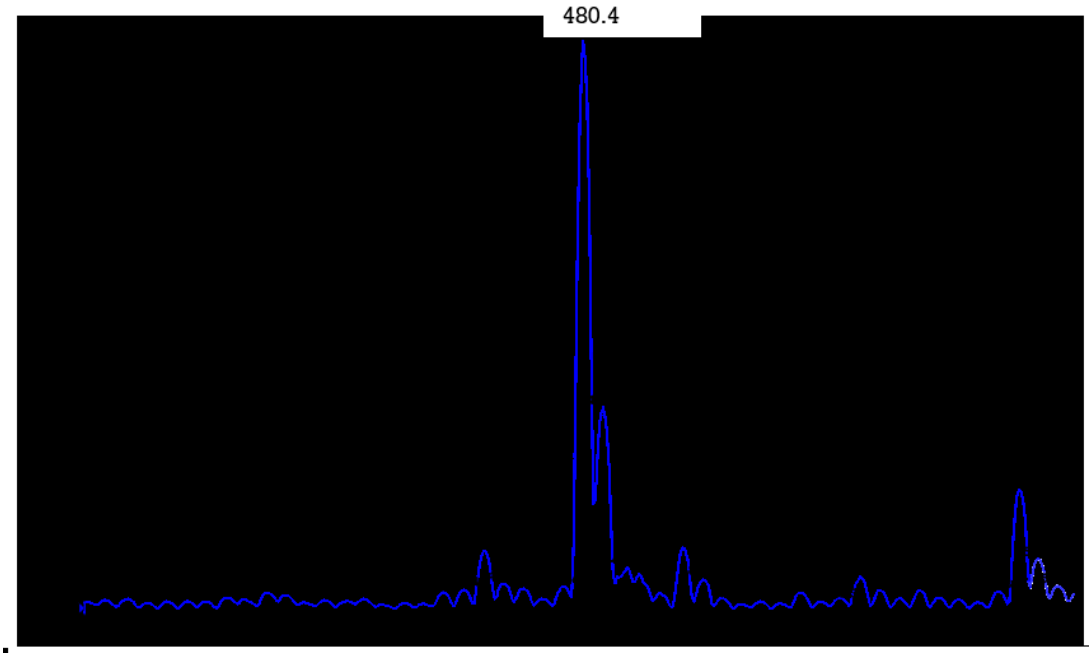

Figure 35. Spectrum obtained in positive mode with a Q1 scan from 450 to 650 Da that confirms the presence of NOR IMA (zoom from 455 to 505 *m/z* to see the isotopic pattern of the pseudo-molecular ion at 484.4 *m/z*).

Through Q1MI scan mode, the XIC signal of the pseudo-molecular ion at 480.4 *m/z* was monitored ramping the DP value from 0 to 400 V. The XIC highest intensity was reached with DP = 110 V (figure 36). In the same way the value of 10 V was determined as optimal for EP.

In Product ions (MS2) mode, the fragmentation of the IMA precursor ion was evaluated with different CE values (from 10 to 100 V) applied into the collision cell.

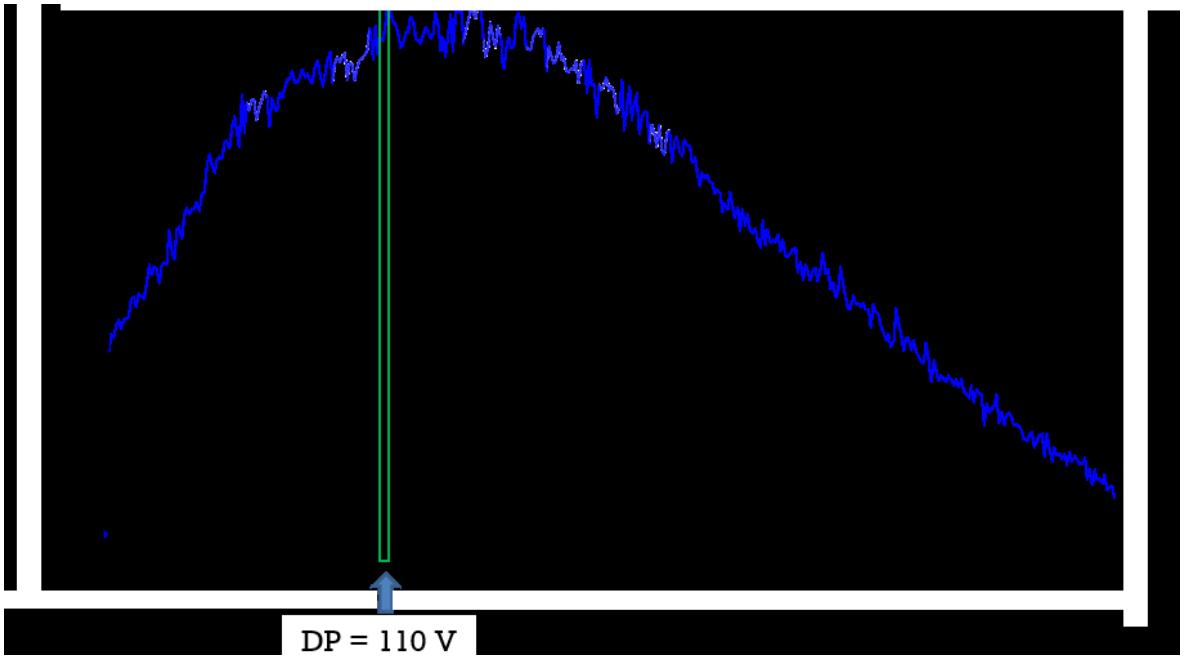

Figure 36. Intensity signal obtained in positive ion mode with Q1 in SIM for 480.4 *m/z*. The apex of the XIC trend was reached at the optimal DP value of 110 V.

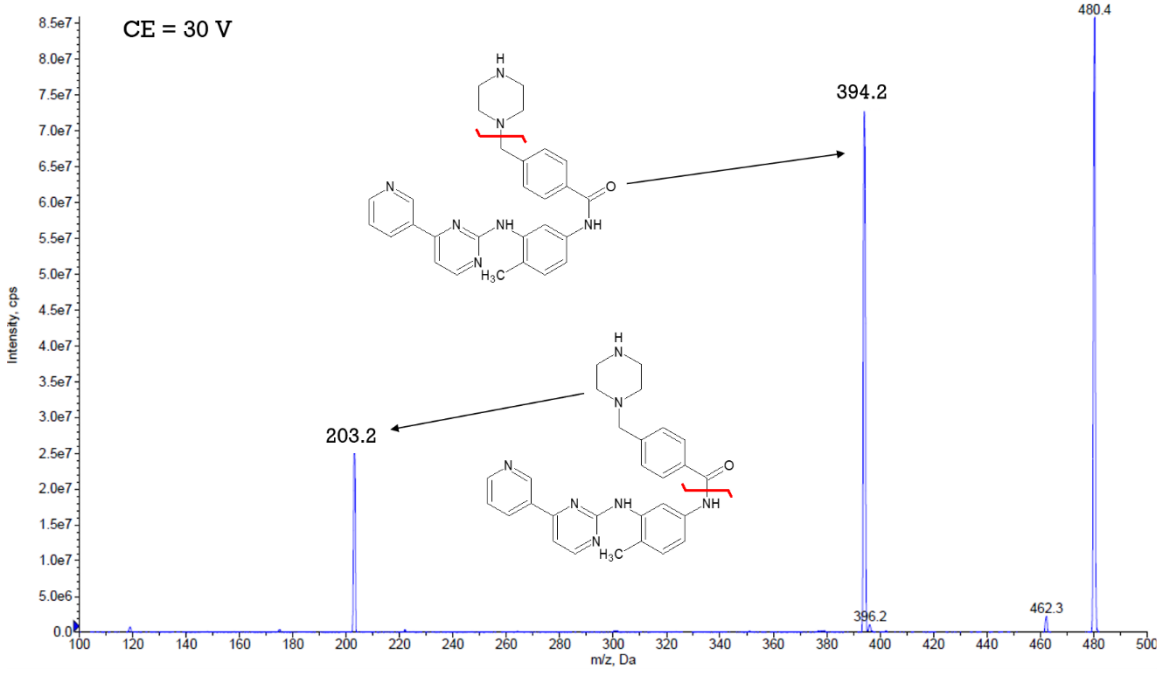

Figure 37. Spectrum recorded in product ion mode showing the fragmentation pattern of NOR IMA precursor ion at 480.4 *m/z* with a CE value of 30 V. The graphic representation of the bond breakage is also shown.

In figure 37, with 30 V of CE applied, the most abundant product ions were found at 394.2 and 203.2 *m/z*, while a third fragment with a similar abundance to the latter was found with 70 V of CE at 378.1 *m/z* (figure 38).

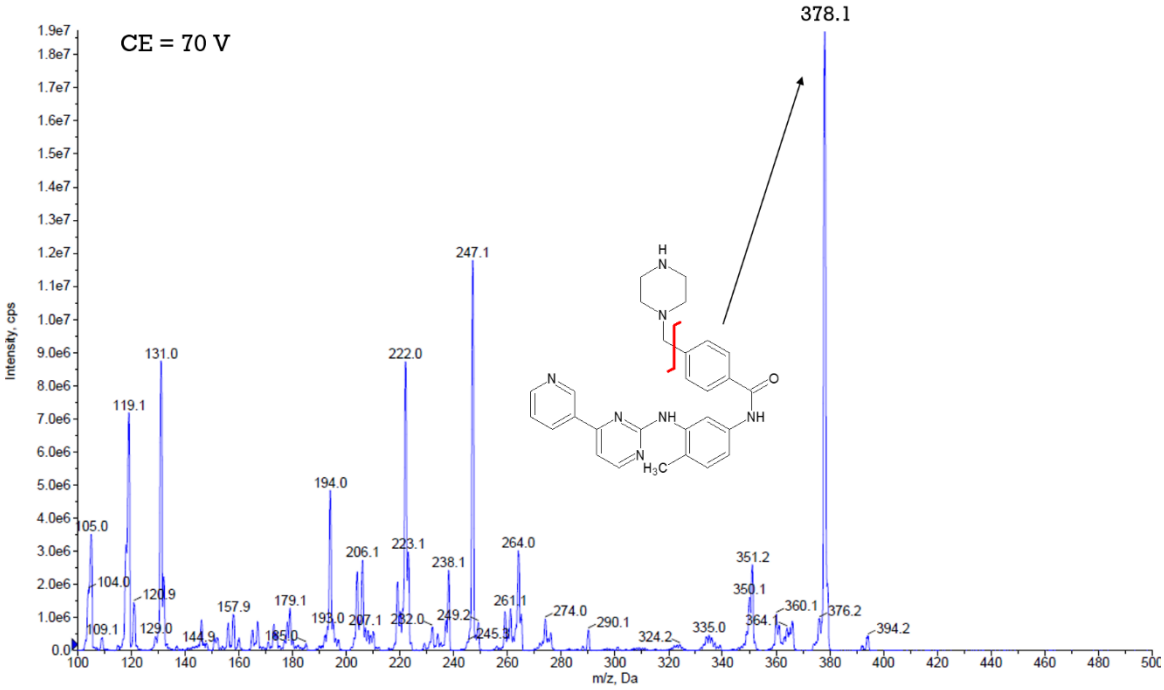

Figure 38. Spectrum recorded in product ion mode showing the fragmentation pattern of NOR IMA precursor ion at 480.4 *m/z* with a CE value of 30 V.

To verify the signal intensity of the SRM transition involving the production of these three fragments and to evaluate the optimal CE value for each of them, an MRM scan was performed: the CE value was ramped from 5 to 130 V while the XICs of the following SRM transitions were monitored:

480.4>394.2 *m/z;*

480.4>203.2 *m/z;*

480.4>378.1 *m/z.*

As can be seen in figure 39, the transition 480.4>394.2 reached the highest signal intensity and so was selected as the quantifier transition while the other two, showing a lower signal, were selected as qualifiers for the identity confirmation of the analyte.

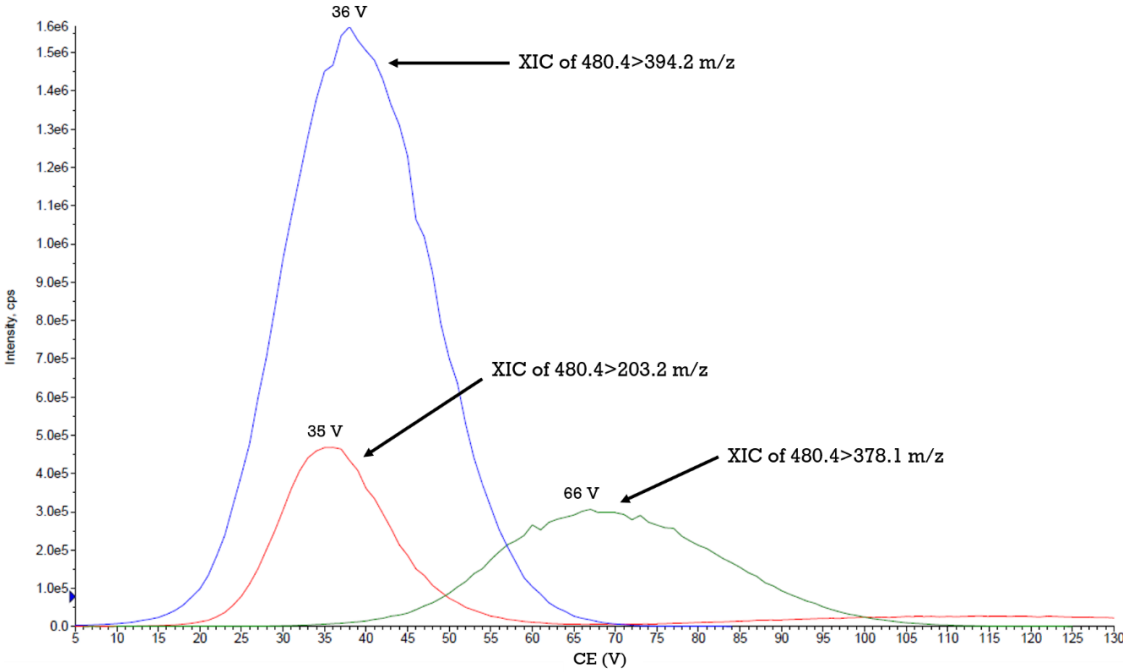

Figure 39. Intensity signal obtained in MRM mode following the transition from the precursor ion at 480.4 *m/z* to the three selected product ions. The XIC intensity of each transition is reported as a function of the CE variation.

The optimal CE values for the formation of each fragment were (figure 39):

36 V for the quantifier product ion at 394.2 *m/z;*

35 V for the first qualifier product ion at 203.2 *m/z;*

66 V for the second qualifier product ion at 378.1 *m/z.*

An optimal CXP value of 10 V for each of the three SRM transitions were obtained thanks to a similar experiment (see section 3.2.2.1).

Moreover, with the precursor ion scan mode it was possible to confirm the direct derivation of the three selected product ions from the precursor ion at 480.4 *m/z*.

The optimized compound-dependent parameters of NOR IMA are reported in table 7.

Precursor ion			Product ions		
Q1 (*m/z*)	DP (V)	EP (V)	Q3 (*m/z*)	CE (V)	CXP (V)
480.4	110	10	394.2	36	10
			203.2	35	10
			378.1	66	10

Table 7. Optimized compound-dependent parameters of NOR IMA.

The compound dependent parameters for the IS IMA-D8 were determined with the same experiments carried out for the analytes and the results are summarised as follows: the monoisotopic mass of IMA-D8 is equal to 501.65 Da, therefore its presence was confirmed by the pseudo-molecular ion $[M+H]^+$ at 502.4 *m/z*. The optimal DP and EP values were equal to 75 V and 10 V, respectively.
The transition selected for the quantification corresponded to 502.4>394.2 *m/z*, while the two qualifier transitions corresponded to 502.4>225.2 and 502.4>378.1 *m/z*. The optimal CE and CXP values for each SRM transition were:

for 502.4>394.2: CE=38 V and CXP=10 V;
for 502.4>225.2: CE=36 V and CXP=10 V;
for 502.4>378.1: CE=72 V and CXP=10 V.

The optimized compound-dependent parameters of IMA-D8 are reported in table 8:

Precursor ion			Product ions		
Q1 (*m/z*)	DP (V)	EP (V)	Q3 (*m/z*)	CE (V)	CXP (V)
502.4	75	10	394.2	38	10
			225.2	36	10
			378.1	72	10

Table 8. Optimized compound-dependent parameters of IMA-D8.

4.1.1.2 Source-dependent parameters optimization

The goal of this experiment was to reach the maximum signal intensity in order to achieve the greatest sensitivity for the analyte of interest in a more realistic working condition. To do that, with the LC-MS/MS apparatus set as described in section 3.2.2.2, a 200 ng/mL solution of IMA in MeOH was infused at 15 µL/min and diluted in a flow of MP composed by 0.1% HCOOH v/v in a mixture of H_2O/MeOH/iPrOH 50:45:5 v/v/v characterised by a flow rate of 400 µL/min. The XIC trend of IMA quantifier transition (494.4>394.2 *m/z*) was monitored by working in SRM mode, thus tuning each source dependent parameter to obtain the highest signal intensity. First, as reported in figure 40, the best TEM value was selected by increasing it from

100 to a maximum of 650 °C in 12 steps that lasted 1 min each (to allow the temperature stabilization).

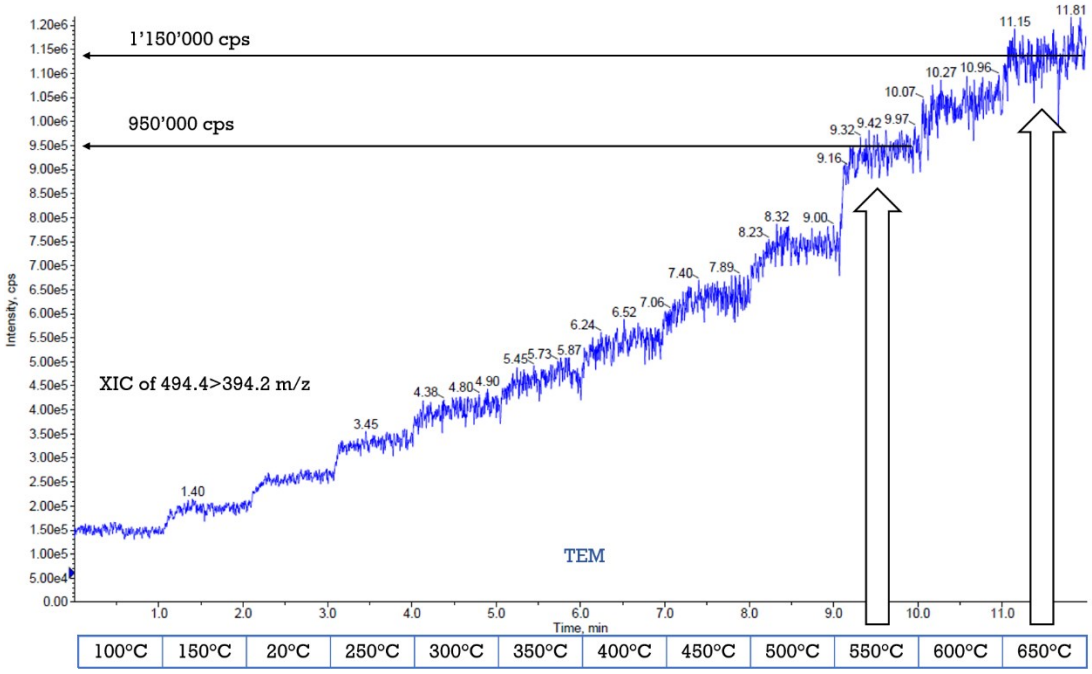

Figure 40. XIC trend of IMA during the variation of the TEM from 100 to 650 °C in 12 steps.

The maximum signal intensity was observed at 650 °C, but 550 °C was selected as the optimal value, as it represented the right balance between a good signal (noticeably higher than the one at 500 °C) and a minor stress for the turbo-heaters.

Regarding CUR, it should have the highest possible value (not lower than 20 psi) to prevent the solvents, or contaminants from entering the analyser. The optimal CUR value was found at 25 psi because, at higher values, a noticeable decrease in the signal was observed.

CAD parameter, which regulates the neutral gas used for the CID process, was left at 8 (medium intensity) because no improvements were observed by deviating from it.

In a similar manner to TEM, the optimal IS value was searched by increasing it from 1500 to 5500 V in ten steps (figure 41). Generally, 5500 V is the value that gives the best ionization yield but, in the case of IMA, the highest XIC intensity was obtained at 2000 V, a value significantly lower than expected.

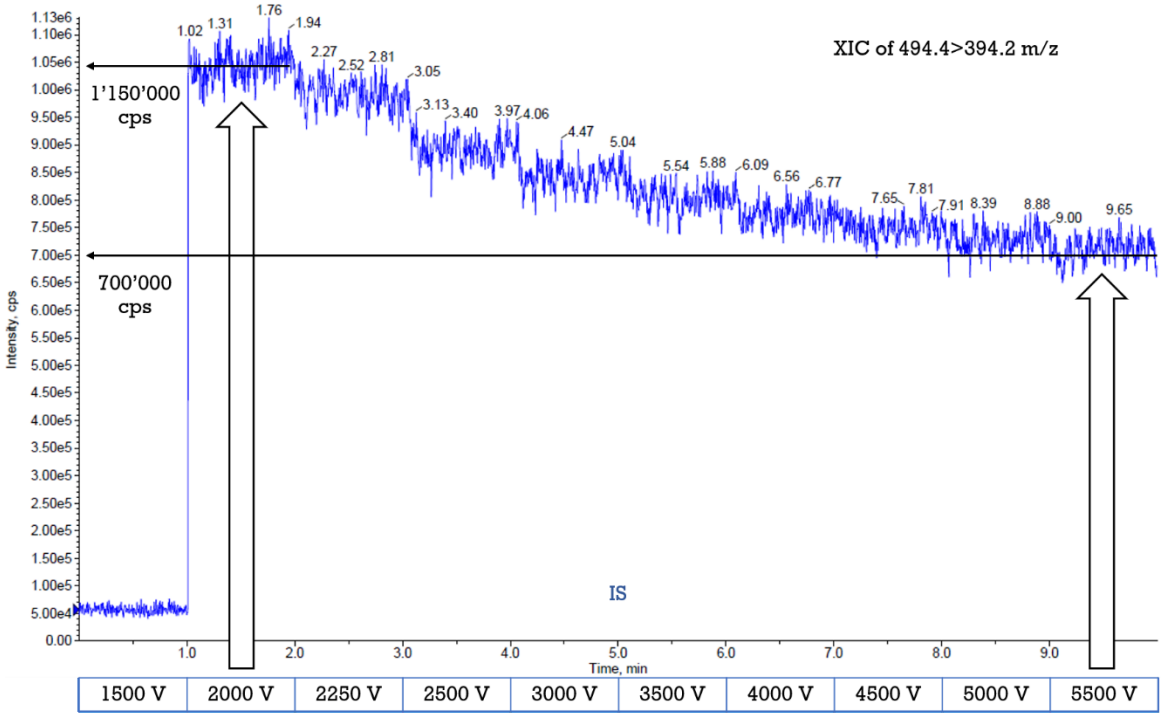

Figure 11. XIC trend of IMA during the variation of the IS from 1'500 to 5'500 V in 10 steps.

Finally, GS1 and GS2 pressures were tuned together by paying attention not to exceed, as summation, the value of 100 psi which is the N_2 generator limit. Various combinations were tested but only GS1: 30 psi and GS2: 60 psi led to a stable and high XIC signal.

The compound- and source-dependent parameters obtained during the process of optimization are reported in table 9 and 10.

Analytes	Precursor ions			Product ions		
	Q1 (*m/z*)	DP (V)	EP (V)	Q3 (*m/z*)	CE (V)	CXP (V)
IMA	494.4	130	10	394.2	37	10
				217.2	35	10
				378.1	69	10
NOR IMA	480.4	110	10	394.2	36	10
				203.2	35	10
				378.1	66	10
IMA-D8	502.4	75	10	394.2	38	10
				225.2	36	10
				378.1	72	10

Table 9. Optimal values of each compound-dependent parameter for IMA, NOR IMA and IMA D8.

Polarity	Positive
CUR	25 psi
CAD	8
IS	2'000 V
TEM	550 °C
GS1	30 psi
GS2	60 psi

Table 10. Optimal values of each source-dependent parameter.

4.1.2 Chromatographic conditions optimization

The development of a chromatographic method implies the determination of the best chromatographic conditions for the separation of two or more analytes. Considering that in this analytical method the detection would be performed with a triple quadrupole analyser (capable of precisely quantifying two co-eluting compounds, contrary to UV detectors), a high chromatographic resolution (R) was not necessary. Anyway, cross-talking issues in some circumstances might occur and the quantification of two co-eluting analytes entails the scan time split between the two, thus halving the number of data points describing each peak. For this reason, a minimum degree of separation between IMA and NOR IMA was required. Other two parameters that were considered during the development of the chromatographic method were the duration of the total run time and the peak width: to obtain narrow peaks gives an advantage for the overall sensitivity and to reduce the overall run time makes the assay less time-consuming.

The column chosen was a Synergi Fusion-RP (4 µm, 80 Å, 50 x 2.0 mm), because of the small internal volume (less than 110 µL) which allowed short equilibration times together with an acceptable sacrifice in R. The SP contained into the column was C18, which offered an adequate hydrophobic selectivity for compounds like IMA and NOR IMA, which only differ for a methyl group. Moreover, the relatively large particle size of 4 µm reduced the system back-pressures during the MP flow rate. In this way, higher flow rates were possible thus leading to shorter equilibration time and, consequently, shorter total run time. This RP column was also coupled with a Fusion-RP security-guard pre-column (4 x 2.0 mm) to block the coarser particles which might come from biological samples and the MP.

Given that IMA was scarcely soluble in MeCN, MeOH was chosen as strong solvent. From preliminary tests (data not shown), the addition of 10% v/v of iPrOH led to peak shape improvements for both IMA and NOR IMA without increasing the back-pressure too much. As weak solvent, type 1 ultrapure H_2O was selected for overall better SNRs. Moreover, both the solvents were added with 0.1% HCOOH v/v to help the ionization of the analytes.

The selected flow rate was 400 µL/min and the column oven was set at 50 °C. High column temperatures increase the efficiency and at the same time help lowering the MP viscosity, which was helpful considering that a mixture of MeOH and iPrOH is way more viscous than MeCN.

Regarding the elution method, the totally isocratic one was discarded because of the poor cleanness of the sample to be analyzed. In fact, the planned extraction method was PP, characterised by a rather dirty extract. The need to constantly clean the column from the interferents carried by the samples injected, led to the choice of a multi-step method (see figure 21 in section 3.2.3).

At the beginning, the initial conditions were the following ones:

- MPA: 0.1% HCOOH v/v in H_2O;
- MPB: 0.1% HCOOH v/v in MeOH/iPrOH 9:1 v/v;
- Column: Synergi Fusion-RP + Fusion-RP security-guard;
- Oven temperature: 50 °C;
- Flow rate: 400 µL/min;
- Equilibration condition: 1% MPB.

The elution step was the first to be tuned, by starting with a long gradient, after a 1 min equilibration step, from 1 to 60% of MPB in 4 min (method A). This method was then compared with a steeper gradient (from 1 to 99% of MPB in 4 min, method B) and, as reported in figure 42, both methods produced a too delayed elution considering the desired short total run time. Moreover, while with method B the analytes eluted earlier, the two peaks exceeded acceptable overlap with a poor R value of 0.5.

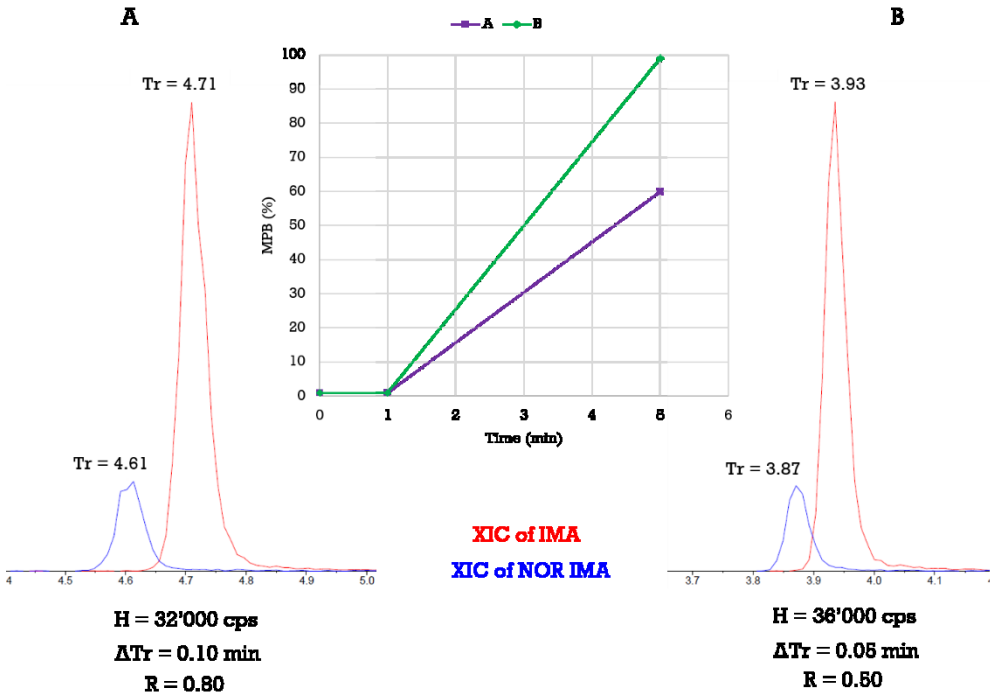

Figure 42. Comparison between the peaks produced by two gradient methods with different slopes. For each method, both sensitivity (reported as peak height, H) and R were reported.

The same gradients were explored by changing the starting condition from 1 to 10% of MPB (figure 43) to anticipate the elution time without lowering R.

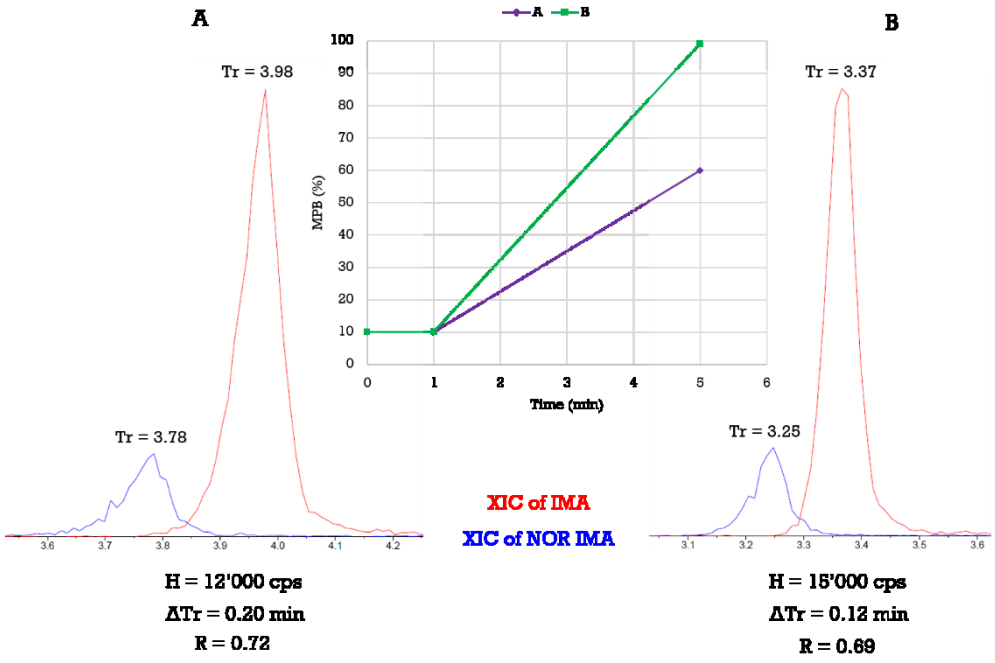

Figure 43. Comparison between the peaks produced by two gradient methods with different slopes. For each method, both sensitivity (reported as peak height, H) and R were reported.

As can be seen in figure 43, the peaks eluted earlier but their widths were too much large with a consequent loss in sensitivity: the peak height shifted from more than 30'000 cps (starting with 1% of MPB) to less than 20'000 cps.

To break the deadlock, also the isocratic regime for the elution step was explored: considering that IMA and NOR IMA eluted with a percentage of MPB ranging from 40 to 50% (estimation made by analysing the gradient method in figure 43A), the two isocratic elutions reported in figure 44 were tested.

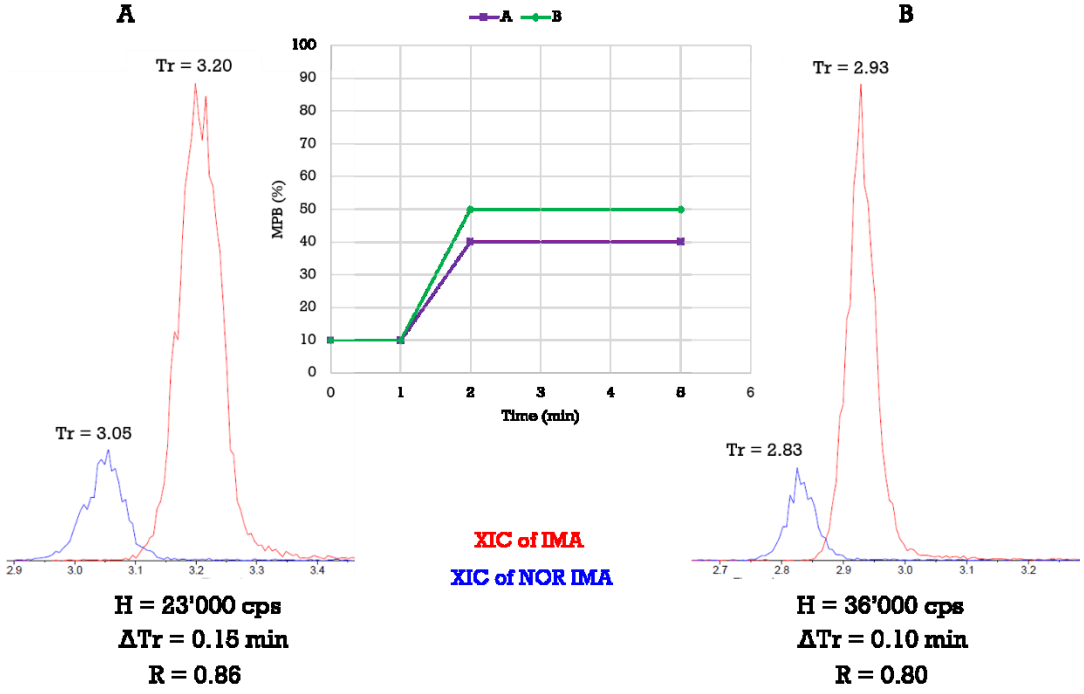

Figure 44. Comparison between the peaks produced by two isocratic elutions with different percentage of MPB. For each method, both sensitivity (reported as peak height, H) and R were reported.

As can be seen, with method B a noticeable gain in sensitivity was obtained compared to A without losing too much in terms of R. That meant a still acceptable overlap and furthermore both IMA and NOR IMA eluted earlier.

Finally, in order to further anticipate the T_r of the analytes in the elution method B (figure 44), a new method was created by avoiding the first conditioning step (lasting 1 min). From the comparison of these last two methods (figure 45), the differences in terms of sensitivity and R were negligible with the exception that, as could be easily expected, with method B the analytes eluted 1 min earlier. For this

reason, the elution method shown in figure 45B was selected as first part of the multi-step chromatographic method.

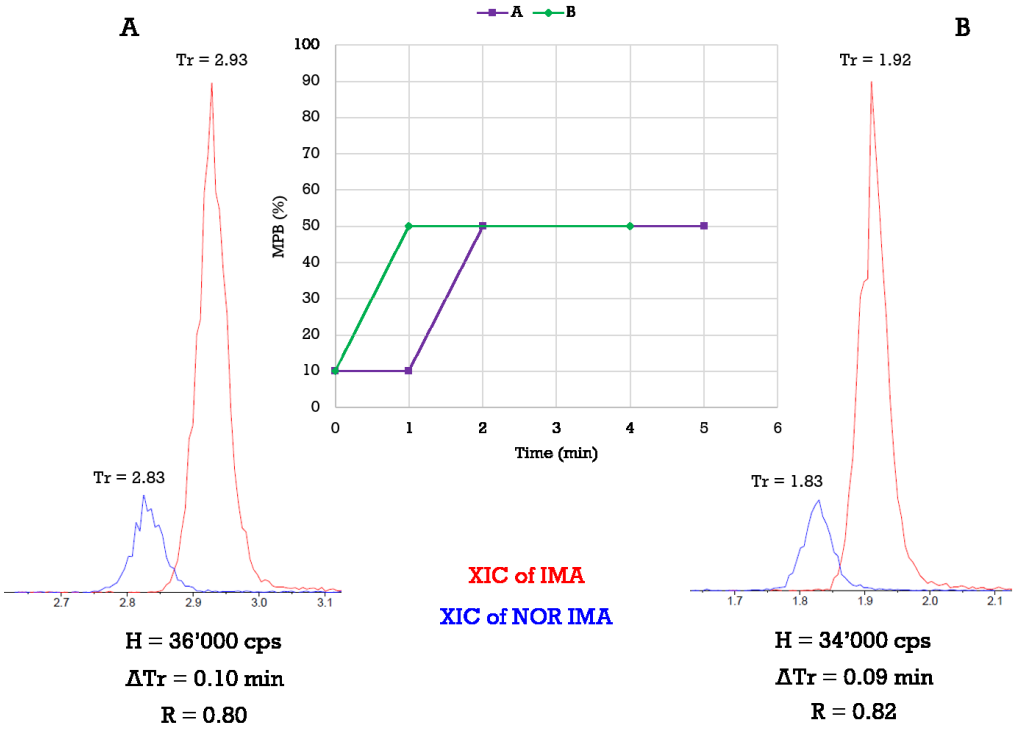

Figure 45. Comparison between the peaks produced by two isocratic elutions: the former (A) with the initial conditioning step and the latter (B) without it. For each method, both sensitivity (reported as peak height, H) and resolution (R) were reported.

Just after the elution of IMA, a washing step with 99% of MPB was introduced. The aim was the elution of the most lipophilic interferents generally present in plasma (e.g. protein residues and phospholipids). During this step, the total flow rate was increased from 400 to 500 µL/min for a stronger wash and, at first, the length was set to 0.75 min. As reported in section 3.2.3, to check the cleaning effectiveness, the elution of three of the most abundant PLs was monitored during the chromatographic run. As can be seen in figure 46, 0.75 min were not enough for an effective removal of the three PLs because they showed a changeable elution profile after consecutive injections.

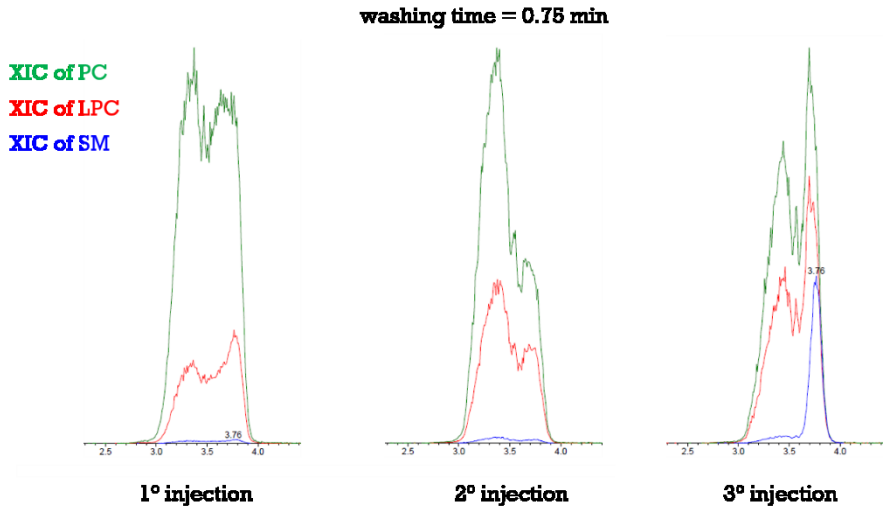

Figure 46. MRM chromatograms of three of the most abundant PLs in human plasma during 0.75 min of wash step from 3 consecutive injections. PC is phosphatidyl choline, LPC is lysophosphatidyl choline and SM is sphingomyelin.

By doubling the washing step duration (figure 47), the elution profile of the 3 PLs remained constant between consecutive injections, thus indicating a correct PLs removal and a more effective cleaning.

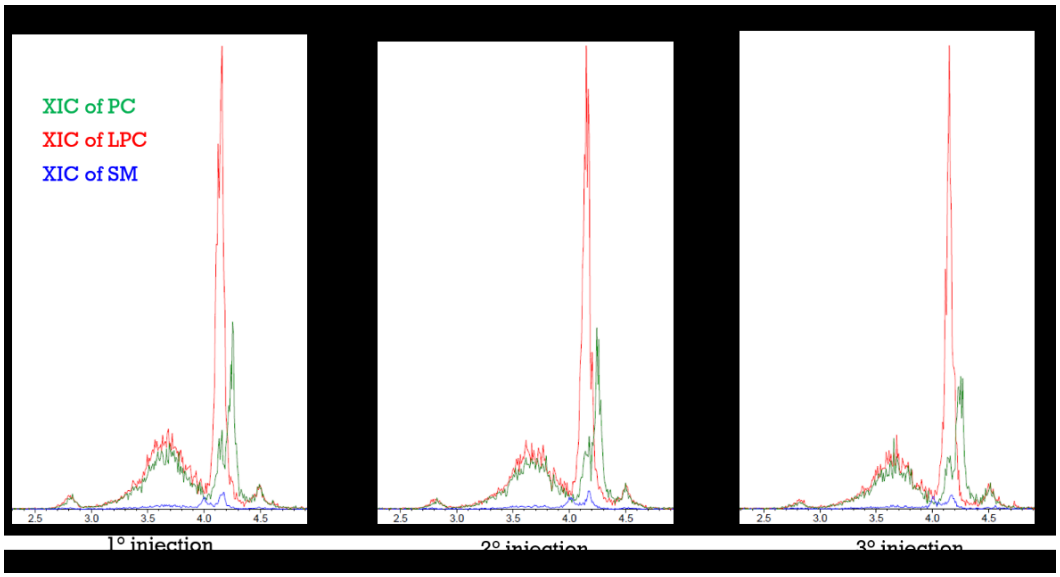

Figure 47. MRM chromatograms of the elution of three of the most abundant PLs in human plasma during 1.50 min of wash step from 3 consecutive injections.

Finally, for the re-equilibration step, the duration selected was 4 min at the same total flow-rate of the wash step. Considering a column volume of about 110 µL, during 4 min at 500 µL/min more than 15 column volumes of MP flow through the

SP, thus allowing a correct re-equilibration. In fact, after consecutive injections, the T_r of both IMA and NOR were reproducible.

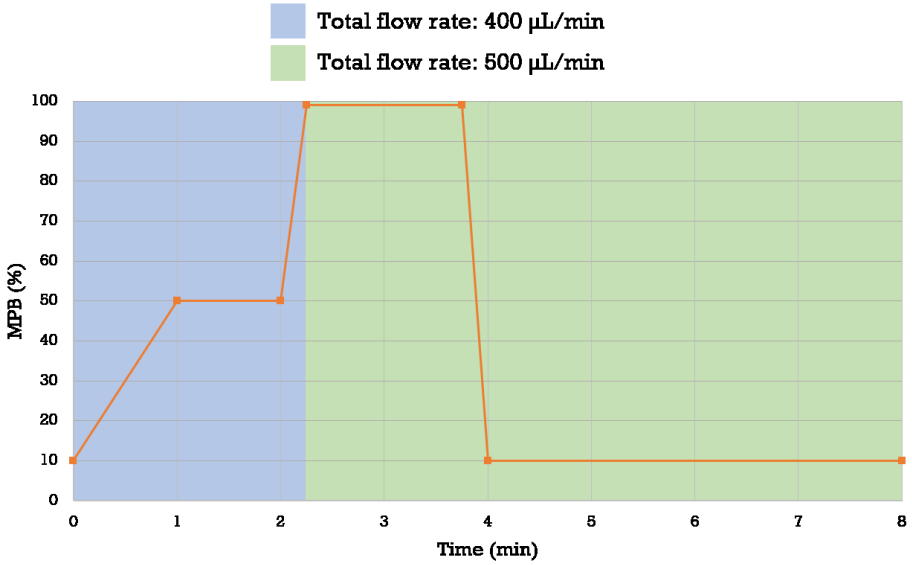

Figure 48. Schematic representation of the developed chromatographic method. The different colors underline the change in total flow rate.

In figure 48, the fully optimized multi-step chromatographic method is reported while an example of an MRM chromatogram, produced by the analysis of a plasma calibrator with the developed LC-MS/MS method, is shown in figure 49.

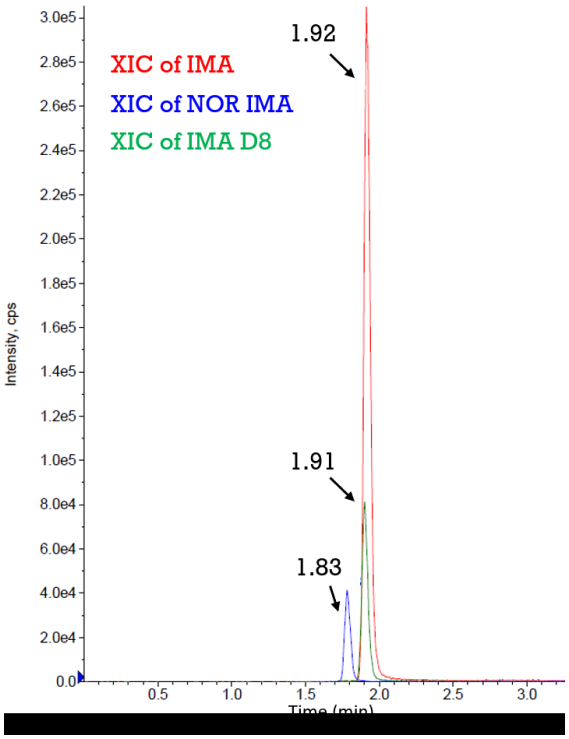

Figure 49. MRM chromatogram of the calibrator C obtained with the developed LC-MS/MS method.

4.1.3 Sample preparation for quantitative analysis

4.1.3.1 Sample extraction optimization

As sample extraction method, PP was chosen because of its speed and simplicity: the possibility to simultaneously minimize errors during preparation and perform a fast sample processing is welcome in the TDM practice. MeOH was selected as the solvent for the PP and it was added in a ratio of 50:1 v/v with respect to the volume of the plasma sample to be extracted (e.g. 1 mL of MeOH was added to 20 µL of plasma sample for the PP). With those proportions, it was possible at the same time to obtain an excellent SNR on the LLoQ of both IMA and NOR IMA (42.3 and 20, respectively, as reported in figure 50) and to avoid the detector saturation during the analysis of the ULoQ.

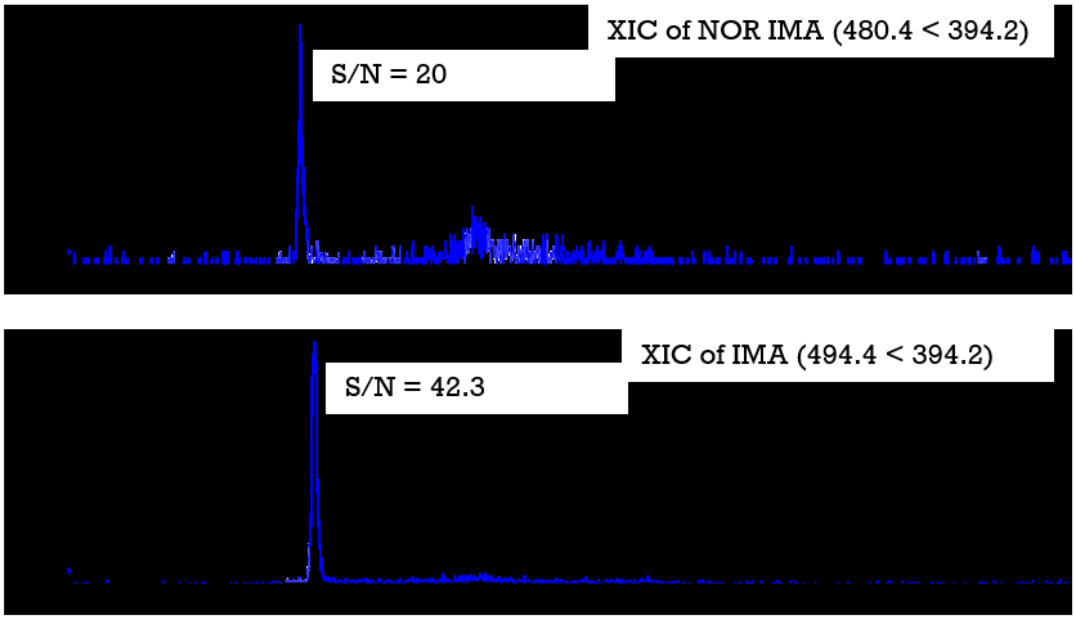

Figure 50. MRM chromatogram of an LLoQ sample reporting the SNR values of both IMA and NOR IMA.

In fact, as reported in figure 51, the signal intensity of IMA during the analysis of the calibrator A (i.e. the ULoQ) was far below the detector saturation limit (2-3 x 10^6 cps). The consequence was an instrumental response which was linear for the whole expected concentration range.

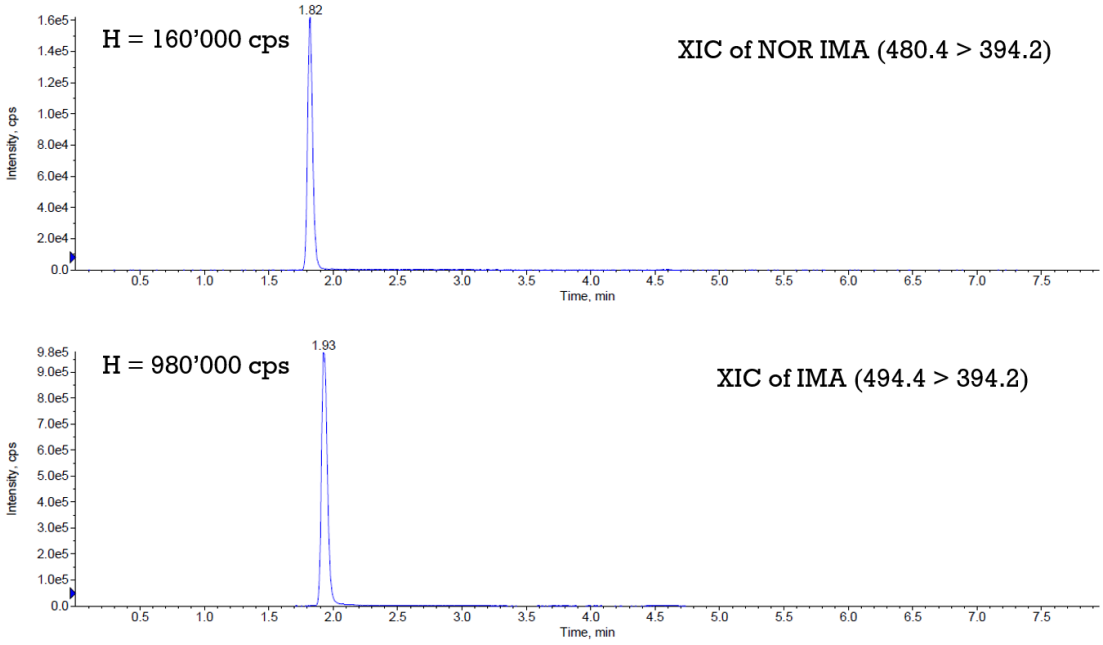

Figure 51. MRM chromatogram of a ULoQ sample reporting the signal intensity (or peak height) of both IMA and NOR IMA.

During the optimization of the sample extraction method, other solvent:sample dilution ratios were tested too. From 5:1 to 40:1 ratio, they were not suitable because, even injecting only 1 µL of the highest calibrator, the signal obtained led to the detector saturation. From 60:1 to 80:1 ratio, NOR IMA was not quantifiable at LLoQ levels.

4.1.3.2 Working solutions preparation

Two different sets of stock solutions for IMA and NOR IMA were prepared in DMSO at the concentration of 6.0 and 1.2 mg/mL respectively. By mixing together the solutions of the first set and diluting the mix with MeOH, seven WSs for the preparation of calibrators were obtained with the following concentrations: 600, 2'000, 5'000, 15'000, 30'000, 60'000, 150'000 ng/mL and 120, 400, 1'000, 3'000, 6'000, 12'000, 30'000 ng/mL (from G to A) for IMA and NOR IMA respectively. Stock solutions belonging to the second set were mixed together and diluted with MeOH obtaining three WSs for the preparation of quality controls (QCs) with the following concentrations: 1'200, 20'000, 120'000 ng/mL and 240, 4'000, 24'000 ng/mL (L, M, H) for IMA and NOR IMA respectively. The stock solution for IMA D8 was prepared in DMSO at a concentration of 1.0 mg/mL and was diluted with MeOH to 500 ng/mL

obtaining the IS WS. All the solutions have been kept in polypropylene tubes and stored at -80 °C.

4.1.3.3 Calibrators and quality controls preparation

A seven-point calibration curve in plasma was prepared freshly every day during the validation study. For each calibrator, 1 µl of the respective WS from G to A was spiked to 19 µl of pooled blank human plasma to obtain the final concentrations reported in table 11.

Sample types	IMA (ng/mL)	NOR IMA (ng/mL)
G	30	6
F	100	20
E	250	50
D	750	150
C	1'500	300
B	3'000	600
A	7'500	1'500
QC L	60	12
QC M	1'000	200
QC H	6'000	1'200

Table 11. Final concentration values of calibrators and QCs for both IMA and NOR IMA.

Each calibration curve included a blank sample (plasma processed without IS) and a zero-blank sample (plasma processed with the IS). QCs were used at least in triplicate for each concentration level and to prepare them, 1.14 mL aliquots of control human plasma were mixed with 60 µL of each WS (L, M and H) obtaining the final concentrations reported in table 11. Several 20 µL-aliquots of the three QCs have been stored at –80 °C to check the stability of the analytes and as controls for future assays.

4.2 LC-MS/MS validation study

The main parameters considered for the validation of this method, accordingly with the FDA and EMA guidelines, were: recovery, linearity of the calibration curve, intra- and inter-day precision and accuracy, limit of quantification, selectivity, stability and reproducibility.

4.2.1 Recovery

The employed extraction method is based on a fast and simple protein precipitation with 50 volumes of MeOH (related to the plasma sample). In table 12, the results of this experiment are reported: the recovery, evaluated in five replicates at three QC concentration levels, was from 86.7 to 92.4% (CV≤8.8%) and from 86.3 to 90.4% (CV≤6.6%) for IMA and NOR IMA, respectively. The recovery of IS was evaluated in five replicates at a concentration of 500 ng/mL and accounted for 101.7 % (CV 5.6%).

Analyte	Nominal concentration (ng/mL)	Recovery (%) ± SD	CV%
IMA	60	92.4 ± 8.1	8.8
	1'000	86.7 ± 7.6	8.7
	6'000	89.0 ± 5.1	5.8
NOR IMA	12	90.4 ± 3.8	4.2
	200	87.0 ± 3.9	4.5
	1'200	86.3 ± 5.7	6.6
IMA-D8 (IS)	500	101.7 ± 5.7	5.6

Table 11. Recovery of the analytes and the IS from human plasma.

4.2.2 Linearity

The calibration curves of IMA and NOR IMA, were freshly prepared every day during the validation study, and showed a good linearity. To generate a calibration curve like the one reported in figure 52, the peak-area ratios between the analyte and the IS compared to the nominal concentrations were plotted and a least-squares linear regression, weighted by the reciprocal of the concentrations, were plotted and a weighted quadratic regression function ($1/x^2$) was applied. The calibration curves prepared on five different days showed good linearity and acceptable

results of the back-calculated concentrations over the validated range of 30–7'500 ng/mL for IMA and 6-1'500 ng/mL for NOR IMA (table 13).

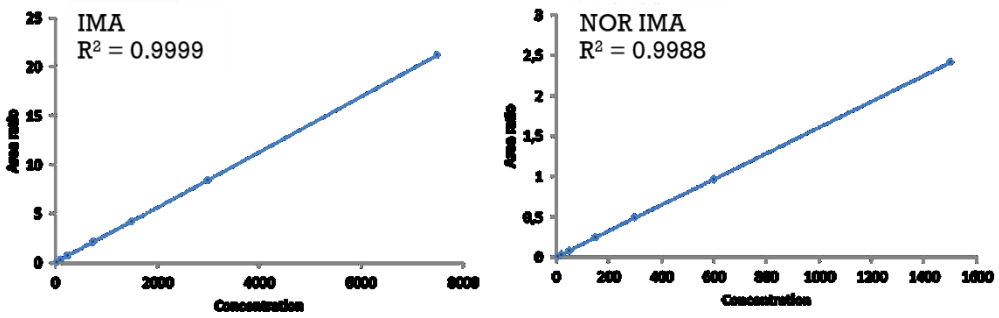

Figure 52. Example of a calibration curves of IMA and NOR IMA in human plasma.

Pearson's coefficient of determination R^2 was ≥0.9939 for each run, the mean accuracy ranges from 96.2 to 103.6% for IMA and from 94.2 to 109.5% for NOR IMA while the precision, expressed as CV%, ranged from 1.4 to 5.9% and from 2.0 to 6.0% for IMA and NOR IMA respectively. The injection of four blank samples after the ULoQ minimized the impact of the carryover effect: no peaks higher than 20% of LLoQ were observed before a sample injection.

Analytes	Nominal concentration (ng/mL)	Mean ± SD	CV%	Accuracy %
IMA	30	30.22 ± 0.42	1.4	100.7
	100	98.83 ± 4.72	4.8	98.8
	250	240.61 ± 10.64	4.4	96.2
	750	777.06 ± 43.00	5.5	103.6
	1'500	1'524.35 ± 90.66	5.9	101.6
	3'000	2'940.27 ± 168.32	5.7	98.0
	7'500	7'548.57 ± 305.64	4.0	100.6
NOR IMA	6	6.15 ± 0.12	2.0	102.5
	20	19.06 ± 0.95	5.0	95.3
	50	47.17 ± 1.66	3.5	94.3
	150	150.33 ± 9.03	6.0	100.2
	300	297.44 ± 15.60	5.2	99.1
	600	588.28 ± 35.02	6.0	98.0
	1'500	1'642.81 ± 60.72	3.7	109.5

Table 12. Linearity, accuracy, and precision data for calibration curves of IMA and NOR IMA in human plasma.

4.2.3 Intra-day and inter-day precision and accuracy

The precision and accuracy of the method were evaluated by analysing three replicates of QC samples (QCL, QCM and QCH) within a single-run analysis for intra-day (or within-run) assessment and between five consecutive runs for inter-day (or between-run) assessment. The accuracy and precision (CV%) obtained are shown in Table 14.

	Analytes	Nominal concentration (ng/mL)	Mean ± SD	CV%	Accuracy %
Intra-day SUN (N=5)	IMA	60	64.75 ± 1.95	3.0	92.7
		1'000	954.74 ± 44.79	4.7	104.7
		6'000	5'849.01 ± 272.86	4.7	102.6
	NOR IMA	12	12.61 ± 0.81	6.4	95.2
		200	191.03 ± 3.69	1.9	104.7
		1'200	1249.87 ± 72.20	5.8	96.0
Inter-day (N=15)	IMA	60	62.29 ± 2.42	3.9	103.8
		1'000	1009.35 ± 71.25	7.1	100.9
		6'000	5967.77 ± 360.60	6.0	99.5
	NOR IMA	12	12.13 ± 0.88	7.2	101.1
		200	196.10 ± 13.01	6.6	98.0
		1'200	1275.31 ± 82.43	6.5	106.3

Table 13 Intra- and inter-day precision and accuracy of the method for the analysis of IMA and its main metabolite NOR IMA in human plasma samples.

An intra- and inter-day CV≤4.7% and ≤7.1% for IMA and ≤6.4% and ≤7.2% for NOR IMA depicted the method as very precise. Moreover, it was accurate too, thus showing an intra- and inter-day accuracy ranging from 92.7 ad 104.7% and from 99.5 and 103.8% for IMA. A similar accuracy was observed for its main metabolite, with an intra- and inter-day accuracy values ranging from 95.2 to 104.7% and from 98.0 and 106.3%.

4.2.4 Limit of quantification

The LLoQ was defined as the lowest concentration that could be measured (SNR≥5) with a precision within 20% and accuracy between 80% and 120%. Figure 50 in section 4.1.3.1 shows the obtained SNR (20 for IMA and 42.3 for NOR IMA) by analysing a sample at the LLoQ concentration value which, based on the

concentration range expected in patients' samples, was fixed at 30 and 6 ng/mL for IMA and NOR IMA, respectively. Through the analysis of six replicates, both the accuracy and the precision were determined: the quantification of six samples at the LLoQ concentration level showed an accuracy and CV% of, respectively, 92.7% and 10.4% for IMA and 101.0% and 12.1% for NOR IMA.

4.2.5 Matrix effect and selectivity

The method was not significantly affected by endogenous components in the matrix or by others in the sample. In fact, spiking six different sources of human plasma with IMA and NOR IMA at a concentration corresponding to the LLoQ, the precision expressed as CV% was 8.7 and 8.3% for IMA and NOR IMA, respectively and the accuracy was 92.4% for IMA and 94.1% for NOR IMA, respectively. There were no significant variations (<15%) in the peak area of each analyte in the six lots of matrix. Moreover, thanks to the post-column infusion test (figure 24), it was observed that the intensity of the analyte signal (figure 53), infused at a constant concentration, did not undergo variations at the retention time of the analytes. Therefore, it was possible to exclude the presence of any matrix effect of ion suppression or enhancement.

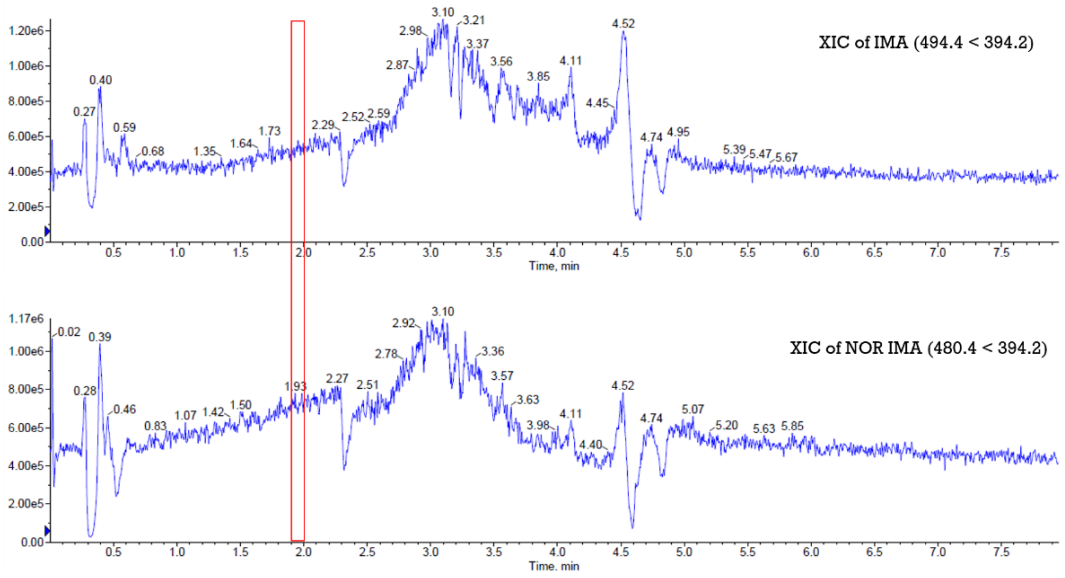

Figure 53. Evaluation of the matrix effect through a post-column infusion experiment: the XIC trend of both IMA and NOR IMA shows both ion enhancement and ion suppression areas. These phenomena did not affect the analytes of interest, whose retention times were highlighted with the red rectangle.

4.2.6 Stability

The stability of IMA and its main metabolite, under different conditions, was assessed by analysing QC samples, prepared in triplicate. The two analytes in human plasma were stable for 4 h at RT (Table 15).

	Analytes	Nominal concentration (ng/mL)	Mean ± SD	CV%	Accuracy %
T = 4 h (RT)	IMA	60	61.81 ± 1.76	2.8	103.0
		1'000	1'093.04 ± 15.71	1.4	109.3
		6'000	5'619.59 ± 198.02	5.3	93.7
	NOR IMA	12	11.31 ± 0.82	7.2	94.2
		200	203.50 ± 4.60	2.3	101.7
		1'200	1'185.84 ± 45.64	3.8	98.8

Table 15. Short term stability of IMA and NOR IMA in human plasma samples at RT.

Concerning the stability in autosampler (set at 4 °C) of the extracted samples, it was assessed for 24 h (table 16), thus allowing analysis of more than 150 samples in a single run without the issue of compound degradation.

	Analytes	Nominal concentration (ng/mL)	Mean ± SD	CV%	Accuracy %
T = 24 h AS (4°C)	IMA	60	59.67 ± 3.91	6.6	99.5
		1'000	1'063.54 ± 94.05	8.8	106.4
		6'000	6'370.64 ± 139.07	2.2	106.2
	NOR IMA	12	11.35 ± 0.06	0.5	94.6
		200	203.37 ± 17.96	8.8	101.7
		1'200	1'378.75 ± 3.66	0.3	114.9

Table 16. Stability of IMA and its main metabolite NOR IMA, in extracted plasma samples, after 24 h of storage into the autosampler set at 4 °C.

IMA and NOR IMA were stable in human plasma over three freeze/thaw cycles: precision as CV% and accuracy were ≤5.7% and within 96.9–108.2%, respectively for IMA and, ≤5.7% and within 106.6–108.6% for NOR IMA (Table 17).

	Analytes	Nominal concentration (ng/mL)	Mean ± SD	CV%	Accuracy %
3 x FT cycles	IMA	60	64.90 ± 3.71	5.7	108.2
		1'000	1090.37 ± 16.46	1.5	109.0
		6'000	5812.34 ± 50.38	0.9	96.9
	NOR IMA	12	12.97 ± 0.74	5.7	108.1
		200	213.27 ± 4.72	2.2	106.6
		1'200	1302.80 ± 14.28	1.1	108.6

Table 17. Stability of IMA and its main metabolite NOR IMA, in human plasma samples, after 3 freeze-thaw cycles.

Several aliquots of QC samples were stored, in the same way as the QC WS, at -80 °C in order to complete the assessment of the long-term stability. This part of the validation (together with the ISR) will be conducted in the next months in order to define the stability of the analytes in plasma and WS at 3, 6 and 9 months.

4.3 Simultaneous quantification of IMA and its main metabolite NOR IMA in GIST patients' plasma for TDM

After the validation, the LC-MS/MS method was considered suitable for the quantification of both IMA and NOR IMA in real samples. In fact, up to 49 plasma samples of patients enrolled in the abovementioned clinical study (see section 3.4.1) were analyzed in a single run. The obtained C_{min} values for both IMA and NOR IMA, with the developed and validated method, are shown in Table 18. As per protocol, for privacy reasons each patient was identified with a progressive number based on the enrollment order. Each plasma sample was identified with an ID that is composed by the patient identification number followed by the sampling number. By way of example, sample ID 4_3 indicates the plasma obtained from patient number 4 at the third withdrawal.

In the next days, this quantification will be repeated to assess another validation criterion: the ISR. If at least 33 samples (66.7%) will show a percentage difference (%diff) of the results within ±20% compared to the first analysis, the ISR will be a success.

Patient N°	Age	Sex	sample ID	IMA (ng/mL)	NOR IMA (ng/mL)
Pt1	79	M	1_2	859	230
			1_3	709	183
			1_4	1012	252
Pt2	66	M	2_3	1449	277
			2_4	1658	314
Pt4	76	M	4_3	2990	427
			4_4	3358	491
			4_5	2282	307
Pt7	69	F	7_3	< LLOQ	< LLOQ
			7_4	931	215
			7_5	828	197
Pt8	69	M	8_3	760	111
			8_4	708	139
Pt10	61	M	10_3	338	181
			10_4	398	226
			10_5	281	144
Pt12	75	M	12_2	1149	217
			12_3	825	177
			12_4	605	138
Pt14	78	F	14_2	1361	198
			14_3	1174	174
			14_4	1345	201
Pt16	52	F	16_2	1164	205
			16_3	2766	404
Pt17	65	F	17_3	673	152
			17_4	730	137
			17_5	982	176
			17_6	666	153
Pt18	81	F	18_3	896	240
			18_4	848	188
			18_5	1207	284
Pt19	54	F	19_2	700	138
			19_3	770	122
Pt20	63	M	20_2	502	113
Pt21	55	M	21_2	< LLOQ	81
Pt22	52	M	22_1	2617	314
			22_3	700	116
			22_4	1032	196
Pt23	55	M	23_1	171	55
			23_2	548	87
Pt24	52	M	24_1	258	84
			24_2	502	159
Pt25	76	M	25_1	< LLOQ	< LLOQ
Pt26	58	F	26_1	862	282
			26_2	1051	281
Pt27	76	M	27_2	1188	264
			27_3	1243	305
Pt29	76	M	29_1	1330	195
Pt30	44	M	30_2	932	212
Median age, years (median [range]): 65 [44-81]					
Gender (male/female): 15/7					

Table 18. C_{min} values of both IMA and NOR IMA determined in 49 plasma samples from GIST patients employing the developed and validated LC-MS/MS method. Additional data such as age and gender are reported.

4.4 Study of the light-induced geometric isomerization of SUN and N-DES SUN in human plasma by LC-MS/MS

4.4.1 Formation of the E-isomer

The E-isomer mean percentages of SUN and N-DES SUN, respect to the sum of E- and Z-isomers, obtained for increasing time of exposure to the LED lamp at the three concentration levels tested, are reported in figures 54 and 55.

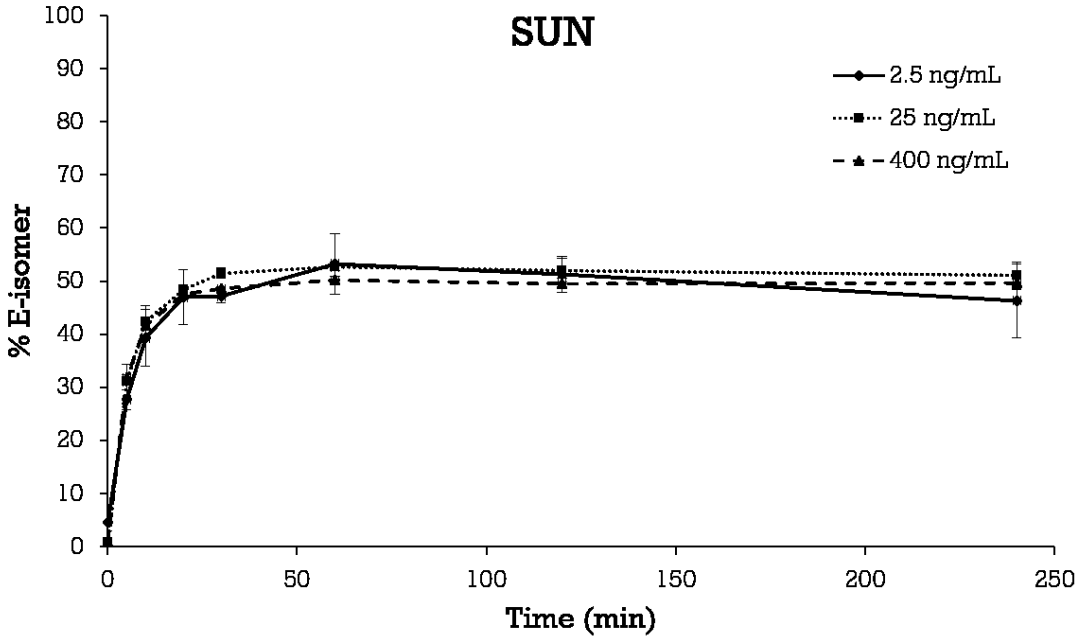

Figure 54. Trend of the E-SUN formation under exposure to LED lamp at the three concentration levels.

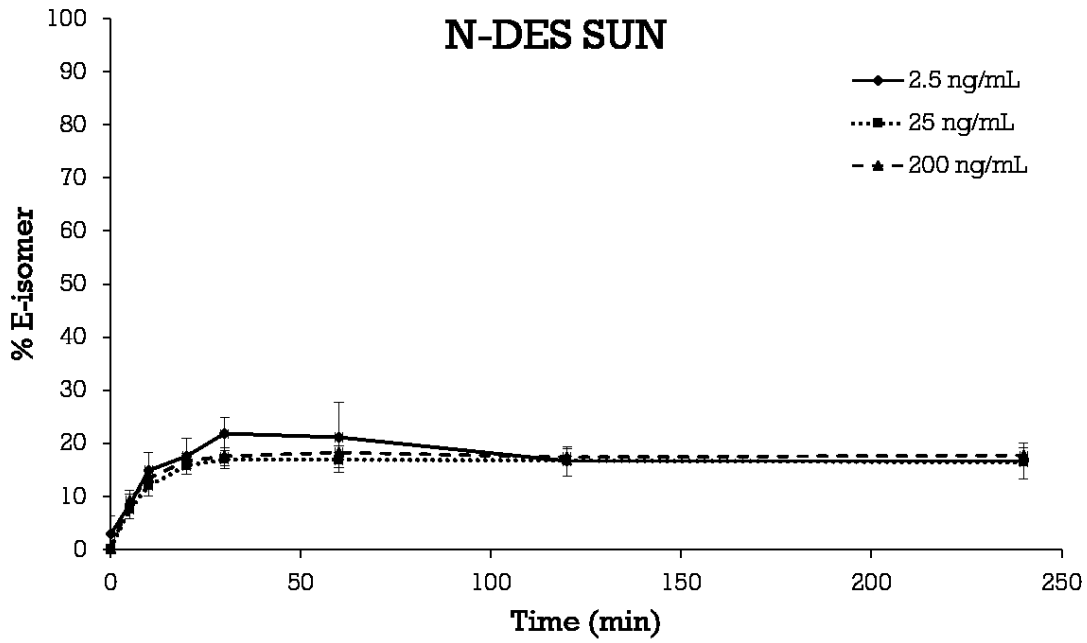

Figure 55. Trend of the E-N-DES SUN formation under LED lamp exposure at the three concentration levels.

Under the applied experimental conditions, for both the compounds, the photo transformation of the Z-isomer into the E-one proceeded very quickly: the E-isomer reached its maximum percentage within 30 min of light exposure, and it seemed to be not influenced by the different concentrations tested.

The maximum percentage achieved by E-SUN was 53.2 ± 5.7% while its main metabolite N-DES SUN, in the same conditions, reached a considerably lower percentage of the E-isomer: 21.8 ± 3.1%.

Both HCOOH and TFA were used to test the influence of an acidic environment on the photo transformation from Z- to E-isomers. When the protein precipitation was performed with acidified MeOH, both the compounds reached a higher percentage of the E-isomer. With regard to SUN (figure 56), the E-isomer gain (up to 58.9 ± 12.5% and 57.4 ± 9.8 in presence of HCOOH and TFA, respectively) was of 11%, regardless of the kind of acid used.

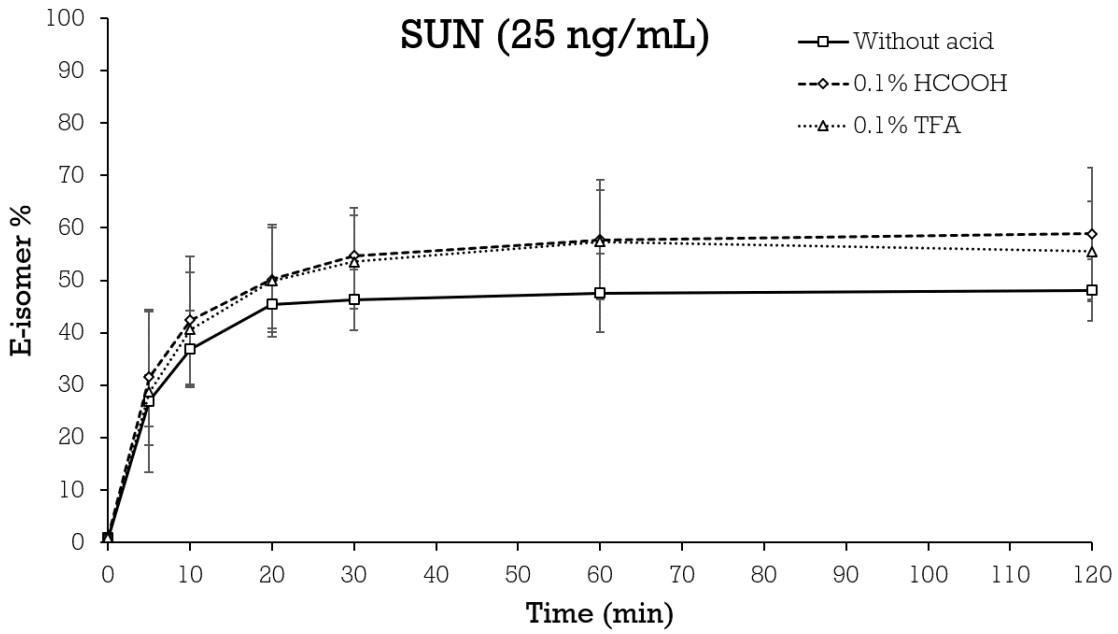

Figure 56. Trend of E-SUN formation under exposition to LED lamp at the medium concentration level and the comparison of the same phenomenon in presence of 0.1% TFA and 0.1% HCOOH v/v.

N-DES SUN (figure 57), on the contrary, behaved differently: apart from showing a higher E-isomer maximum percentage increase than SUN, the increase amount was different depending on the tested acid: it increased up to 26.7 ± 3.6% (22% higher than in absence of acid) with TFA and even up to 32.2 ± 5.8% (48% higher than without acid) with HCOOH.

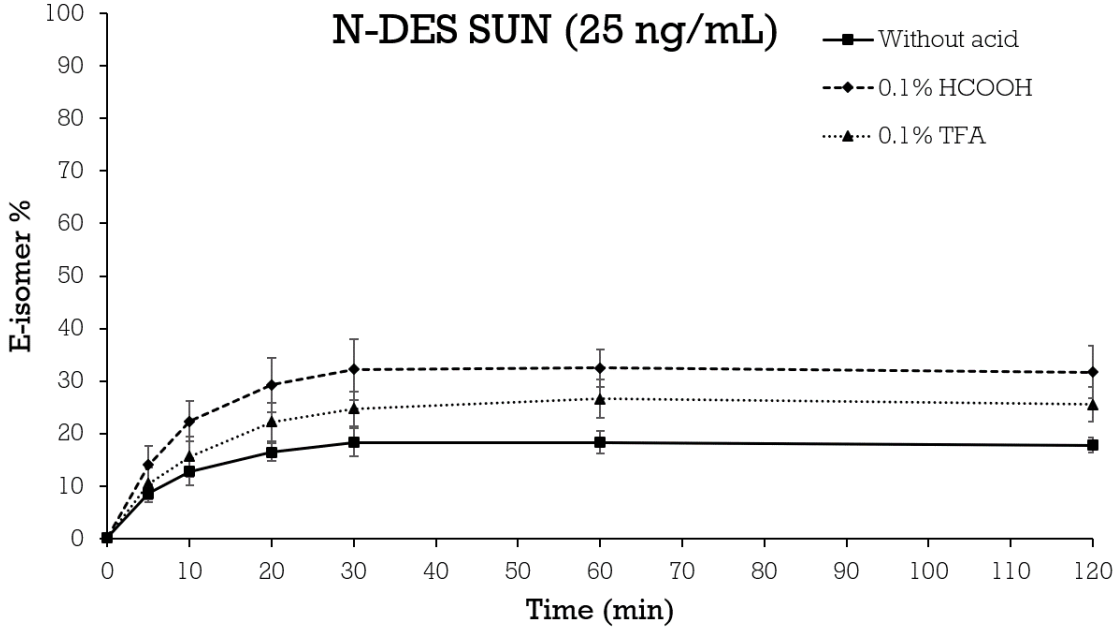

Figure 57. Trend of E-N-DES SUN formation under exposition to LED lamp at the medium concentration level in absence of acids and in presence of 0.1% TFA and 0.1% HCOOH v/v.

4.4.2 Reconversion from the E- to Z-isomer into the autosampler

In figure 58 the Z-isomer mean percentages of the two compounds were reported against the duration of the protection from the light (i.e. into the autosampler) at different temperatures. The E- to Z-isomer reconversion of both compounds appeared very slow when the autosampler was set at 4 °C: as can be seen in figure 58, after 12 h of sample storage at those conditions, the mean percentages of the Z-isomer were 56.6 ± 4.9% and 82.3 ± 1.7% for SUN and N-DES SUN respectively. An acceleration of the reconversion was observed by raising the temperature from 4 to 25 °C: higher E-isomer percentages were achieved (73.4 ± 7.1% and 93.6 ± 1.9% for SUN and N-DES SUN after just 1.5 h and, by waiting for 7 h at the same conditions, the completion of the SUN reconversion was reached (99% of Z-isomer). The same result was achieved in only 4 h by N-DES SUN (figure 59). The temperature effect was even greater at 40 °C, with shorter time for the total reconversion: after 2 h, Z-SUN accounted for 99.0 ± 0.1% while the Z-isomer of N-DES SUN took 30 min less to achieve a similar result (99.6 ± 0.1%).

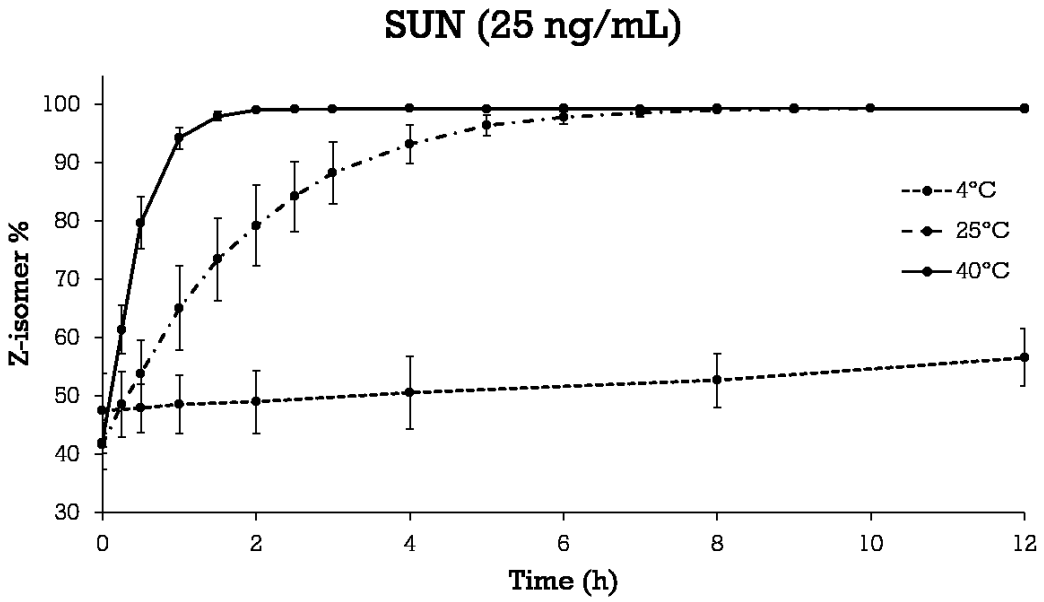

Figure 58. Trend of the E- to Z-isomer reconversion of pre-exposed solutions containing SUN at the medium concentration level stored into the autosampler set at three temperatures value.

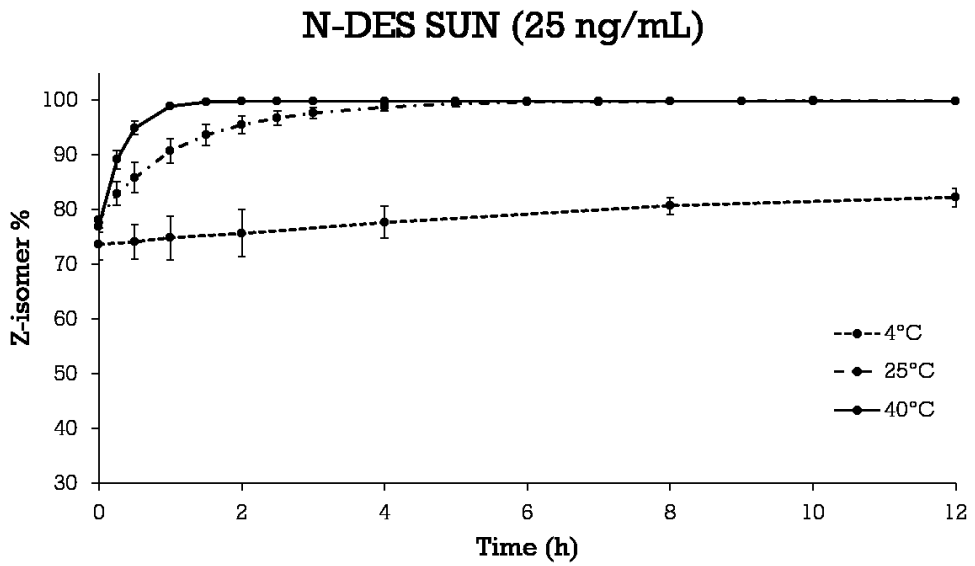

Figure 59. Trend of E- to Z-isomer reconversion of pre-exposed solutions containing N-DES SUN at the medium concentration level stored into the autosampler set at three temperatures value.

The influence of different concentration values of the analytes was investigated at the highest temperature value (40 °C). The Z-isomer mean percentages of SUN and its metabolite were reported in figures 60 and 61 at the L, M, and H (2.5, 25 and 400 ng/mL for SUN and 2.5, 25 and 200 ng/mL for N-DES SUN) concentration levels against the duration of storage into the autosampler. The superimposition of the three curves showed, for both the compounds, the independency of the E- to Z-isomer reconversion rate from the initial concentration of both the analytes.

Figure 60. Trend of the E- to Z-isomer reconversion of pre-exposed solutions containing SUN at three concentration levels stored into the autosampler set at 40 °C.

Figure 61. Trend of the E- to Z-isomer reconversion of pre-exposed solutions containing N-DES SUN at three concentration levels stored into the autosampler set at 40 °C.

The influence of acid addition to the extraction solvent was investigated at 40 °C and for the M concentration level.

Figure 62. Trend of the E- to Z-isomer reconversion of pre-exposed solutions containing SUN at the M concentration level stored into the autosampler set at 40 °C using MeOH with or without 0.1% v/v of HCOOH as extraction solvent.

The addition of HCOOH (0.1% v/v) to the MeOH used for the protein precipitation caused a noticeably slowdown of the E- to Z-isomer reconversion rate for both compounds: in samples extracted with MeOH added by 0.1% of HCOOH, after 5 h of storage into the autosampler, the Z-isomer mean percentages were 60.7 ± 3.0% (99.8 ± 0.0% in absence of acids) for SUN, and 82.1 ± 0.2% (99.3 ± 0.2% in absence of acids) for N-DES SUN (figure 62 and 63, respectively).

Figure 63. Trend of the E- to Z-isomer reconversion of pre-exposed solutions containing N-DES SUN at the M concentration level stored into the autosampler set at 40 °C using MeOH with or without 0.1% v/v of HCOOH as extraction solvent.

4.4.3 Reconversion from E- to Z-isomer into a heated water bath

Even shorter time for the quantitative E- to Z-isomer reconversion was required with temperatures higher than 40 °C obtained using a heated water bath.
In fact, as shown in table 19 and figure 65, 5 min of water bath heated at 70 °C was enough to reach the 99% of Z-isomer for both SUN and N-DES SUN.

Concentration Level	SUN %	N-DES SUN %
L	97.9 ± 0.9	99.2 ± 0.0
M	98.9 ± 0.2	99.7 ± 0.0
H	98.7 ± 0.3	99.5 ± 0.1

Table 19. Z-isomer mean percentages of SUN and N-DES SUN obtained after 5 min of heated water bath at 70 °C.

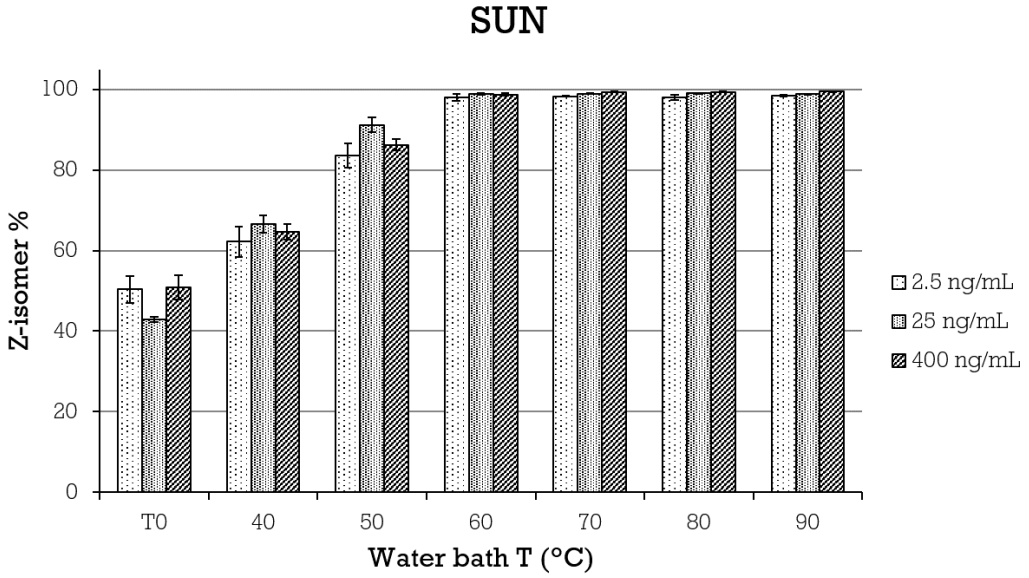

Figure 64. Z-isomer percentages of pre-exposed samples containing SUN at the three concentration levels L, M, and H, before (T0) and after 5 min incubation into the heated water bath set at 40, 50, 60, 70, 80, and 90 °C.

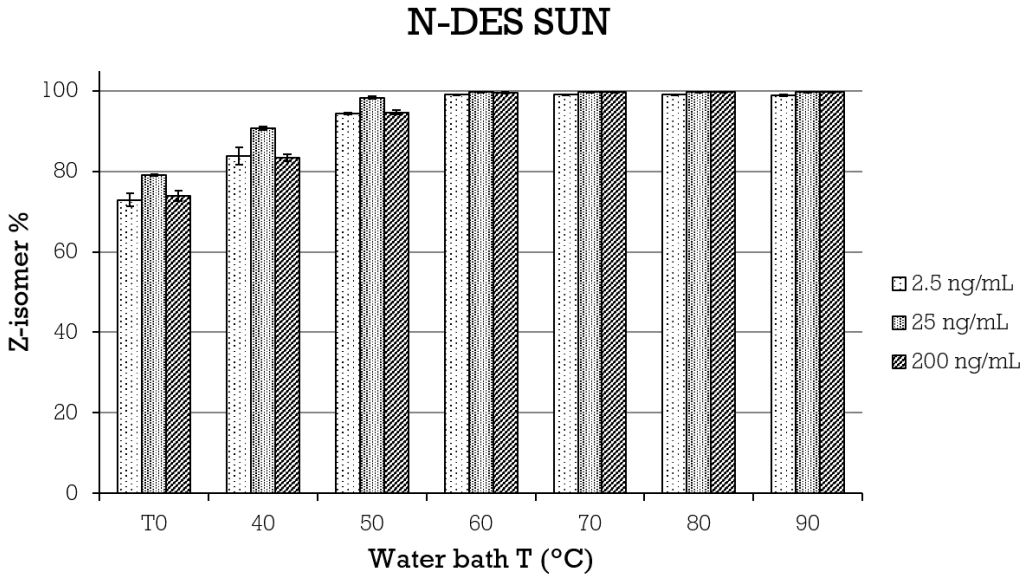

Figure 65. Z-isomer percentages of pre-exposed samples containing N-DES SUN at the three concentration levels L, M, and H, before (T0) and after 5 min incubation into the heated water bath set at 40, 50, 60, 70, 80, and 90 °C.

The experiment was conducted in triplicate at each concentration level (L, M and H) and, in the same way as the previous one, the reconversion kinetics appeared to be independent of the concentration of both the analytes (see figure 64, 65 and table 19).

The influence of acid added to the extraction solvent was investigated for the M concentration level: as already seen in the autosampler experiment (section 4.4.2),

in samples extracted with MeOH added with 0.1% v/v of TFA or HCOOH, the E- to Z-isomer reconversion rate considerably slowed down for both the compounds (figure 66 and 67): Z-SUN mean percentages after 5 min in water bath heated at 70 °C were 49.7 ± 4.4% and 54.6 ± 1.0% with HCOOH and TFA respectively, while Z-N-DES SUN mean percentages were 71.4 ± 3.5% and 79.5 ± 1.3% with HCOOH and TFA, respectively.

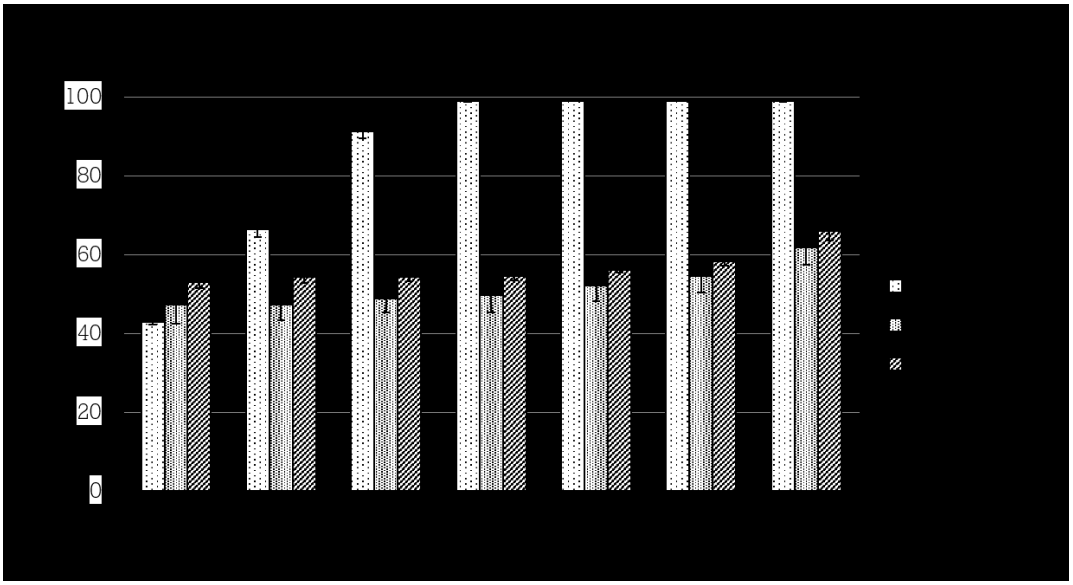

Figure 66. Acid addition effect on the E- to Z-isomer reconversion of pre-exposed solutions containing SUN at M concentration level before (T0) and after 5 min incubation into the heated water bath set at 40, 50, 60, 70, 80, and 90 °C.

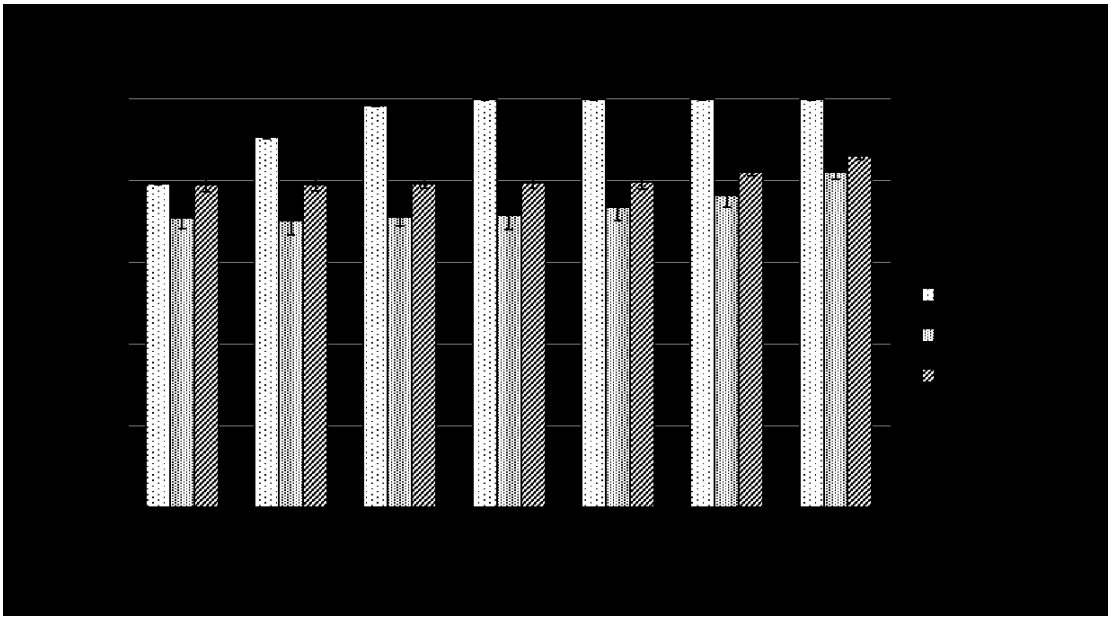

Figure 67. Acid addition effect on the E- to Z-isomer reconversion of pre-exposed solutions containing N-DES SUN at M concentration level before (T0) and after 5 min incubation into the heated water bath set at 40, 50, 60, 70, 80, and 90 °C.

4.4.4 Stability test of SUN and N-DES SUN at high temperatures

In table 20 the percentage changes of Z-isomer before and after one and two heated water bath (5 min at 70° C) cycles are reported at the three concentration levels L, M and H for both SUN and N-DES SUN. The greater Z-isomer decrease was of 3.6 and 3.9% for SUN and N-DES SUN respectively, therefore it is possible to exclude a significant degradation of both analytes even after two heated water bath cycles.

SUN	L		M		H	
	Mean ± SD	Var%	Mean ± SD	Var%	Mean ± SD	Var%
T0	3'000.7 ± 170.6	0.0	194'947.0 ± 3'499.3	0.0	2'114'347.9 ± 22'103.0	0.0
HWB #1	2'886.0 ± 214.4	-3.8	192'455.8 ± 1'264.9	-1.3	2'071'523.6 ± 7'363.5	-2.0
HWB #2	2'889.9 ± 97.8	-3.7	190'922.7 ± 5'863.4	-2.1	2'038'574.2 ± 55'198.0	-3.6
N-DES SUN	Mean ± SD	Var%	Mean ± SD	Var%	Mean ± SD	Var%
T0	7'558.4 ± 266.8	0.0	478'115.8 ± 2'716.9	0.0	2'800'540.5 ± 19'907.8	0.0
HWB #1	7'265.1 ± 764.3	-3.9	483'868.5 ± 14'824.0	1.2	2'718'749.2 ± 68'035.7	-2.9
HWB #2	7296.0 ± 224.5	-3.5	483'055.2 ± 4'614.5	1.0	2'733'897.5 ± 103'503.6	-2.4

Table 20. Z-isomer peak areas before (T0) and after one and two heated water bath cycles (HWB#) and percentage changes (Var%) respect to the T0 peak area for SUN and N-DES SUN at the three concentration levels (L, M, and H).

4.5 Validation of the optimized LC-MS/MS method for the simultaneous quantification of SUN and N-DES SUN in human plasma

The main parameters considered for the validation of the methods, accordingly with the FDA guidelines, were recovery, linearity of the calibration curve, intra- and inter-day precision and accuracy, limit of quantification, selectivity and stability. Moreover, the optimized method was tested with real samples from one patient in order to perform ISR to verify the reliability of the reported subject sample analyte concentrations.

4.5.1 Recovery

The extraction method employed is based on a fast and simple protein precipitation with five volumes of MeOH (related to the plasma sample). In table 21, the results of this experiment are reported: the recovery, evaluated in five replicates at three QC concentration levels, was from 93.9 to 111.1% (CV≤9.2%) and from 95.7 to 108.1% (CV≤12.3%) for SUN and N-DES SUN respectively. The recovery of IS was evaluated in five replicates at a concentration of 100 ng/mL and accounted for 104.9% (CV 5.2%).

Analyte	Nominal concentration (ng/mL)	Recovery (%) ± SD	CV%
SUN	0.25	100.5 ± 9.3	9.2
	25	93.9 ± 5.4	5.8
	400	111.1 ± 1.0	0.9
N-DES SUN	0.25	104.6 ± 12.9	12.3
	25	95.7 ± 5.9	6.1
	200	108.1 ± 2.9	2.7
SUN-D10 (IS)	100	104.9 ± 5.4	5.2

Table 21. Recovery (%) of SUN, N-DES SUN and IS from human plasma samples extracted with five volumes of MeOH.

4.5.2 Linearity of the calibration curve

The calibration curves of SUN and its main metabolite N-DES SUN, which were freshly prepared every day during the validation study, showed a good linearity.

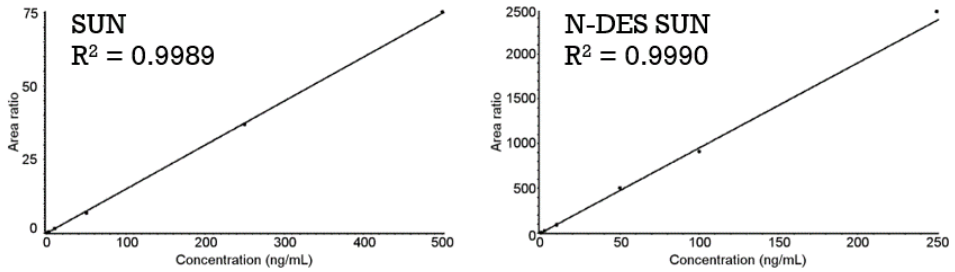

Figure 68. Example of calibration curves of both SUN and N-DES SUN in human plasma samples.

To generate a calibration curve like the one reported in figure 68, the peak-area ratios between the analyte and the IS compared to the nominal concentrations were plotted and a least-squares linear regression, weighted by the reciprocal of the concentrations, were plotted and a weighted quadratic regression function ($1/x^2$) was applied. The calibration curves prepared on five different days showed good linearity and acceptable results of the back-calculated concentrations over the validated range of 0.1–500 ng/mL for SUN and 0.1-250 ng/mL for N-DES SUN (table 22). Pearson's coefficient of determination R^2 was ≥0.9939 for each run, the mean accuracy ranges from 95.8 to 102.9% for SUN and from 92.3 to 106.2% for N-DES SUN while the precision, expressed as CV%, ranged from 1.6 to 7.7 % and from 0.8 to 10.8% for SUN and N-DES SUN respectively. The injection of three samples of MP after the ULoQ injection, minimized the impact of the carryover effect: no peaks higher than 20% of LLOQ were observed before a sample injection.

Analytes	Nominal concentration (ng/mL)	Mean ± SD	CV%	Accuracy %
SUN	0.1	0.10 ± 0.00	1.6	101.0
	0.5	0.48 ± 0.04	7.7	95.8
	2.5	2.41 ± 0.14	5.6	96.5
	10	10.25 ± 0.47	4.6	102.5
	50	49.38 ± 2.04	4.1	98.8
	250	256.67 ± 12.29	4.8	102.7
	500	514.50 ± 16.16	3.1	102.9
N-DES SUN	0.1	0.10 ± 0.00	0.8	101.2
	0.5	0.47 ± 0.02	3.9	94.2
	2.5	2.31 ± 0.11	4.8	92.3
	10	9.72 ± 1.05	10.8	97.2
	50	51.48 ± 2.96	5.7	103.0
	100	104.93 ± 9.07	8.6	104.9
	250	265.41 ± 19.16	7.2	106.2

Table 22. Linearity, accuracy, and precision data for calibration curves of SUN and N-DES SUN.

4.5.3 Intra-day and inter-day precision and accuracy

The precision and accuracy of the method were evaluated by analysing three replicates of QC samples (QCL, QCM and QCH) within a single-run analysis for intra-day assessment and between five consecutive runs for inter-day assessment. The accuracy and precision (CV%) obtained are shown in table 23.

	Analytes	Nominal concentration (ng/mL)	Mean ± SD	CV%	Accuracy %
Intra-day SUN (N=5)	SUN	0.25	0.25 ± 0.03	11.0	98.5
		25	25.93 ± 0.69	2.7	103.7
		400	447.86 ± 5.10	1.1	112.0
	N-DES SUN	0.25	0.26 ± 0.03	11.7	103.7
		25	26.71 ± 2.57	9.6	106.9
		200	223.30 ± 6.28	2.8	111.7
Inter-day (N=15)	SUN	0.25	0.26 ± 0.02	6.1	102.5
		25	25.40 ± 1.27	5.0	101.6
		400	423.48 ± 29.23	6.9	105.9
	N-DES	0.25	0.25 ± 0.02	9.1	99.1
		25	24.18 ± 1.76	7.3	96.7
		200	214.45 ± 14.17	6.6	107.2

Table 23. Intra- and inter-day precision and accuracy of the assay for SUN and N-DES SUN in human plasma samples.

An intra- and inter-day CV≤11.0% and ≤6.9% for SUN and ≤11.7% and ≤9.1% for N-DES SUN depicted the method as very precise. Moreover, it was accurate too, thus showing an intra- and inter-day accuracy ranging from 98.5 ad 112.0% and from 101.6 and 105.9% for SUN. A similar accuracy was observed for its main metabolite, with an intra- and inter-day values ranging from 103.7 to 111.7% and from 96.7 and 107.2%.

4.5.4 Limit of quantification

The LLoQ was defined as the lowest concentration that could be measured (SNR≥5) with a precision within 20% and accuracy between 80% and 120%. Figure 69 shows the obtained SNR (20.1 for SUN and 25.3 for N-DES SUN) analysing a sample at the LLoQ concentration value which, based on the concentration range expected in

patients' samples, was fixed at 0.1 ng/mL for both SUN and its main metabolite. Through the analysis of six replicates, both the accuracy and the precision were determined: the accuracy and CV% were, respectively, 87.4% and 14.7% for SUN, 107.8% and 8.0% for N-DES SUN.

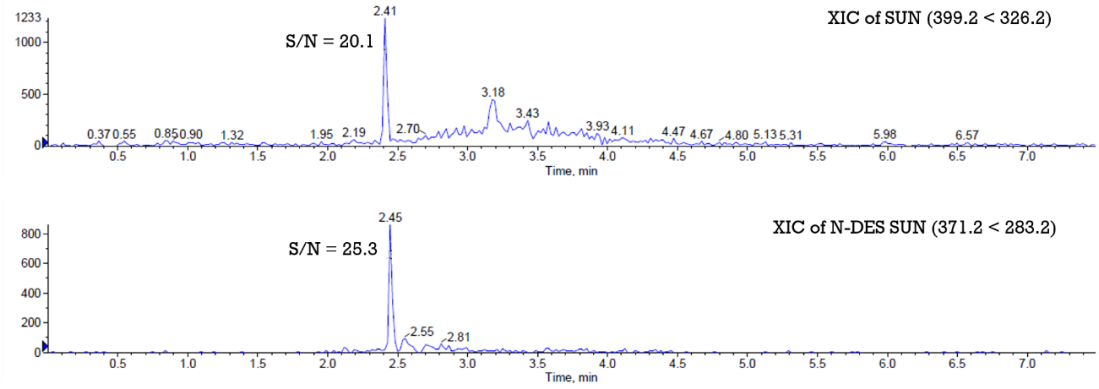

Figure 69. MRM chromatogram of an LLoQ sample reporting the SNR values of both SUN and N-DES SUN.

4.5.5 Matrix effect and selectivity

The method was not significantly affected by endogenous components in the matrix or other components in the sample. In fact, spiking six different sources of human plasma with SUN and N-DES SUN at a concentration corresponding to the LLoQ, the precision was 8.4% and 5.9% for SUN and N-DES SUN, respectively, and the accuracy was 89.5% for SUN and 114.9% for N-DES SUN, respectively. There were no significant variations (<15%) in the peak area of each analyte in the six lots of matrix. Moreover, thanks to the post-column infusion test (figure 24), with which it was observed that the signal intensity of the analyte infused at a constant concentration (figure 70), did not undergo variations at the retention time of the analytes under examination: therefore, it was possible to exclude the presence of any matrix effect of ion suppression or enhancement.

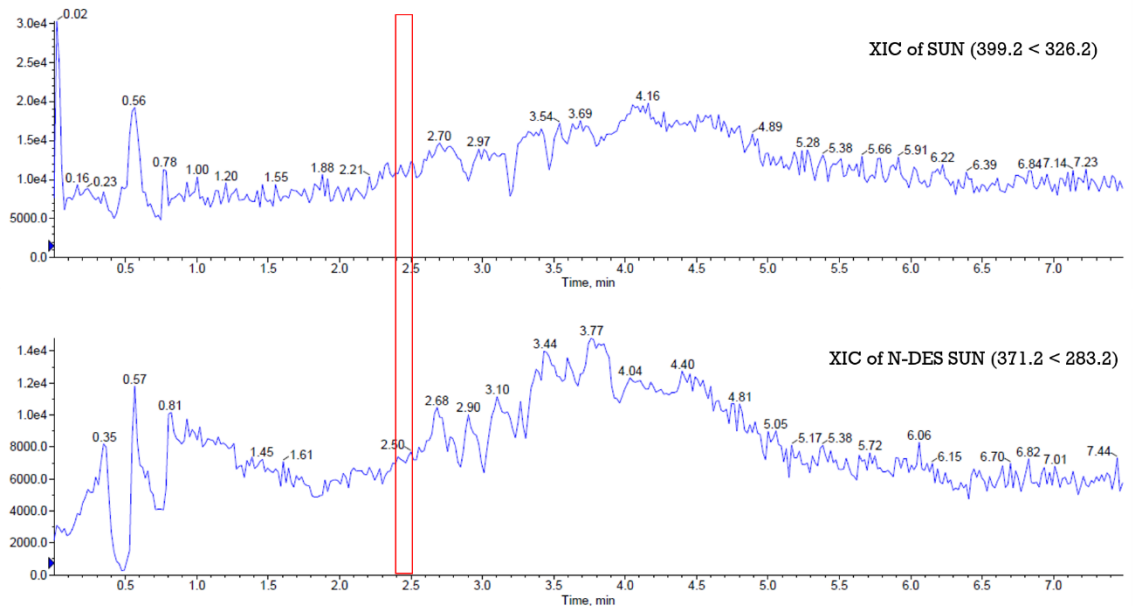

Figure 70. Evaluation of the matrix effect through a post-column infusion experiment: the XIC trend of both SUN and N-DES SUN shows both ion enhancement and ion suppression areas. These phenomena did not affect the analytes of interest, whose retention times were highlighted with the red rectangle.

4.5.6 Stability

The stability of SUN and its main metabolite, under different conditions, was assessed by analysing QC samples, prepared in triplicate. All these analytes in human plasma were stable for 4 h at RT (Table 24):

	Analytes	Nominal concentration (ng/mL)	Mean ± SD	CV%	Accuracy %
T = 4 h (RT)	SUN	0.25	0.23 ± 0.01	5.9	90.6
		25	23.37 ± 0.86	3.7	93.5
		400	440.84 ± 22.23	5.0	110.2
	N-DES SUN	0.25	0.25 ± 0.03	12.6	101.0
		25	22.81 ± 1.12	4.9	91.2
		200	227.44 ± 4.10	1.8	113.7

Table 24. Short term (4 h) stability of SUN and N-DES SUN in human plasma samples at RT.

Precision, expressed as CV%, and accuracy in this short-term stability test were ≤5.9% and within 90.6–110.2% for SUN and ≤12.6% and within 91.2–113.7% for N-DES SUN.

For the peculiarity of this method, it is particularly important to assess the stability in autosampler after the extraction. In fact, in order to enhance and stabilize the

conversion to the active Z-isomer the autosampler temperature is set at 40 °C, while standard methods usually consider an autosampler temperature of 4 °C. With a precision and accuracy ≤8.4% and within 90.6–104.6%, respectively, for SUN and ≤7.2% and within 100.8–104.8%, respectively, for N-DES SUN, the stability of the extracted samples for 48 h in the autosampler at 40 °C was demonstrated (table 25).

	Analytes	Nominal concentration (ng/mL)	Mean ± SD	CV%	Accuracy %
T = 48 h AS (40°C)	SUN	0.25	0.23 ± 0.02	8.4	90.6
		25	23.94 ± 1.95	8.1	95.8
		400	418.56 ± 24.90	5.9	104.6
	N-DES SUN	0.25	0.25 ± 0.02	7.2	101.3
		25	25.20 ± 0.45	1.8	100.8
		200	209.57 ± 7.56	3.6	104.8

Table 25. Stability of SUN and N_DES SUN, in extracted plasma samples, after 48 h of storage into the autosampler set at 40 °C.

SUN and N-DES SUN were stable in human plasma over two freeze/thaw cycles: precision expressed as CV% and accuracy were ≤8.6% and within 99.9–108.2% for SUN and, ≤12.4% and within 101.9–106.1% for N-DES SUN (table 26).

	Analytes	Nominal concentration (ng/mL)	Mean ± SD	CV%	Accuracy %
2 x FT cycles	SUN	0.25	0.26 ± 0.02	6.5	105.9
		25	24.97 ± 0.74	3.0	99.9
		400	432.80 ± 37.2	8.6	108.2
	N-DES SUN	0.25	0.26 ± 0.02	9.2	104.8
		25	26.52 ± 0.26	1.0	106.1
		200	203.82 ± 25.24	12.4	101.9

Table 26. Stability of SUN and N-DES SUN, in human plasma samples, after 2 freeze-thaw cycles.

Several aliquots of QC samples were stored, in the same way as the QC WS, at -80°C in order to complete the assessment of the long-term stability. Concerning the WS, the assessment will be carried out in the next months, while, in plasma samples, both SUN and N-DES SUN appeared to be stable even after 9 months, showing a precision and accuracy values ≤7.4% and within 92.9–109.6% for SUN, and ≤3.1% and within 86.2–104.4% for N-DES SUN (table 27).

	Analytes	Nominal concentration (ng/mL)	Mean ± SD	CV%	Accuracy %
T = 9 months (-80 °C)	SUN	0.25	0.27 ± 0.02	7.4	109.6
		25	23.21 ± 0.59	2.5	92.9
		400	394.08 ± 11.80	3.0	98.5
	N-DES SUN	0.25	0.26 ± 0.00	0.0	104.4
		25	21.55 ± 0.66	3.1	86.2
		200	207.24 ± 4.76	2.3	103.6

Table 27. Long term (9 months) stability of SUN and N-DES SUN in human plasma samples stored at -80 °C.

4.5.7 Incurred Samples Reanalysis

The ISR was carried out by quantifying nine real samples belonging to a patient who had taken 37.5 mg of SUN. The sampling was performed following the schedule reported in section 3.6.4 which ensured an adequate coverage of the target concentration profile. The quantification was done twice for each sample on two different days. The results of the first analysis are reported against sampling time in figure 70, thus obtaining a pharmacokinetic curve, while the comparison of the results between the two analysis is reported in table 28.

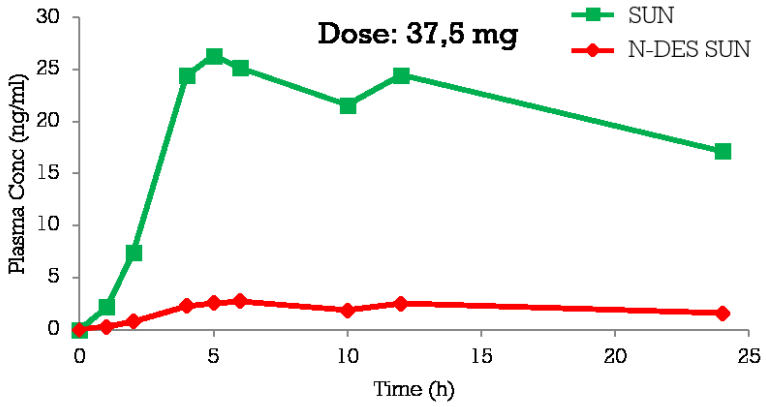

Figure 70. Pharmacokinetic curve obtained plotting both SUN and N-DES SUN concentration values against sampling time.

The optimized method showed a good reproducibility on real sample analysis since, excluding the first non-quantifiable sample, the two runs were considered equivalent: 100% of the retested samples showed a percentage difference (%diff) of the results within ±20% compared to the first analysis.

	N-DES SUN (ng/mL)		%diff	SUN (ng/mL)		%diff
	1st analysis	2nd analysis		1st analysis	2nd analysis	
T0	<LLoQ	<LLoQ	NA	<LLoQ	<LLoQ	NA
1h	0,28	0,26	-6,67	2,27	2,16	-4,87
2h	0,87	0,79	-10,37	8,15	7,37	-10,09
4h	2,42	2,25	-7,20	23,97	24,39	1,77
5h	2,51	2,52	0,56	24,34	26,32	7,84
6h	2,37	2,74	14,50	23,24	25,15	7,90
10h	1,79	1,83	2,10	19,60	21,58	9,64
12h	2,12	2,49	16,30	22,49	24,45	8,34
24h	1,50	1,55	3,47	15,16	17,14	12,27

Table 28. Comparison expressed as percentage variation between the results of the two analysis performed in two different days on the same real samples.

5 DISCUSSION

The projects described in this PhD thesis are included in the wider context of anticancer treatment optimization, that is highly desirable in clinical practice. The two drugs considered in this work, IMA and SUN, are potent oral TKIs and represent, respectively, the first- and the second-line pharmacological treatment for patients with inoperable, metastatic or recurrent GIST. This malignant neoplasm is characterised by a marked unresponsiveness to standard chemotherapy regimens and the introduction of the targeted cancer therapy with the TKI drug class provided evident changes to the anticancer therapy strategies and, in some cases, strongly improved the patients' outcome. However, there is now growing evidence that targeted cancer therapy action is not without drawbacks or complications.

In fact, it is believed that targeted therapy is characterized by fewer and less severe adverse events than classic chemotherapy, such as diarrhea, nausea, vomiting, alopecia or neutropenia. This is only partly true, since also targeted therapy could produce severe off-target toxicities related to cross-reactivity between the target in cancer and in healthy tissues[115]. It is increasingly appreciated that the response to targeted drugs is influenced by several factors, such as the genetic heterogeneity of drug targets (determining tumor sensitivity), the patient's genetic background, his/her adherence to treatment, and environmental factors affecting the pharmacokinetics[116]. To date, patients treated with oral TKI receive a fixed starting dose and posology adjustments are only performed on the basis of clinical evidences of toxicity or inadequate efficacy. This "one-dose-fits-all" paradigm unfortunately does not take into consideration individual features that alter some physiological processes such as adsorption, distribution, metabolism or elimination and, therefore, can lead to highly different concentrations of the drugs in patient's bloodstream. This high inter-patient variability in drug plasma levels might favor the selection of resistant tumor clones (in case of sub-therapeutic drug exposure) or might lead to the development of undesirable effects (in case of overexposure). In this respect, the great majority of targeted therapies are characterized by a wide spread of plasma concentrations with standard dosage regimens, and the C_{min} of up to 23-fold among patients[117]. A useful approach to reach the goal of a more rational drug dosing according to patients' characteristics, is the application of TDM. Considering the low therapeutic index, the large inter-individual variability in the

systemic exposure, and the positive exposure-efficacy relationship of SUN and IMA, there is a strong rationale for TDM of these drugs.

Enabling high levels of precision and reliability, LC-MS/MS represents the Gold-Standard for the quantification of drugs in patient's plasma and it is the analytical technique used for a TDM purpose. The work performed during this PhD period concerns the development and the validation, according to the FDA and EMA guidelines of two HPLC-MS/MS methods for the quantification, on one hand of IMA and its main metabolite NOR IMA, and on the other hand of SUN and its main active metabolite N-DES SUN.

5.1 LC-MS/MS method development for the simultaneous quantification of IMA and its main metabolite, NOR IMA, in human plasma

IMA is a potent and selective inhibitor of different tyrosine kinases including the Abl kinase, KIT, PDGFRα, PDGFRβ, and DDR1: the inhibition of the tyrosine kinase phosphorylation activity produce the blockade of the downstream signalling for proliferation and survival pathways within the cell.

IMA is indicated as adjuvant treatment after the resection of GIST and also as first-line standard therapy for inoperable, metastatic, or recurrent GISTs. The standard dosage is 400 mg/day while, for patients with KIT exon 9-mutated GIST, the NCCN and ESMO guidelines recommend a higher dosage of 800 mg/day because of the positive correlation with a longer PFS.

IMA displays a large inter-patient variability in plasma exposure and a relationship between C_{min} and therapy outcome, thus representing a good candidate for TDM. Although several levels of evidences recommend TDM for IMA, no consensus is still reached for the definition of a precise C_{min} threshold that could be correlated with the treatment efficacy in GIST patients. In the literature, two different cut-off values have been suggested for IMA: the first is 1'110 ng/mL after one month from treatment initiation, and the second is 760 ng/mL after more than three months from therapy starting. Regarding the association between IMA plasma levels and toxicity, it was only defined in patients affected by CML, where concentrations above 3'000 ng/mL have been linked to a higher risk of toxicity occurrence.

The development of a simple, rapid and of course reliable analytical method for the quantification of this drug could have a double benefit: on one side, to make IMA TDM applicable in clinical practice, and, on the other side, to deepen the knowledge on the correct C_{min} threshold for GIST patients treated with IMA. With these aims, the method should be able to detect IMA and its main metabolite within a wide range of concentrations (the IMA steady state plasma levels found in the clinic vary between 256 and 4'582 ng/mL) by analysing a small amount of plasma.

In the literature, several methods were published for the quantification of IMA and/or its metabolite NOR IMA or other TKIs, as reported in table 29.

Analytes	Plasma volume (µL)	Extraction method	Run time (min)	Linear range (ng/mL)	Reference
IMA, NOR IMA and IMA-D8	200	PP	2.5	4-10'000	Bakhtiar et al. 2002
IMA and IMA-D8	200	PP with supernatant filtration	2	1-10'000	Guetens et al. 2003
IMA, NOR IMA and IMA-D8	200	PP with supernatant evaporation and re-dissolution	14	30-10'000	Parise et al. 2003[117]
IMA and IMA-D8	200	LLE	6	10-5'000	Titier et al. 2005
IMA, IMA-D8 and other TKIs	100	PP with supernatant dilution	20	1-10'000	Haouala et al. 2009
IMA and other TKIs	250	PP with supernatant dilution	20	78,1-10.000	De Francia et al. 2009
IMA and IMA-D8	200	LLE	2.5	10-4'000	Awidi et al. 2010
IMA, NOR IMA, IMA-D8 and other TKIs	50	PP	7	50-5'000 (IMA); 10-1'000 (NOR)	Couchman et al. 2012
IMA, NOR IMA, IMA-D8 and dasatinib	50	PP	<5	50-10'000 (IMA), 10-2'000 (NOR)	Birch et al. 2012
IMA and other TKIs	50	PP	10	20-10'000	Lankheet et al. 2012
IMA, IMA-D8 and other TKIs	100	PP with supernatant dilution	9	100-5'000	Gotze et al. 2012
IMA, NOR IMA and IMA-D8	50	PP with supernatant dilution	6	10-2'000	Zhang et al. 2012
IMA and tamsulosin (IS)	100	PP	4	500-10'000	Rezende et al. 2013
IMA NOR IMA and palonosetron (IS)	400	PP	3.8	8-5'000 (IMA); 3-700 (NOR)	Zhang et al. 2014
IMA and other TKIs	300	LLE	6	1,64-100	Abdelhameed et al. 2016
IMA, NOR IMA and IMA-D8	100	LLE	3.5	10-10'000	Zhuang et al. 2017
IMA, IMA-D8 and other TKIs	200	SPE	7	2,5-5'000	Wojnicz et al. 2017

Table 29. List of already published assays for the quantification of IMA and (in some of them) its main metabolite, NOR IMA.

Only seven methods, among those published, considered the quantification of both IMA and its active metabolite, NOR IMA[105,118–123]. The method proposed by Bakhtiar

et al. presents a noticeably wide linear range that adequately cover clinical relevant plasma levels (4-10'000 ng/mL) for both IMA and NOR IMA[118]. Moreover, this method is fast, with a chromatographic run time of only 2.5 min, with a sample preparation based on a simple PP with MeCN. One drawback of this method is represented by the requirement of a high plasma volume (200 µL), representing an element in common with the assay developed by Parise et al., which in addition, is characterized by a long run time of 14 min and by a multi-step sample preparation[119]. The combination of these factors make this method quite complex and, above all, time-consuming, thus hindering the possibility of an easy application into the clinical routine. The first assay for IMA proposed by Zhang et al.(2012), although requiring a lower sample volume (50 µL), displays a concentration range that is inadequate to cover the clinically relevant plasma levels of IMA (ULoQ of only 2'000 ng/mL)[121]. The second assay published by the same author (in 2014), instead, is based on the highest sample volume (400 µL) among the methods reported in table 29[122]. Birch et al. proposed a LC-MS/MS method with a suitable linear range (50-10'000 ng/mL for IMA and 10-2'000 ng/mL for NOR IMA), a chromatographic run time shorter than 5 min and characterized by a simple PP as sample extraction technique[120]. However, the precipitating solvent is composed by a mixture of butyl acetate and butanol (4:1): the use of less toxic and cheaper solvents would be more appropriate in light of a frequent application of the method in the clinical setting. The method described by Zhuang et al. displays a wide linear range for IMA (10-10'000 ng/mL), is characterized by a chromatographic run time of only 3.5 min, but the rapidity of the analysis results mitigated by the time-consuming sample preparation performed with LLE[123]. Finally, the method developed by Couchman et al. appears to be the most suitable for the clinical setting among those reported in the literature: the sample preparation is performed with a simple PP which, combined with a chromatographic run of 7 min, further shortens the time of each analysis. Moreover the adequate linear range (50-5'000 ng/mL for IMA and 10-1'000 ng/mL for NOR IMA) and the limited sample volume employed (50 µL) make this method fitted for the TDM purpose[105].

A further improvement of the method developed by Couchman et al. represents the correct way in the direction of a method as much suitable as possible to the clinical

routine. For this reason, the aim of this work was to develop a new LC-MS/MS assay from scratch with the aim of further reduce the sample volume, to cover a wider linear range for both the analytes while keeping an adequate rapidity in terms of both extractive process and chromatographic run time.

Thanks to an accurate optimization of both the compound- and source-dependent parameters of the mass spectrometer, the instrumental sensitivity reached for IMA and NOR IMA was so high that it brought two immediate advantages.

First, the sample volume required for the analysis was lowered to 20 µL, allowing to reduce the sampling volume, with direct benefits on patient's compliance and leading to a great matrix-saving during the preparation of both calibrators and QCs.

Secondly, the amount of MeOH added for the PP was increased from a normal plasma to solvent ratio of 4:1 to 50:1. This makes PP more efficient in terms of sample cleaning than it generally is: each interferents that might cause some matrix effect and dirty both the column and the source components is diluted with a volume of organic solvent 10-fold higher than the standard usually applied. Therefore, the high sensitivity obtained during the manual tuning of the instrument made both analytes quantifiable in a considerably wide concentration range (from 30 to 7'500 ng/mL for IMA and from 6 to 1'500 ng/mL for NOR IMA) even if the sample is highly diluted in MeOH with the abovementioned beneficial effects.

Moreover, during the development of the chromatographic method, some measures were adopted to obtain, at the same time, a short total run time, an adequate chromatographic separation between IMA and NOR IMA to prevent any possibility of cross-talking phenomena and a correct removal of the endogenous interferents from the column between consecutive injections.

The adequate chromatographic resolution was achieved thanks to the choice of a suitable C18 column (Synergi Fusion-RP) and to the setup of a fine-tuned multi-step chromatographic method with 0.1% HCOOH in H_2O as MPA and 0.1% HCOOH in a mixture of MeOH/iPrOH 9:1 v/v as MPB. The combination of the relatively large particle size of the column and the high flow rate of 400 µL/min (raised to 500 µL/min during the wash and re-equilibration steps) of the MP allow to cram a controlled elution, an efficient column cleaning from the most lipophilic interferents and a correct re-equilibration in only 8 min of total runtime.

The method was successfully validated according to the FDA and EMA guidelines for the validation of bioanalytical methods. The calibration curve was linear in the considered concentration range (R^2 was ≥0.9939 for each run) and was characterized by a good precision and accuracy. Both intra- and inter-day precisions were ≤7.1% and ≤7.2% for IMA and NOR IMA, respectively, while intra- and inter-day accuracy comprehensively ranged from 92.7 to 106.3% considering both IMA and NOR IMA. Recovery of the analytes was high and reproducible over the concentrations tested, ranging from 80 to 90% for both IMA and NOR IMA with a precision always ≤8.8%. Moreover, the method was selective and not significantly affected by endogenous components in the matrix or other components in the sample (matrix effect). Short-term stabilities were also assessed: both IMA and NOR IMA resulted stable in plasma samples after 4 hours at room temperature, after three freeze-thaw cycles and in extracted samples into the autosampler for 24 hours at 4°C. To complete the validation process, long-term stability needs to be assessed both in plasma and in WS and ISR needs to be performed as an additional test to define the method reproducibility. These analyses will be performed in the immediate future.

The method set up during this work was applied for the simultaneous quantification of IMA and NOR IMA in 49 plasma samples from GIST patients involved in the clinical study titled: *"Pilot study to evaluate the feasibility of an innovative approach to monitor patients with gastrointestinal stromal tumor treated with imatinib"* N. EudraCT 2017-002437-36, Code: CRO-2017-19). The first consideration emerging from this analysis regards the high inter-patient variability in C_{min} values: patients' IMA concentrations ranged from a minimum of 171 ng/mL to a maximum of 3'358 ng/mL, reflecting the wide variability reported in the literature about IMA exposure in patients treated at the same starting dose (table 30). C_{min} values higher than 760 ng/mL were associated with a longer PFS in GIST patients treated with IMA for more than 3 months. Surprisingly, in only 61.2% of the analyzed samples, the C_{min} was higher than or equal to the threshold value for IMA efficacy. Consequently, the 38.8% of the analyzed samples revealed an under-exposition to the drug and, therefore, a risk for a reduced therapeutic effect.

Patient N°	Age	Sex	sample ID	IMA (ng/mL)	NOR IMA (ng/mL)
Pt1	79	M	1_2	859	230
			1_3	709	183
			1_4	1012	252
Pt2	66	M	2_3	1449	277
			2_4	1658	314
Pt4	76	M	4_3	2990	427
			4_4	3358	491
			4_5	2282	307
Pt7	69	F	7_3	< LLOQ	< LLOQ
			7_4	931	215
			7_5	828	197
Pt8	69	M	8_3	760	111
			8_4	708	139
Pt10	61	M	10_3	338	181
			10_4	398	226
			10_5	281	144
Pt12	75	M	12_2	1149	217
			12_3	825	177
			12_4	605	138
Pt14	78	F	14_2	1361	198
			14_3	1174	174
			14_4	1345	201
Pt16	52	F	16_2	1164	205
			16_3	2766	404
Pt17	65	F	17_3	673	152
			17_4	730	137
			17_5	982	176
			17_6	666	153
Pt18	81	F	18_3	896	240
			18_4	848	188
			18_5	1207	284
Pt19	54	F	19_2	700	138
			19_3	770	122
Pt20	63	M	20_2	502	113
Pt21	55	M	21_2	< LLOQ	81
Pt22	52	M	22_1	2617	314
			22_3	700	116
			22_4	1032	196
Pt23	55	M	23_1	171	55
			23_2	548	87
Pt24	52	M	24_1	258	84
			24_2	502	159
Pt25	76	M	25_1	< LLOQ	< LLOQ
Pt26	58	F	26_1	862	282
			26_2	1051	281
Pt27	76	M	27_2	1188	264
			27_3	1243	305
Pt29	76	M	29_1	1330	195
Pt30	44	M	30_2	932	212
Median age, years (median [range]): 65 [44-81]					
Gender (male/female): 15/7					

Table 30. C_{min} values of both IMA and NOR IMA determined in 49 plasma samples from GIST patients employing the developed and validated LC-MS/MS method. In green: C_{min} values above the threshold of 760 ng/mL; in yellow: samples with a non-quantifiable amount of IMA; in red: C_{min} values above the threshold of 3'000 ng/mL. Additional data such as age and gender are reported.

In addition, among the 30 samples showing a concentration equal to or above the threshold of 760 ng/mL, 2 sequential samples, belonging to the same patient, were particularly interesting: one of them displayed a C_{min} of 2'990 ng/mL while the latter, 3'358 ng/mL.

The results of a study on IMA-treated CML patients suggest that concentrations higher than 3'000 ng/mL should be avoided since they were associated with toxicity development. The type of toxicities associated with elevated drug concentrations were:

- hematological toxicities: anemia, neutropenia, and leukopenia;
- non hematological toxicities: nausea, vomiting, diarrhea, edema, arthralgia, myalgia, skin rash, muscle spasms, headache and asthenia.

To investigate whether this high exposure to the drug, also in case of GIST pathology, could be linked to the onset of adverse events, the clinical history of the patient showing high IMA plasma levels was retraced. As reported in the clinical record, this patient experienced some drug side effects during treatment: in particular, toxicities of mild, moderate and severe grades were observed. Mild adverse events were: anemia, limbs and hands muscle spasms, hypercreatininemia, creatine phosphokinase increase; those of moderate and severe grade were nausea and vomiting (graded according to the Common Terminology Criteria for Adverse Events – CTCAE version 4.03). As aforementioned, most of these toxicities have already been associated with high IMA concentrations in CML patients. For this reason, it can be hypothesized that the cut-off of 3'000 ng/mL could be considered a meaningful threshold value above which the probability of developing toxicities, even of severe grade, is higher regardless the pathology. Clearly, this hypothesis is only provisional since it is based on a single observation.

Finally, in 3 plasma samples, IMA signal was lower than the LLoQ (30 ng/mL) and this could be considered an indicator of non-adherence to therapy.

From the analysis of the first 49 samples, a spectrum of different situations was revealed:

- only 61.2% of them showed an adequate C_{min} level;
- a correlation between high C_{min} values (close or above 3'000 ng/mL) and the toxicity occurrence (although in one patient);
- the identification of a possible non-adherence to therapy in the 6% of the analyzed samples.

Thus, the preliminary analysis of this small set of patients' samples clearly suggests that TDM application in clinical routine would allow the maximization of therapy efficacy through the identification of sub-optimal responses, severe adverse drug reactions or concerns about therapy adherence.

In light of this, it would be important to exactly define the threshold C_{min} values of both efficacy and risk of toxicity development in patients affected by GIST and treated with IMA.

5.2 LC-MS/MS method optimization for the simultaneous quantification of SUN and its main metabolite N-DES SUN in human plasma

As a multi-targeted TKI, SUN inhibits several tyrosine kinase receptors (including PDGFRα, PDGFRβ, VEGFR1, VEGFR2, VEGFR3 and KIT) involved in tumor growth, tumor neo-angiogenesis and metastatic cancer progression. It was approved by the FDA in January 2006 and by EMA in June of the same year for the treatment of unresectable and/or metastatic malignant GIST in adult patients after treatment failure (resistance or intolerance) with IMA.

For SUN, TDM approach has been suggested as potentially useful due to its low therapeutic index, the existence of a positive exposure-efficacy/toxicity relationship and of a large interindividual variability in systemic exposure. To calculate the target plasma concentration for TDM analysis, the sum between the trough levels of SUN and its metabolite N-DES SUN (total C_{min}) has been applied. In fact, for GIST patients taking SUN 37,5 mg continuously daily, a minimal total Cmin of 37,5 ng/mL has been associated with an objective response. Instead, dose limiting toxicities have been reported especially when total Cmin were higher than 90 ng/mL. Thus, a robust and adequately ranged assay for the simultaneous quantification of SUN and N-DES SUN is necessary to foster the application of TDM of this drug in clinical routine.

A sensitive and robust LC-MS/MS assay that could potentially fulfil this need had already been developed in our group: compared to the other already published quantitative assays for SUN, the strengths were the ease and rapidity of the processing procedure and the use of limited quantity of biological samples.

However, one important issue was not considered during the method development: both SUN and its metabolite undergo a photoisomerization in solution and in real sample. The partial transformation from Z-isomer to the E-one obliges to take some particular precautions during collection, handling, and analysis of biological samples containing SUN. In many published methods, to avoid the isomerization, both the blood sampling and the whole handling procedures were conducted under

light protection conditions and this clearly represents an obstacle for the development of a clinically suitable quantification method for the two compounds.

Between the two geometric isomers of SUN, Z-SUN is the most thermodynamically favored one thanks to an additional intramolecular HB between the pyrrole N-H and the C=O group of oxindole that strengthen the co-planarity of the indole and pyrrole moieties through the formation of a further, fused seven-membered ring (see figure 14 in section 1.2.3.2). In the case of E-isomer, the abovementioned co-planarity is absent both in the solid and in the solution state, as it appears from the remarkable downfield shift observed in the ^{1}H NMR spectrum for the pyrrole N-H (d = 13.75 ppm in DMSO-D_6) compared to other N H signals in SUN (indole N-H at d = 10.94 ppm and carbo-amidic N-H at d = 7.79 ppm)[124]. Despite the photodegradation rate from Z- to E-isomer in solution of SUN and N-DES SUN depends on many factors, in all the cases reported in the literature it proceeded very quickly in organic or organic/aqueous phases being the maximum percentage of E-isomer (30–40% for both analytes) reached within 5–30 min of light exposition. Although all the experiments conducted in this PhD project were conducted in deproteinized plasma samples to optimize an LC-MS/MS method applicable in clinical routine, the obtained results partially confirm these data: 30 min of exposition to LED lamp were enough to achieve the maximum percentage of the E-isomer for both SUN and N-DES SUN. During the same experiments, however, the E-isomer maximum percentage of N-DES SUN resulted less than half the E-SUN (53.2 ± 5.7% for E-SUN vs 21.8 ± 3.1% for E-N-DES SUN) which contrasted with what reported in literature. Moreover, in the experiments conducted in this thesis, the E-isomer formation was not influenced by the initial concentration of the analytes, conversely to what reported by Padervand et al.. In fact, they observed a slowdown in the isomerization process with the increase of SUN initial concentration due to the hypothesis decreased light penetration. Anyway, they increased the SUN concentration from 1 to 250 μg/mL, which was way higher than the concentrations tested in this PhD project ranged 2.5–400 and 2.5–200 ng/mL for SUN and N-DES SUN, respectively, which are closer to clinical concentrations (50–100 ng/mL). By working with low concentration of the analytes, probably there was not any shielding phenomenon

from light. In addition, after the acidic addition to the extraction solvent (MeOH), the formation of the E-isomer resulted increased up to 10 percentage points. This acid effect on the isomerization of SUN and its metabolite was also reported and discussed by Padervand et al.: at low pH, the C2 carbonyl group tends to tautomerize to an enol group reducing the C=O availability for intramolecular HB formation with the N-H group of the pyrrole ring, responsible for the thermodynamic stability of the Z-isomer (figure 14 of section 1.1.1.2). In these conditions, the rotation around the exocyclic double bond is facilitated and this might be the reason for the increased percentage of the E-isomer detected for both SUN and N-DES SUN.

The isomerization process is totally reversible and, by placing the solution in the dark, the reconversion into the thermodynamically Z-isomer is favored. This phenomenon was observed and reported by Lankheet et al: they obtained different E:Z proportions in samples over time since, when samples were placed into the autosampler, they were protected from the light and the reconversion already took place during the analytical run. Since no further data regarding the reconversion rate, such as isomers percentages and timing, are available and nothing was reported about the behavior in plasma matrix, during this PhD project a kinetics of the E- to Z- reconversion in dark conditions was carried out by storing the extracted plasma samples into the autosampler. At low temperatures, the reconversion proceeded very slowly (after 4 h at 4 °C, the Z-isomer mean percentages were 50.6 ± 6.2% for SUN and 77.7 ± 2.9% for N-DES SUN), while it underwent to a considerable acceleration as the temperature rose up to 40 °C. In fact, the Z-isomer percentage reached the 99% within 2 and 1.5 h for SUN and N-DES SUN, respectively. Anyway, while no differences were observed at the three concentrations tested, when the deproteinization was carried out with acids, the increase of reconversion rate with the temperature was inhibited. Since 40°C was the temperature limit for the autosampler, to further reduce the time required for the quantitative (99%) reconversion of the E- to the Z- isomer, the extracted plasma sample containing SUN and N-DES SUN were put into a heated water bath. After only 5 min of water bath incubation at 70 °C, the mean percentages of SUN and N-DES SUN reached the 99% at each concentration tested. The value of 70 °C was chosen as the best compromise between high reconversion rate and minimum

evidence of solvent evaporation and analytes degradation. In fact, the Z-isomer peak areas of both SUN and N-DES SUN, after two water bath incubations of the samples, showed a maximum decrease of only 3.9%, thus demonstrating the absence of a significant degradation. As observed with the autosampler experiment, also in this case the presence of acids considerably slowed down the E- to Z-isomer reconversion rate for both compounds. In fact, in samples containing acids, the Z-isomer mean percentages after 5 min in water bath heated at 70 °C were within 55% and 80% for SUN and N-DES SUN, respectively.

The experimental results obtained from the abovementioned study were exploited to improve and complete the assay already developed in our institute. By simply implementing the standard sample handling procedure with 5 min of water bath incubation at 70 °C, to conduct the whole workflow (from the blood withdrawal to the sample injection into the HPLC) was possible for the personnel without light protection conditions. In fact, the fraction of Z-isomer which isomerize to E-isomer during time under environmental light exposure, could be totally reconverted to the Z-form in only 5 min just before the sample introduction to the autosampler. Some authors bypassed the light protection procedure summing the SRM responses of both separated isomers of each analyte. Consequently, the E-isomer formation was not considered a problem. However, in order to apply this trick, a quantifiable peak of both the isomers is necessary in any analytical run and this consideration could explain a quite high value as LLoQ (2.5 ng/mL). In the method developed during this PhD project, the LLoQ is 25-fold lower for both the analytes (the calibration range was 0.1-500 ng/mL for SUN and 0.1-250 ng/mL for N-DES SUN) and this makes it adequate not only for TDM practice (trough levels range from 10 to 200 ng/mL for SUN and from 5 to 100 ng/mL for N-DES SUN) but also for further pharmacokinetic studies, in which really low concentrations should be detected in order to very accurately determine parameters as half-life.

The LC-MS/MS assay, after the upgrade of the HWB, was validated according to the FDA and EMA guidelines for the validation of bioanalytical methods. The calibration curve was linear in the considered concentration range (R^2 was ≥0.9939 for each run) and was characterized by a good precision and accuracy. Both intra- and inter-

day precisions were ≤11.7% and ≤9.1% for SUN and N-DES SUN, respectively, while intra- and inter-day accuracy comprehensively ranged from 98.5 to 112.0% considering both SUN and N-DES SUN. Recovery of the analytes was high and reproducible over the concentrations tested, ranging from 93.9 to 111.1% for both SUN and N-DES SUN with a precision always ≤12.3%. Moreover, the method was selective and not significantly affected by endogenous components in the matrix or by other components in the sample (matrix effect). Short-term stabilities were also assessed: both SUN and N-DES SUN resulted stable in plasma samples after 4 hours at RT, after two freeze-thaw cycles and in extracted samples into the autosampler for 48 h at 40 °C. Long term stability in plasma samples was assessed (both SUN and N-DES SUN resulted stable for 9 months at -80 °C) while the one in WS has not been evaluated yet: it will be performed in the immediate future. Moreover, the assay reproducibility was assessed also in real samples with the ISR.

6 CONCLUSIONS

TDM is the practice of monitoring drug concentrations in patient's bloodstream, the interpretation of these data and the consequent adaptation of the drug dose in order to optimize treatment efficacy. Anticancer drugs are considered good candidates for TDM approach considering that they are administered at fixed doses or according to body surface area or body weight despite their low therapeutic index and the large inter-patient variability in systemic exposures clinically observed. Even though, TDM has been rarely implemented in clinical practice. Several factors hinder its introduction to the management of anticancer therapies. A successful clinical implementation demands a well-established drug exposure-therapeutic/toxic effects relationship as well as the availability of specialized personnel and adequate instrumental equipment. Most importantly, to properly apply TDM, highly sensitive, accurate and precise analytical methods are mandatory. These analytical methods have to be fast and easy to use in order to simplify TDM transfer to the clinical routine. Current analytical methods often do not satisfyingly meet these features, being, in most cases, complex, time-consuming and requiring highly specialized laboratories and/or laborious sample processing.
IMA and SUN are tyrosine kinase inhibitors used to treat several malignancies, including GIST. TDM of these drugs is strongly recommended, but still not well implemented in the clinical practice, due to some drug-related difficulties, including those aforementioned. In this regard, in order to foster the application of IMA and SUN TDM, the work performed during this PhD project was focused on both the method development from scratch for IMA quantification and the optimization of an already developed LC-MS/MS method for SUN and their validation according to FDA and EMA guidelines. The main purpose considered during methods development was to overcome the obstacles, related to each drug, hindering TDM introduction in the clinical routine.

More in detail, the LC-MS/MS method developed for the quantification of IMA and NOR IMA in human plasma resulted fast, based on a simple sample preparation, characterised by adequate precision, accuracy and robustness for analysis of very small sample volumes, thus fully accomplishing the intended purpose of simplicity,

rapidity, feasibility and practicality to make the method suitable for the TDM practice.
Moreover, the method was tested in the context of the clinical study *"Pilot study to evaluate the feasibility of an innovative approach to monitor patients with gastrointestinal stromal tumor treated with imatinib"* for the quantification of 49 real plasma samples from GIST patients. The method proved to be effective in quantifying plasma concentrations of both IMA and NOR IMA, highlighting possible cases of under-exposure, over-exposure and non-adherence to the therapy.

About SUN, the main difficulty to apply TDM in clinical practice was represented by the need to perform the whole analytical workflow, from the blood withdrawal to the final analysis, under light protection conditions. The reason was a photoisomerization reaction involving both the drug and its main metabolite, N-DES SUN, in solution. To overcome the issue of the isomerization in presence of light without carrying out the sample handling in the dark, was the key factor to optimize an LC-MS/MS assay, already developed by our group, for the quantification of SUN and N-DES SUN in human plasma.
First, the behavior of SUN and its metabolite was studied in human plasma to find the proper conditions to trigger the reverse reaction. Then, the addition of a simple pre-analytical step allowed to substitute, in only 5 minutes, an entire sample handling in light protection conditions. The upgraded LC-MS/MS method was finally validated according to the FDA and EMA guidelines showing robustness, precision, accuracy and reproducibility even with real samples.

As future perspective, to further support the TDM practice from the analytical point of view, other analytical assays will be developed for other drugs belonging to the targeted therapy. Moreover, thanks to the sensitivity and selectivity guaranteed by the LC-MS/MS technique, micro-sampling approaches like dried blood spot and capillary sampling will be taken into consideration to provide a better patient's compliance.

REFERENCES

1. Rubin, J. L. *et al.* Epidemiology, survival, and costs of localized gastrointestinal stromal tumors. *Int. J. Gen. Med.* **4**, 121–130 (2011).

2. van der Zwan, S. M. & DeMatteo, R. P. Gastrointestinal stromal tumor: 5 years later. *Cancer* **104**, 1781–1788 (2005).

3. AIOM. Sarcome dei tessuti molli e GIST, informazoni per i pazienti (2017)

4. DeMatteo, R. P. *et al.* Two hundred gastrointestinal stromal tumors: recurrence patterns and prognostic factors for survival. *Ann. Surg.* **231**, 51–58 (2000).

5. Nilsson, B. *et al.* Gastrointestinal stromal tumors: the incidence, prevalence, clinical course, and prognostication in the preimatinib mesylate era--a population-based study in western Sweden. *Cancer* **103**, 821–829 (2005).

6. Demetri, G. D. *et al.* NCCN Task Force report: update on the management of patients with gastrointestinal stromal tumors. *J. Natl. Compr. Cancer Netw. JNCCN* **8 Suppl 2**, S1-41; quiz S42-44 (2010).

7. Keung, E. Z. & Raut, C. P. Management of Gastrointestinal Stromal Tumors. *Surg. Clin. North Am.* **97**, 437–452 (2017).

8. AIOM. Linee guida sarcomi dei tessuti molli e GIST (2016)

9. Woodall, C. E. *et al.* An evaluation of 2537 gastrointestinal stromal tumors for a proposed clinical staging system. *Arch. Surg. Chic. Ill 1960* **144**, 670–678 (2009).

10. Corless, C. L., Fletcher, J. A. & Heinrich, M. C. Biology of gastrointestinal stromal tumors. *J. Clin. Oncol.* **22**, 3813–3825 (2004).

11. Lanke, G. & Lee, J. H. How best to manage gastrointestinal stromal tumor. *World J. Clin. Oncol.* **8**, 135–144 (2017).

12. Koh, J. S. *et al.* Gastrointestinal stromal tumors: overview of pathologic features, molecular biology, and therapy with imatinib mesylate. *Histol. Histopathol.* **19**, 565–574 (2004).

13. Hirota, S. *et al.* Gain-of-function mutations of c-kit in human gastrointestinal stromal tumors. *Science* **279**, 577–580 (1998).

14. Wozniak, A. *et al.* Tumor genotype is an independent prognostic factor in primary gastrointestinal stromal tumors of gastric origin: a european

multicenter analysis based on ConticaGIST. *Clin. Cancer Res.* **20**, 6105–6116 (2014).

15. Joensuu, H. *et al.* Management of malignant gastrointestinal stromal tumors. *Lancet Oncol.* **3**, 655–664 (2002).

16. Langer, C. *et al.* Prognostic factors influencing surgical management and outcome of gastrointestinal stromal tumors. *Br. J. Surg.* **90**, 332–339 (2003).

17. Blanke, C. D. *et al.* Long-term results from a randomized phase II trial of standard- versus higher-dose imatinib mesylate for patients with unresectable or metastatic gastrointestinal stromal tumors expressing KIT. *J. Clin. Oncol.* **26**, 620–625 (2008).

18. Demetri, G. D. *et al.* Efficacy and Safety of Imatinib Mesylate in Advanced Gastrointestinal Stromal Tumors. *N. Engl. J. Med.* **347**, 472–480 (2002).

19. van Oosterom, A. T. *et al.* Safety and efficacy of imatinib (STI571) in metastatic gastrointestinal stromal tumors: a phase I study. *Lancet* **358**, 1421–1423 (2001).

20. Lim, K. T. & Tan, K. Y. Current research and treatment for gastrointestinal stromal tumors. *World J. Gastroenterol.* **23**, 4856–4866 (2017).

21. ESMO/European Sarcoma Network Working Group. Gastrointestinal stromal tumors: ESMO Clinical Practice Guidelines for diagnosis, treatment and follow-up. *Ann. Oncol. Off. J. Eur.* **25 Suppl 3**, iii21-26 (2014).

22. Gastrointestinal Stromal Tumor Meta-Analysis Group (MetaGIST). Comparison of two doses of imatinib for the treatment of unresectable or metastatic gastrointestinal stromal tumors: a meta-analysis of 1,640 patients. *J. Clin. Oncol.* **28**, 1247–1253 (2010).

23. Gold, J. S. & Dematteo, R. P. Combined surgical and molecular therapy: the gastrointestinal stromal tumor model. *Ann. Surg.* **244**, 176–184 (2006).

24. Quek, R. & George, S. Gastrointestinal stromal tumor: a clinical overview. *Hematol. Oncol. Clin. North Am.* **23**, 69–78, viii (2009).

25. Peng, B., Lloyd, P. & Schran, H. Clinical pharmacokinetics of imatinib. *Clin. Pharmacokinet.* **44**, 879–894 (2005).

26. von Mehren, M. & Widmer, N. Correlations between imatinib pharmacokinetics, pharmacodynamics, adherence, and clinical response in advanced metastatic gastrointestinal stromal tumor (GIST): an emerging role for drug blood level testing? *Cancer Treat. Rev.* **37**, 291–299 (2011).

27. AIFA. Allegato I Riassunto delle caratteristiche del prodotto (Glivec)

28. Delbaldo, C. *et al.* Pharmacokinetic-pharmacodynamic relationships of imatinib and its main metabolite in patients with advanced gastrointestinal stromal tumors. *Clin. Cancer Res.* **12**, 6073–6078 (2006).

29. Dutreix, C. *et al.* Pharmacokinetic interaction between ketoconazole and imatinib mesylate (Glivec) in healthy subjects. *Cancer Chemother. Pharmacol.* **54**, 290–294 (2004).

30. O'Brien, S. G. *et al.* Effects of imatinib mesylate (STI571, Glivec) on the pharmacokinetics of simvastatin, a cytochrome p450 3A4 substrate, in patients with chronic myeloid leukaemia. *Br. J. Cancer* **89**, 1855–1859 (2003).

31. Din, O. S. & Woll, P. J. Treatment of gastrointestinal stromal tumor: focus on imatinib mesylate. *Ther. Clin. Risk Manag.* **4**, 149–162 (2008).

32. Nikolova, Z. *et al.* Bioequivalence, safety, and tolerability of imatinib tablets compared with capsules. *Cancer Chemother. Pharmacol.* **53**, 433–438 (2004).

33. Jakhetiya, A. *et al.* Targeted therapy of gastrointestinal stromal tumors. *World J. Gastrointest. Surg.* **8**, 345–352 (2016).

34. Giorgi, U. D. & Verweij, J. Imatinib and gastrointestinal stromal tumors: Where do we go from here? *Mol. Cancer Ther.* **4**, 495–501 (2005).

35. Zalcberg, J. R. *et al.* Outcome of patients with advanced gastro-intestinal stromal tumors crossing over to a daily imatinib dose of 800 mg after progression on 400 mg. *Eur. J. Cancer* **41**, 1751–1757 (2005).

36. Blanke, C. D. *et al.* Phase III randomized, intergroup trial assessing imatinib mesylate at two dose levels in patients with unresectable or metastatic gastrointestinal stromal tumors expressing the kit receptor tyrosine kinase: S0033. *J. Clin. Oncol.* **26**, 626–632 (2008).

37. Roskoski, R. Classification of small molecule protein kinase inhibitors based upon the structures of their drug-enzyme complexes. *Pharmacol. Res.* **103**, 26–48 (2016).

38. Adams, V. R. & Leggas, M. Sunitinib malate for the treatment of metastatic renal cell carcinoma and gastrointestinal stromal tumors. *Clin. Ther.* **29**, 1338–1353 (2007).

39. George, S. *et al.* Clinical evaluation of continuous daily dosing of sunitinib malate in patients with advanced gastrointestinal stromal tumor after imatinib failure. *Eur. J. Cancer* **45**, 1959–1968 (2009).

40. Le Tourneau, C., Raymond, E. & Faivre, S. Sunitinib: a novel tyrosine kinase inhibitor. A brief review of its therapeutic potential in the treatment of renal carcinoma and gastrointestinal stromal tumors (GIST). *Ther. Clin. Risk Manag.* **3**, 341–348 (2007).

41. Goodman, V. L. *et al.* Approval summary: sunitinib for the treatment of imatinib refractory or intolerant gastrointestinal stromal tumors and advanced renal cell carcinoma. *Clin. Cancer Res.* **13**, 1367–1373 (2007).

42. Dar, A. C. & Shokat, K. M. The evolution of protein kinase inhibitors from antagonists to agonists of cellular signaling. *Annu. Rev. Biochem.* **80**, 769–795 (2011).

43. FDA. Riassunto delle caratteristiche del prodotto (Glivec).

44. Bello, C. L. *et al.* Effect of food on the pharmacokinetics of sunitinib malate (SU11248), a multi-targeted receptor tyrosine kinase inhibitor: results from a phase I study in healthy subjects. *Anticancer. Drugs* **17**, 353–358 (2006).

45. Desar, I. M. E. *et al.* Pharmacokinetics of sunitinib in an obese patient with a GIST. *Ann. Oncol.* **20**, 599–600 (2009).

46. Faivre, S. *et al.* Safety, Pharmacokinetic, and Antitumor Activity of SU11248, a Novel Oral Multitarget Tyrosine Kinase Inhibitor, in Patients With Cancer. *J. Clin. Oncol.* **24**, 25–35 (2006).

47. Study Of SU011248 Plus Gefitinib (Iressa) In Patients With Advanced Renal Cell Carcinoma - Study Results - ClinicalTrials.gov. Available at: https://clinicaltrials.gov/ct2/show/results/NCT00113529. (Accessed: 4th November 2018)

48. AIFA. Allegato I Riassunto delle caratteristiche del prodotto (Sutent)

49. Lyseng-Williamson, K. A. Regorafenib: a guide to its use in advanced gastrointestinal stromal tumor (GIST) after failure of imatinib and sunitinib. *BioDrugs* **27**, 525–531 (2013).

50. Demetri, G. D. *et al.* Efficacy and safety of regorafenib for advanced gastrointestinal stromal tumors after failure of imatinib and sunitinib (GRID): an international, multicentre, randomised, placebo-controlled, phase 3 trial. *Lancet* **381**, 295–302 (2013).

51. AIFA. Allegato I Riassunto delle caratteristiche del prodotto (Stivarga).

52. FDA. Riassunto delle caratteristiche del prodotto (Stivarga).

53. Poveda, A. *et al.* GEIS guidelines for gastrointestinal sarcomas (GIST). *Cancer Treat. Rev.* **55**, 107–119 (2017).

54. Home - ClinicalTrials.gov.

55. Feng, W. *et al.* Compliance and persistency with imatinib. *J. Clin. Oncol.* **24**, 6038–6038 (2006).

56. Tsang, J., Rudychev, I. & Pescatore, S. L. Prescription compliance and persistency in chronic myelogenous leukemia (CML) and gastrointestinal stromal tumor (GIST) patients (pts) on imatinib (IM). *J. Clin. Oncol.* **24**, 6119–6119 (2006).

57. Yu, H. *et al.* Practical guidelines for therapeutic drug monitoring of anticancer tyrosine kinase inhibitors: focus on the pharmacokinetic targets. *Clin. Pharmacokinet.* **53**, 305–325 (2014).

58. Reynolds, D. J. & Aronson, J. K. ABC of monitoring drug therapy. Making the most of plasma drug concentration measurements. *BMJ* **306**, 48–51 (1993).

59. Hon, Y. Y. & Evans, W. E. Making TDM work to optimize cancer chemotherapy: a multidisciplinary team approach. *Clin. Chem.* **44**, 388–400 (1998).

60. Alnaim, L. Therapeutic drug monitoring of cancer chemotherapy. *J. Oncol. Pharm. Pract.* **13**, 207–221 (2007).

61. Teng, J. F. T., Mabasa, V. H. & Ensom, M. H. H. The role of therapeutic drug monitoring of imatinib in patients with chronic myeloid leukemia and metastatic or unresectable gastrointestinal stromal tumors. *Ther. Drug Monit.* **34**, 85–97 (2012).

62. Herviou, P. *et al.* Therapeutic drug monitoring and tyrosine kinase inhibitors. *Oncol. Lett.* **12**, 1223–1232 (2016).

63. Taylor, G. I. Disintegration of water drops in an electric field. *Proc R Soc Lond A* **280**, 383–397 (1964).

64. F.R.S, L. R. XX. On the equilibrium of liquid conducting masses charged with electricity. *Lond. Edinb. Dublin Philos. Mag. J. Sci.* **14**, 184–186 (1882).

65. Stauffer, E., Dolan, J. A. & Newman, R. CHAPTER 8 - Gas Chromatography and Gas Chromatography—Mass Spectrometry. in *Fire Debris Analysis* (eds. Stauffer, E., Dolan, J. A. & Newman, R.) 235–293 (Academic Press, 2008). doi:10.1016/B978-012663971-1.50012-9

66. Bioanalytical Method Validation Guidance for Industry. 44 (2018).

67. EMA. Guideline on bioanalytical method validation (2011).

68. Shah, V. P. *et al.* Analytical methods validation: bioavailability, bioequivalence and pharmacokinetic studies. Conference report. *Eur. J. Drug Metab. Pharmacokinet.* **16**, 249–255 (1991).

69. FDA. Bioanalytical Method Validation (draft guidance). 34 (2013)

70. Booth, B. *et al.* Workshop Report: Crystal City V—Quantitative Bioanalytical Method Validation and Implementation: The 2013 Revised FDA Guidance. *AAPS J.* **17**, 277–288 (2014).

71. Spector, R., Park, G. D., Johnson, G. F. & Vesell, E. S. Therapeutic drug monitoring. *Clin. Pharmacol. Ther.* **43**, 345–353 (1988).

72. Relling, M. V. *et al.* Patient characteristics associated with high-risk methotrexate concentrations and toxicity. *J. Clin. Oncol.* **12**, 1667–1672 (1994).

73. Evans, W. E. & Relling, M. V. Clinical pharmacokinetics-pharmacodynamics of anticancer drugs. *Clin. Pharmacokinet.* **16**, 327–336 (1989).

74. *DeVita, Hellman, and Rosenberg's Cancer: Principles and Practice of Oncology*. (LWW, 2011).

75. Moore, M. J. & Erlichman, C. Therapeutic drug monitoring in oncology. Problems and potential in antineoplastic therapy. *Clin. Pharmacokinet.* **13**, 205–227 (1987).

76. Widmer, N. *et al.* Review of therapeutic drug monitoring of anticancer drugs part two--targeted therapies. *Eur. J. Cancer* **50**, 2020–2036 (2014).

77. Bardin, C. *et al.* Therapeutic drug monitoring in cancer – Are we missing a trick? *Eur. J. Cancer* **50**, 2005–2009 (2014).

78. Galpin, A. J. & Evans, W. E. Therapeutic drug monitoring in cancer management. *Clin. Chem.* **39**, 2419–2430 (1993).

79. McLeod, H. L. Therapeutic drug monitoring opportunities in cancer therapy. *Pharmacol. Ther.* **74**, 39–54 (1997).

80. Decosterd, L. A. *et al.* Therapeutic drug monitoring of targeted anticancer therapy. *Biomark. Med.* **9**, 887–893 (2015).

81. Baccarani, M. *et al.* Chronic myeloid leukemia: ESMO Clinical Practice Guidelines for diagnosis, treatment and follow-up. *Ann. Oncol.* **23 Suppl 7**, vii72-77 (2012).

82. Verheijen, R. B. *et al.* Practical Recommendations for Therapeutic Drug Monitoring of Kinase Inhibitors in Oncology. *Clin. Pharmacol. Ther.* **102**, 765–776 (2017).

83. Demetri, G. D. *et al.* Imatinib plasma levels are correlated with clinical benefit in patients with unresectable/metastatic gastrointestinal stromal tumors. *J. Clin. Oncol.* **27**, 3141–3147 (2009).

84. Judson, I. *et al.* Imatinib pharmacokinetics in patients with gastrointestinal stromal tumor: a retrospective population pharmacokinetic study over time. EORTC Soft Tissue and Bone Sarcoma Group. *Cancer Chemother. Pharmacol.* **55**, 379–386 (2005).

85. Eechoute, K. *et al.* A long-term prospective population pharmacokinetic study on imatinib plasma concentrations in GIST patients. *Clin. Cancer Res.* **18**, 5780–5787 (2012).

86. Bouchet, S. *et al.* Relationship between imatinib trough concentration and outcomes in the treatment of advanced gastrointestinal stromal tumors in a real-life setting. *Eur. J. Cancer* **57**, 31–38 (2016).

87. Judson, I. Therapeutic drug monitoring of imatinib--new data strengthen the case. *Clin. Cancer Res.* **18**, 5517–5519 (2012).

88. Yoo, C. *et al.* Cross-sectional study of imatinib plasma trough levels in patients with advanced gastrointestinal stromal tumors: impact of gastrointestinal resection on exposure to imatinib. *J. Clin. Oncol.* **28**, 1554–1559 (2010).

89. Houk, B. E. *et al.* Relationship between exposure to sunitinib and efficacy and tolerability endpoints in patients with cancer: results of a pharmacokinetic/pharmacodynamic meta-analysis. *Cancer Chemother. Pharmacol.* **66**, 357–371 (2010).

90. Goulooze, S. C., Galettis, P., Boddy, A. V. & Martin, J. H. Monte Carlo simulations of the clinical benefits from therapeutic drug monitoring of sunitinib in patients with gastrointestinal stromal tumors. *Cancer Chemother. Pharmacol.* **78**, 209–216 (2016).

91. Lankheet, N. A. G. *et al.* Pharmacokinetically guided sunitinib dosing: a feasibility study in patients with advanced solid tumors. *Br. J. Cancer* **110**, 2441–2449 (2014).

92. Mizuno, T. *et al.* Impact of genetic variation in breast cancer resistance protein (BCRP/ABCG2) on sunitinib pharmacokinetics. *Drug Metab. Pharmacokinet.* **27**, 631–639 (2012).

93. Oberoi, R. K., Mittapalli, R. K., Fisher, J. & Elmquist, W. F. Sunitinib LC–MS/MS Assay in Mouse Plasma and Brain Tissue: Application in CNS Distribution Studies. *Chromatographia* **76**, (2013).

94. Maafi, M. & Lee, L. Y. Actinometric and Φ-order photodegradation properties of anti-cancer Sunitinib. *J. Pharm. Biomed. Anal.* **110**, 34–41 (2015).

95. Padervand, M., Ghaffari, S., Attar, H. & Nejad, M. M. Reverse phase HPLC determination of sunitinib malate using UV detector, its isomerisation study, method development and validation. *J. Anal. Chem.* **72**, 567–574 (2017).

96. Etienne-Grimaldi, M. C., Renée, N., Izzedine, H. & Milano, G. A routine feasible HPLC analysis for the anti-angiogenic tyrosine kinase inhibitor, sunitinib, and its main metabolite, SU12662, in plasma. *J. Chromatogr. B Analyt. Technol. Biomed. Life. Sci.* **877**, 3757–3761 (2009).

97. de Bruijn, P. *et al.* Bioanalytical method for the quantification of sunitinib and its n-desethyl metabolite SU12662 in human plasma by ultra performance liquid chromatography/tandem triple-quadrupole mass spectrometry. *J. Pharm. Biomed. Anal.* **51**, 934–941 (2010).

98. Zhou, Q. & Gallo, J. M. Quantification of sunitinib in mouse plasma, brain tumor and normal brain using liquid chromatography-electrospray ionization-tandem mass spectrometry and pharmacokinetic application. *J. Pharm. Biomed. Anal.* **51**, 958 (2010).

99. Rodamer, M., Elsinghorst, P. W., Kinzig, M., Gütschow, M. & Sörgel, F. Development and validation of a liquid chromatography/tandem mass spectrometry procedure for the quantification of sunitinib (SU11248) and its active metabolite, N-desethyl sunitinib (SU12662), in human plasma: application to an explorative study. *J. Chromatogr. B Analyt. Technol. Biomed. Life. Sci.* **879**, 695–706 (2011).

100. Musijowski, J., Piórkowska, E. & Rudzki, P. J. Determination of sunitinib in human plasma using liquid chromatography coupled with mass spectrometry. *J. Sep. Sci.* **37**, 2652–2658 (2014).

101. Qiu, F., Bian, W., Li, J. & Ge, Z. Simultaneous determination of sunitinib and its two metabolites in plasma of Chinese patients with metastatic renal cell carcinoma by liquid chromatography–tandem mass spectrometry. *Biomed. Chromatogr.* **27**, 615–621 (2013).

102. Andriamanana, I., Gana, I., Duretz, B. & Hulin, A. Simultaneous analysis of anticancer agents bortezomib, imatinib, nilotinib, dasatinib, erlotinib, lapatinib, sorafenib, sunitinib and vandetanib in human plasma using LC/MS/MS. *J. Chromatogr. B Analyt. Technol. Biomed. Life. Sci.* **926**, 83–91 (2013).

103. Lankheet, N. A. G. *et al.* Quantification of sunitinib and N-desethyl sunitinib in human EDTA plasma by liquid chromatography coupled with electrospray ionization tandem mass spectrometry: validation and application in routine therapeutic drug monitoring. *Ther. Drug Monit.* **35**, 168–176 (2013).

104. Haouala, A. *et al.* Therapeutic Drug Monitoring of the new targeted anticancer agents imatinib, nilotinib, dasatinib, sunitinib, sorafenib and lapatinib by LC tandem mass spectrometry. *J. Chromatogr. B Analyt. Technol. Biomed. Life. Sci.* **877**, 1982–1996 (2009).

105. Couchman, L. *et al.* An automated method for the simultaneous measurement of azole antifungal drugs in human plasma or serum using turbulent flow liquid chromatography-tandem mass spectrometry. *Anal. Bioanal. Chem.* **404**, 513–523 (2012).

106. Lankheet, N. a. G. *et al.* Method development and validation for the quantification of dasatinib, erlotinib, gefitinib, imatinib, lapatinib, nilotinib,

sorafenib and sunitinib in human plasma by liquid chromatography coupled with tandem mass spectrometry. *Biomed. Chromatogr.* **27**, 466–476 (2013).

107. van Erp, N. P. *et al.* A validated assay for the simultaneous quantification of six tyrosine kinase inhibitors and two active metabolites in human serum using liquid chromatography coupled with tandem mass spectrometry. *J. Chromatogr. B Analyt. Technol. Biomed. Life. Sci.* **937**, 33–43 (2013).

108. Ngai, M. H., So, C. L., Sullivan, M. B., Ho, H. K. & Chai, C. L. L. Photoinduced Isomerization and Hepatoxicities of Semaxanib, Sunitinib and Related 3-Substituted Indolin-2-ones. *ChemMedChem* **11**, 72–80 (2016).

109. Sistla, A. & Shenoy, N. Reversible Z-E Isomerism and Pharmaceutical Implications for SU5416. *Drug Dev. Ind. Pharm.* **31**, 1001–1007 (2005).

110. Xia, Y.-Q. & Jemal, M. Phospholipids in liquid chromatography/mass spectrometry bioanalysis: comparison of three tandem mass spectrometric techniques for monitoring plasma phospholipids, the effect of mobile phase composition on phospholipids elution and the association of phospholipids with matrix effects. *Rapid Commun. Mass Spectrom.* **23**, 2125–2138 (2009).

111. González, O. *et al.* Bioanalytical chromatographic method validation according to current regulations, with a special focus on the non-well defined parameters limit of quantification, robustness and matrix effect. *J. Chromatogr. A* **1353**, 10–27 (2014).

112. Mei, H. *et al.* Investigation of matrix effects in bioanalytical high-performance liquid chromatography/tandem mass spectrometric assays: application to drug discovery. *Rapid Commun. Mass Spectrom.* **17**, 97–103 (2003).

113. Bonfiglio, null, King, null, Olah, null & Merkle, null. The effects of sample preparation methods on the variability of the electrospray ionization response for model drug compounds. *Rapid Commun. Mass Spectrom.* **13**, 1175–1185 (1999).

114. Fast, D. M. *et al.* Workshop report and follow-up--AAPS Workshop on current topics in GLP bioanalysis: Assay reproducibility for incurred samples--implications of Crystal City recommendations. *AAPS J.* **11**, 238–241 (2009).

115. Gharwan, H. & Groninger, H. Kinase inhibitors and monoclonal antibodies in oncology: clinical implications. *Nat. Rev. Clin. Oncol.* **13**, 209–227 (2016).

116. Klümpen, H.-J., Samer, C. F., Mathijssen, R. H. J., Schellens, J. H. M. & Gurney, H. Moving towards dose individualization of tyrosine kinase inhibitors. *Cancer Treat. Rev.* **37**, 251–260 (2011).

117. Parise, R. A., Ramanathan, R. K., Hayes, M. J. & Egorin, M. J. Liquid chromatographic–mass spectrometric assay for quantitation of imatinib and its main metabolite (CGP 74588) in plasma. *J. Chromatogr. B* **791**, 39–44 (2003).

118. Bakhtiar, R. *et al.* High-throughput quantification of the anti-leukemia drug STI571 (Gleevec) and its main metabolite (CGP 74588) in human plasma using liquid chromatography-tandem mass spectrometry. *J. Chromatogr. B Analyt. Technol. Biomed. Life. Sci.* **768**, 325–340 (2002).

119. Parise, R. A., Ramanathan, R. K., Hayes, M. J. & Egorin, M. J. Liquid chromatographic-mass spectrometric assay for quantitation of imatinib and its main metabolite (CGP 74588) in plasma. *J. Chromatogr. B Analyt. Technol. Biomed. Life. Sci.* **791**, 39–44 (2003).

120. Birch, M. *et al.* Simple methodology for the therapeutic drug monitoring of the tyrosine kinase inhibitors dasatinib and imatinib. *Biomed. Chromatogr.* **27**, 335–342 (2013).

121. Zhang, M., Moore, G. A., Fernyhough, L. J., Barclay, M. L. & Begg, E. J. Determination of imatinib and its active metabolite N-desmethyl imatinib in human plasma by liquid chromatography/tandem mass spectrometry. *Anal. Bioanal. Chem.* **404**, 2091–2096 (2012).

122. Zhang, Y. *et al.* LC-MS-MS determination of imatinib and N-desmethyl imatinib in human plasma. *J. Chromatogr. Sci.* **52**, 344–350 (2014).

123. Zhuang, W. *et al.* Simultaneous quantification of imatinib and its main metabolite N-demethyl-imatinib in human plasma by liquid chromatography-tandem mass spectrometry and its application to therapeutic drug monitoring in patients with gastrointestinal stromal tumor. *Biomed. Chromatogr.* **31**, (2017).

124. Sidoryk, K. *et al.* Physicochemical characteristics of sunitinib malate and its process-related impurities. *J. Pharm. Sci.* **102**, 706–716 (2013).

Ringraziamenti

Vorrei innanzitutto ringraziare l'ex coordinatore Mauro Stener e l'attuale coordinatrice Barbara Milani assieme ai miei due supervisori Giuseppe Toffoli e Federico Berti per avermi permesso, in questi tre anni di dottorato, di portare avanti il mio progetto di ricerca. Ringrazio poi la mia tutor e co-supervisore Elena Marangon per avermi formato nelle prime parti del mio progetto e avermi tramandato un approccio molto accurato nei confronti della chimica analitica. Insieme a lei, anche Bianca e Luciana hanno contribuito alla mia formazione e le ringrazio infinitamente di essermi sempre state accanto sia a livello lavorativo, sia come buonissime amiche. I miei ringraziamenti vanno anche a Bruno, il quale ha contribuito con la sua enorme esperienza a rendere la spettrometria di massa sempre stimolante e mi ha sempre dato una mano nel momento del bisogno con costante gentilezza. Ringrazio tutti gli altri membri del gruppo "Fasi 1" Sara, Valentina, Martina, Ariana e Michela; ognuna di loro è stata un elemento fondamentale nella mia crescita professionale e personale. Un ringraziamento va a tutti i membri della Farmacologia Sperimentale Clinica, in particolare ad Antonella, per la sua infinità cordialità e gentilezza, e al "gruppo mensa" per aver allietato quotidianamente dei pranzi altrimenti non proprio esaltanti. Inoltre, alla neo-maestra Eva, sempre presente per me sia nel bene che nel male durante il mio dottorato, faccio un enorme in bocca al lupo per il suo futuro. Ringrazio il mio coinquilino Andrea per avermi sopportato in questi tre lunghi anni e per le lunghe chiacchierate, serie o meno, accompagnate dalla canonica birra del King's. Un grande grazie sia alla mia ragazza Anna, sempre solare e positiva, per avermi costantemente fatto sorridere e per avermi "salvato", sia al mio migliore amico e compagno di sventure di dottorato Marco. Ultimi, ma non certo per importanza, i miei genitori, mio fratello e tutti i miei parenti: li ringrazio dal primo all'ultimo per esserci sempre stati e per aver sempre creduto in me.